universität wien

DISSERTATION

Titel der Dissertation

Separation, Identification and Quantitation of Metabolites in Biological Systems by Liquid Chromatography and Tandem Mass Spectrometry

Verfasser

Magister Roland Johann Reischl

angestrebter akademischer Grad

Doktor der Naturwissenschaften (Dr. rer. nat.)

Wien, 2012

Studienkennzahl lt. Studienblatt:	A 091 419
Dissertationsgebiet lt. Studienblatt:	Analytische Chemie
Betreuerin / Betreuer:	o.Prof. Dr. Wolfgang Lindner

Danksagung

Ein sehr herzlicher Dank gilt Herrn Professor Lindner, der die ganzen Jahre über ein wahrer Mentor war, der meine Entwicklung in zahllosen regen Diskussionen stets gefördert und meine Ambitionen nach Kräften unterstützt hat.

Norbert Maier, Michael Lämmerhofer, Wolfgang Bicker und Alexander Leitner, haben mit sehr viel Engagement und enormer fachlicher Kompetenz einen wichtigen Beitrag zu dieser Arbeit geleistet

Vielen Dank an die gesamte Arbeitsgruppe, die ein lockeres, freundschaftliches und doch extrem motivierendes Umfeld waren. In diesem Umfeld war das Arbeiten stets eine Freude und die Festaktivitäten haben den Laboralltag versüßt.

Mein allergrößter Dank gilt meiner Mutter, die mich mit sehr viel Liebe und Herzenswärme so erzogen hat, dass ich mich stets frei entfalten und eigenständige Entscheidungen treffen konnte. Meinem Vater, der mir all dies ermöglicht hat und der mir das naturwissenschaftliche Interesse mitgegeben hat, bin ich dafür sehr dankbar.

Meine Schwestern Claudia und Sabine waren mir immer ein unglaublicher familiärer Rückhalt. Ebenso wie Andreas Lackner, der mich den ganzen Weg über begleitet hat und dessen Freundschaft immer über allen Höhen und Tiefen stand. Diese Menschen haben meinem Leben das Fundament gegeben, das ich für diese lange Ausbildung gebraucht habe.

Faxe, Fritzi und David; Martin, Maxi und Metla; Hias, Marco und Gadman und auch du, liebe Alex. Ihr habt die Stunden abseits der Arbeit erfüllt und mich oft den Stress vergessen lassen.

Danke, Reinhard Pell, der als treuer Sitznachbar stets ein offenes Ohr für häufig auch unwissenschaftliche Kommentare gehabt hat.

Table of Contents

I. GENERAL PART

Metabolism is a key requirement to sustain basic functions in any biological system and defines life as such. The turnover of molecular components involved in biochemical reactions leaves chemical traces. The identification and determination of the involved molecules at their physiological levels deliver key answers on the function and the state of any living cell. The challenges of analyzing these molecules in biological samples call for a reduction of complexity and also for analytical methods providing exceptional levels of selectivity to enrich and trace these targets in a reliable and sensitive fashion. This thesis deals with various aspects of method development and application of highly selective analytical protocols for the precise detection of crucial biomolecules and metabolites in trace amounts

In the frame of these studies, special focus was given to the analysis of amino acids, with the intention to cover the full range of their biological relevance. In this context, amino acids were investigated as essential parts of biomarkers for ethanol consumption. Further experiments aimed for the establishment of sensitive enantioselective separation procedures for amino acids as single entities. Moreover, they have been studied as essential building blocks in peptides and proteins.

High performance liquid chromatography was the method of choice, due to its broad applicability and the availability of a broad assortment of selectors capable of separating molecules in solution with respect to almost any given property. Applying this technique in combination with different selectivity principles, analytes were separated with regard to differences in size, lipophilicity, acidity and chirality.

Considering the zwitterionic nature of the amino acids, their chromatographic separation is a nontrivial task. To eliminate their zwitterionic properties, they were derivatized in order to transform them to acidic analytical species, thus greatly facilitating analysis with reversed phase chromatography as well as chiral ion exchangers. This was achieved employing various N-derivatization strategies. In the case of enantioselective separations, the introduction of additional supportive interaction sites, such as hydrogen donors and acceptors, or aromatic moieties to enhance selector – selectand interactions, proved to be particularly useful. This measure also improved the detectability with electro spray ionization mass spectrometers via introduction of groups promoting ionization and implementing highly characteristic fragmentation patterns. Finally, these favourable features were

combined to create analytical methods, which included derivatization strategies to introduce enhanced chromatographic selectivity and increased sensitivity of detection.

In the following chapters the determination of a novel biomarker for recent ethanol consumption with reversed phase LC-MS will be presented. Furthermore, the application of zwitterionic chiral stationary phases for the enantioselective separation of amino acid derivatives is discussed. Two different labelling strategies have been developed for the chemoselective and enantioselective separation of amino acids in biological fluids by one dimensional LC with MS/MS detection. Finally, the structural determination of protein complexes by employing labelling strategies in combination with 2 dimensional chromatographic separation and high resolution mass spectrometry will be demonstrated.

II. Ethanol

Ethanol may be the most influential recreational drug in the history of mankind. The culture of ethanol production can be dated back thousands of years and its voluntary consumption by human being has major implications on sociological, economical, cultural level, but also serious health consequences. The main effects of alcohol consumption are common knowledge, and scientifically well-established. Besides its positive effects that make it a recreational drug, alcohol abuse has a severe negative impact on health. It is connected to coronary heart disease, various kinds of cancer and liver cirrhosis, and it also frequently causes injuries, traffic accidents, cases of violence and even fatal intoxications. Numerous behavioural studies have provided compelling evidence that alcohol addiction is a well known phenomenon in many societies. The health consequences of chronic and also acute ethanol consumption are a world wide issue. The world health organisation (WHO) publishes annual reports on the consumption and abuse of alcohol. The results presented therein demonstrate that ethanol is causally connected to approximately 2.5 million annual deaths world wide, including illnesses and accidents in context with chronic abuse. In other words, 4% of all worldwide deaths are alcohol related [1]. The global statistics on fatalities caused by drinking are given in Figure II.1.

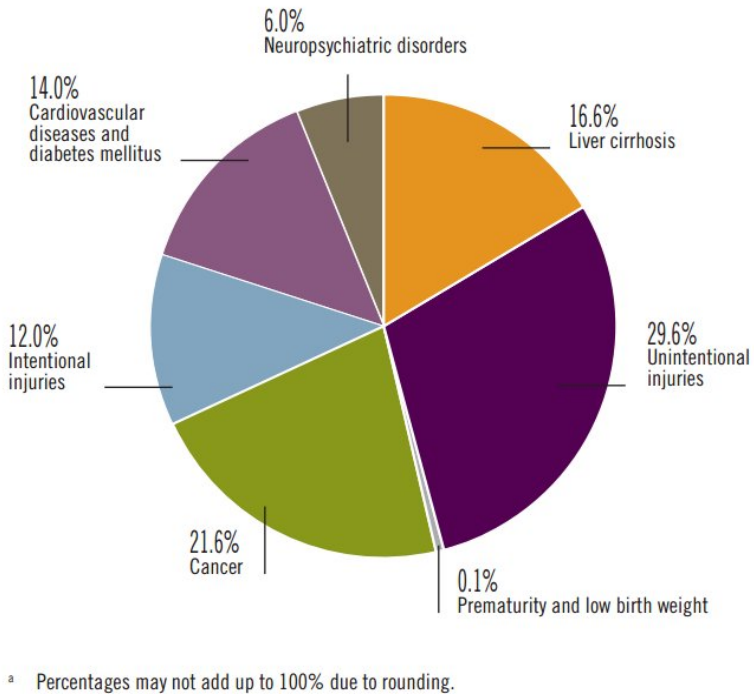

Figure II.1 Percentages of alcohol related causes of death (taken from [1])

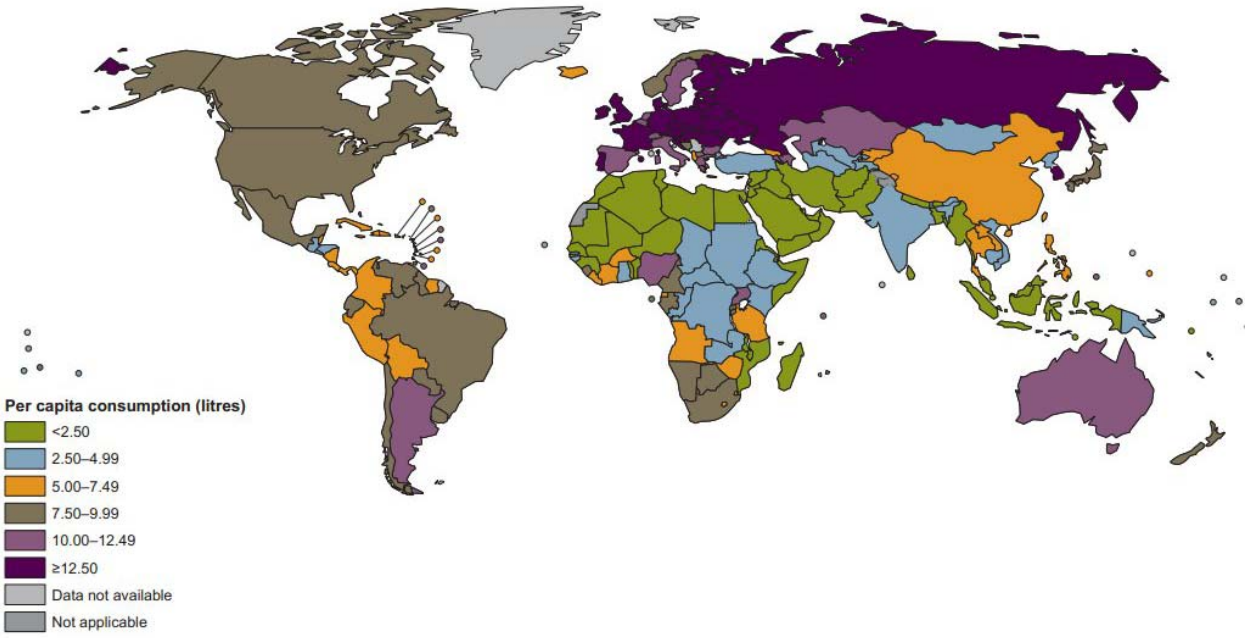

Figure II.2 World wide per capita consumption by persons above 15 years, in litres of pure ethanol (taken from [1])

According to these reports, the population of Europe in total, and especially Eastern Europe, are the world's heaviest drinkers. An overview on the global alcohol consumption is topographically depicted in Figure II.2.

II.1. Ethanol Metabolism

The toxicokinetics of ethanol have been studied intensively. It is well accepted that ethanol is mainly absorbed through the mouth cavity, the stomach and the upper regions of the small intestine. In contrast to the public opinion alcohol is almost quantitatively absorbed independent of what kind of food it is consumed with. In fact, the rate of absorption is dependent on the presence or absence of fat rich matrices in the gastro intestinal tract as well as on the concentration of the consumed beverage. After the uptake, about 10% of the adsorbed ethanol is excreted via exhalation and the urinal tract as such. The remaining 90% are metabolized mainly in the liver. Due to the high grade of metabolic adaptation, the human body quickly eliminates ethanol with a rate of 0.1‰ to 0.2 ‰ per hour independent on the actual blood concentration.

In ethanol metabolism the oxidative degradation is predominant. There are three main oxidative pathways described, amongst which the one via alcohol dehydrogenase is most dominant. All three pathways have acetaldehyde as a first intermediate in common [2]. These metabolic pathways are illustrated in Figure II.3 in a simplified way. It can be seen that in the last metabolic step, alcohol is enzymatically linked to Co-Enzyme A and then either takes part in fatty acid synthesis or enters the citric acid cycle to directly serve for energy production. The amount of energy that can be gained by ethanol breakdown adds up to 29kJ per gram, which is less than that produced from fat (37kJ g^{-1}), but more than that emerging from the breakdown of carbohydrates (16kJ g^{-1}).

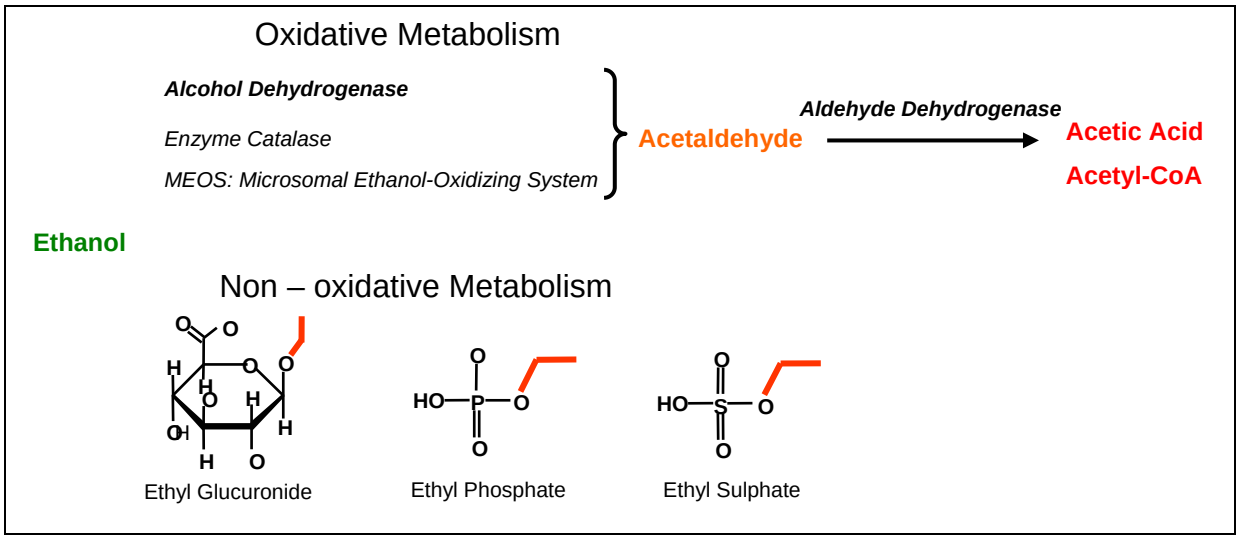

Figure II.3 Schematic presentation of the three major pathways for human ethanol metabolism

The acetaldehyde intermediary formed in the organism is usually readily eliminated by aldehyde dehydrogenase. However, a fraction of eastern Asian populations are aldehyde dehydrogenase deficient. This deficiency results in high acetaldehyde plasma levels as a consequence of alcohol intake [3]. Acetaldehyde itself is has a pronounced toxicity and is classified as a type I carcinogen [4]. Moreover, itseriously affects well being and causes headache, nausea and red blushing of the face. These negative side effects are sometimes purposefully exploited in the medical treatment of alcohol addiction. By medicating patients with the anti-alcohol drug disulfiram, acting as an efficient aldehyde dehydrogenase inhibitor, the unpleasant effects invoked are causing a kind of negative conditioning towards alcohol.

II.2. Clinical Marker

Motivated by clinical and forensic needs, a considerable number of methods were developed for the reliable minimal invasive determination of the alcohol concentration in breath, blood [5] and urine [6]. However, due to its fast metabolism, ethanol as a parent compound can only be measured for several hours. For this reason, several alternative biomarkers for alcohol consumption have been established, allowing for the determination of recent [7,8], intermediate term [8] and chronic consumption [9]. Towards the establishment of methods for the detection of alcohol consumption after several days, our goal was to identify new biomarkers that were different from the well known markers ethyl glucuronide, ethyl phosphate and ethyl sulphate [7], which emerge from the minor non-oxidative metabolism of alcohol. As indicated above, the main part of all absorbed ethanol is oxidatively metabolized via acetaldehyde, which represents a chemically very reactive electrophilic compound. Therefore, we primarily aimed at the identification of a condensation product of acetaldehyde with cysteine, or N-terminal Cys-peptide- in general.

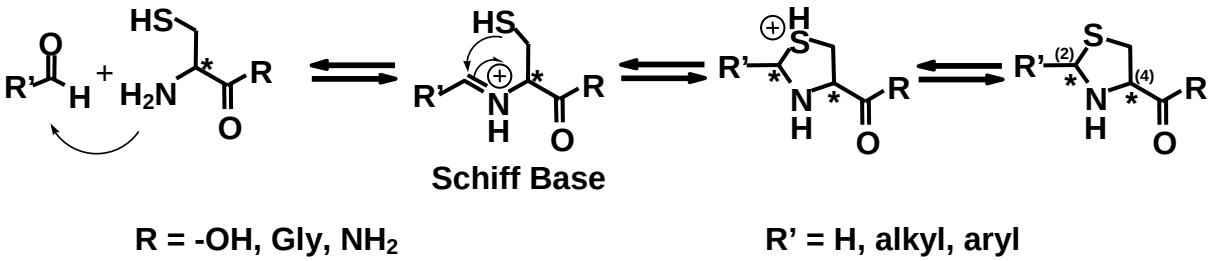

Figure II.4 Reaction scheme for the condensation of aldehydes with cysteine and peptides incorporating N-terminal cysteine

Given the fact that acetaldehyde emerges as a prime product of the major pathways, and that alcohol is generally consumed at gram scale, it is reasonable to expect a higher abundance of the alternative metabolites. Thus, various acetaldehyde – amino acid products were investigated (Figure II.6). However, the primary target was 2-methylthiazolidine-4-carboxylic acid – MTCA (see Figure II.5).

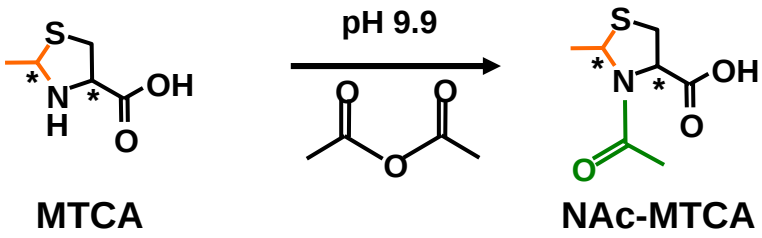

Figure II.5 Main target 2-Methylthiazolidine-4-carboxylic acid (MTCA) and its acetylated derivative

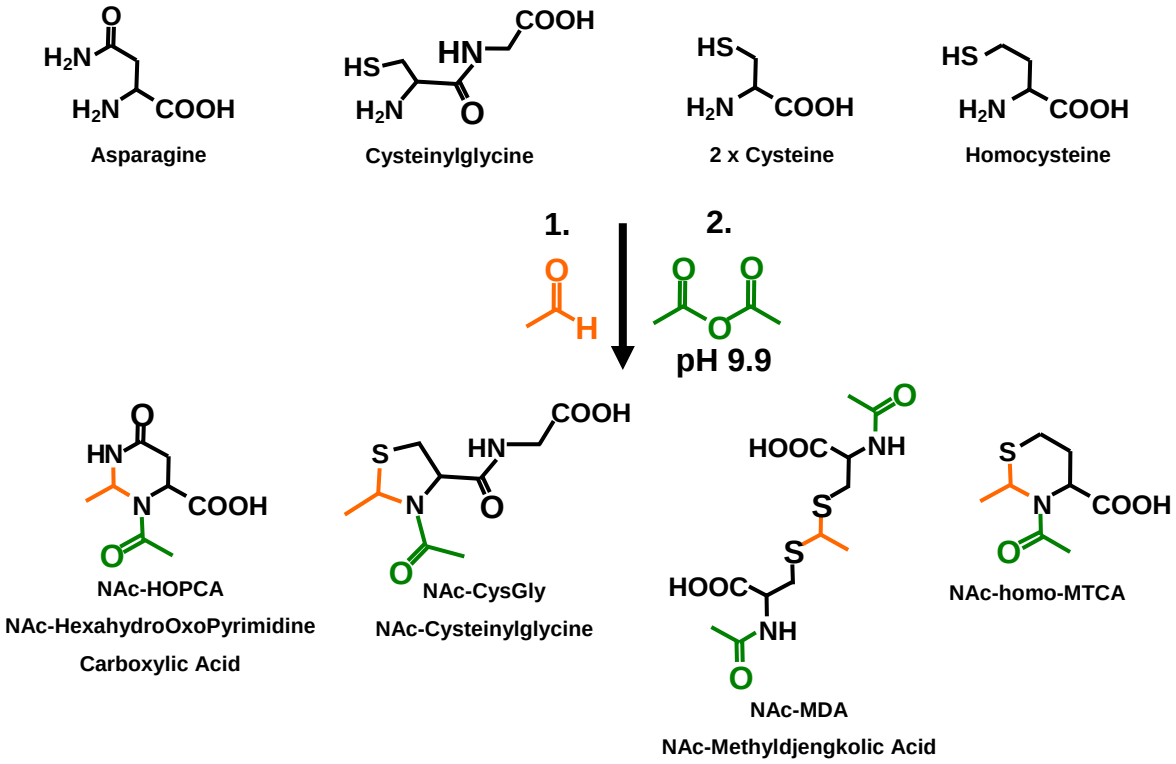

Figure II.6 Condensation of Asn, Cys, CysGly and homoCys with acetaldehyde and consecutive N – acetylation to yield the analytes thereof. The generation of Methyldjengkolic Acid is an alternative possibility to MTCA production

Synthesis of the Acetaldehyde Adducts

In context with these studies, the adducts of cysteine, homo cysteine, asparagine and the dipeptide cysteinylglycine with acetaldehyde were generated via a condensation reaction carried out in water. The reaction mixture was adjusted with 0.1M carbonate buffer to pH 9.9 and acetylated with acetic anhydride to stabilize the generated adducts. Consecutive LC-MS measurements and MS/MS fragmentation experiments were applied for product confirmation (Table II.1).

Preparation of Biological Samples

This protocol was subsequently adapted for derivatization of urine samples.

Adaptation to blood and serum matrices required deproteinization through precipitation prior to sample work up. However, efforts to trace these potential metabolites in these biological matrices were not successful. From this negative results it was concluded, that these types of metabolites, if formed as intermediates of the studied pathways, are present a very low concentration at physiological conditions. As an additional or alternative explanation, poor stability of these condensation products in presence of a huge excess of water was hypothesized.

Further experimental details can be taken from the manuscript presented in Appendix A.

Table II.1 Molecular masses and MS/MS fragments for the investigated acetaldehyde adducts

	$[M-H]^-$ m/z	$Frag^-$ m/z
NAc-MTCA	187.9	56.9 58.9 83.9
NAc-HOPCA	198.9	154.9 126.6 92.9
NAc-homo-MTCA	201.9	159.5 115.2 57.8
NAc-MTCGly	244.8	211.8 198.8 58.9
NAc-MDA	350.8	161.9 83.9 32.8

Results

The developed protocol for capturing acetaldehyde with various amino acids showed good performance in in-vitro studies. A highly sensitive RP-LC/MS method was developed allowing the separation and detection of all in-vitro observed acetaldehyde adducts. However, attempts to detect these potential metabolites in various biological fluids, such as alcohol positive and negative blood, serum and urine, were unsuccessful.

All investigated molecules have their zwitterionic behaviour in common. Therefore, N – acetylation was carried out in order to convert the amino functionalities of the analytes into neutral amide groups. Retention in reversed phase chromatography was then achieved by protonation of the acidic molecules that were generated through derivatization. Even though HOPCA, homo-MTCA and MTCGly could be generated in vitro by simple condensation between the amino acid or peptide educts and acetaldehyde we could not identify any of these targets when we applied the developed analytical method to biological samples such as alcohol positive blood and urine. Methyldjengkolic acid demanded for strongly acidic conditions in synthesis, such conditions could possibly exist in the stomachic milieu. Also NAc-MDA could not be identified neither in urine nor in blood. In contrast to these analytes, MTCA in its N acetylated form was identified in biological samples and therefore it was thoroughly investigated (see below and Appendix A).

Analysis of 2-Methylthiazolidine-4-carboxylic acid – MTCA – a condensation product of cysteine and acetaldehyde as a consequence of alcohol consumption

Roland J. Reischl, Wolfgang Bicker, Thomas Keller, Günther Lamprecht, Wolfgang Lindner

Abstract

Acetaldehyde is a highly electrophilic agent that is endogenously produced as a first intermediate in oxidative alcohol metabolism. Its high reactivity towards biogenic nucleophilic compounds has toxicity and carcinogenicity as a consequence. Acetaldehyde readily undergoes a condensation reaction and a consecutive ring formation with cysteine to form 2-Methylthiazolidine-4-carboxylic acid (MTCA). This reaction product is hydrolytically unstable and can be stabilized by N acetylation. Furthermore N acetylation allows reversed phase chromatography and ESI-MS/MS detection. The LLOQ of MTCA spiked into newborn calf serum was 0,5 mg L^{-1} after acetylation. The measurement of post mortem blood samples showed a very low basal level of our target analyte in alcohol negative patients and strongly enhanced blood levels in patients that were positive in blood alcohol testing. A clear dependency between blood alcohol and MTCA concentration was not determinable. Urinary concentrations of MTCA were much lower and below the LOD in some cases. In a pilot study, the time dependence of MTCA blood levels was analysed after a single per oral dose of 0.5g ethanol per kg bodyweight. The peak concentration of MTCA in blood was determined 250 minutes after the consumption of the alcoholic drink and was still detectable after 780 minutes (13h), in contrast to the corresponding alcohol, which reached a maximum concentration of 0.5 ‰ and levelled off after 7h.

Analytical & Bioanalytical Chemistry, submitted May 15th, 2012

Full length manuscript to be found in Appendix A

II.3. Stereochemical Aspects

In course of the condensation between cysteine and aldehydes an additional chiral centre on C-2 is formed. It has been shown in the literature that the formation of the resulting thiazolidine ring essentially occurs without any stereoinduction, yielding a mixture with 50:50 cis-to-trans ratio [10]. During our studies, this assumption was confirmed by 2-D NMR experiments. However, when formation of the condensation product was carried out followed by acetylation in aqueous environment, a high level of stereochemical induction was observed in subsequent RP-LC-MS measurements (Figure II.7). Employing 2D – NMR (HMBC) spectroscopy cis-stereochemistry could be assigned for the major diastereomer. (see Figure II.8). Interestingly, when MTCA was acetylated in non-aqueous conditions in pyridine, the transformation led to a trans-cis ratio of 55:45. This ratio was shifted even further in favour of the trans product upon performing the acetylation reaction under strictly anhydrous conditions, using freshly dried pyridine (63:37 trans:cis) (Figure II.7). The detailed mechanism for this stereochemical induction remains unclear. However, from the experimental observation it can be assumed that water plays a key role in the stereoselective acetylation process, stabilizing some type of pro-chiral transition state.

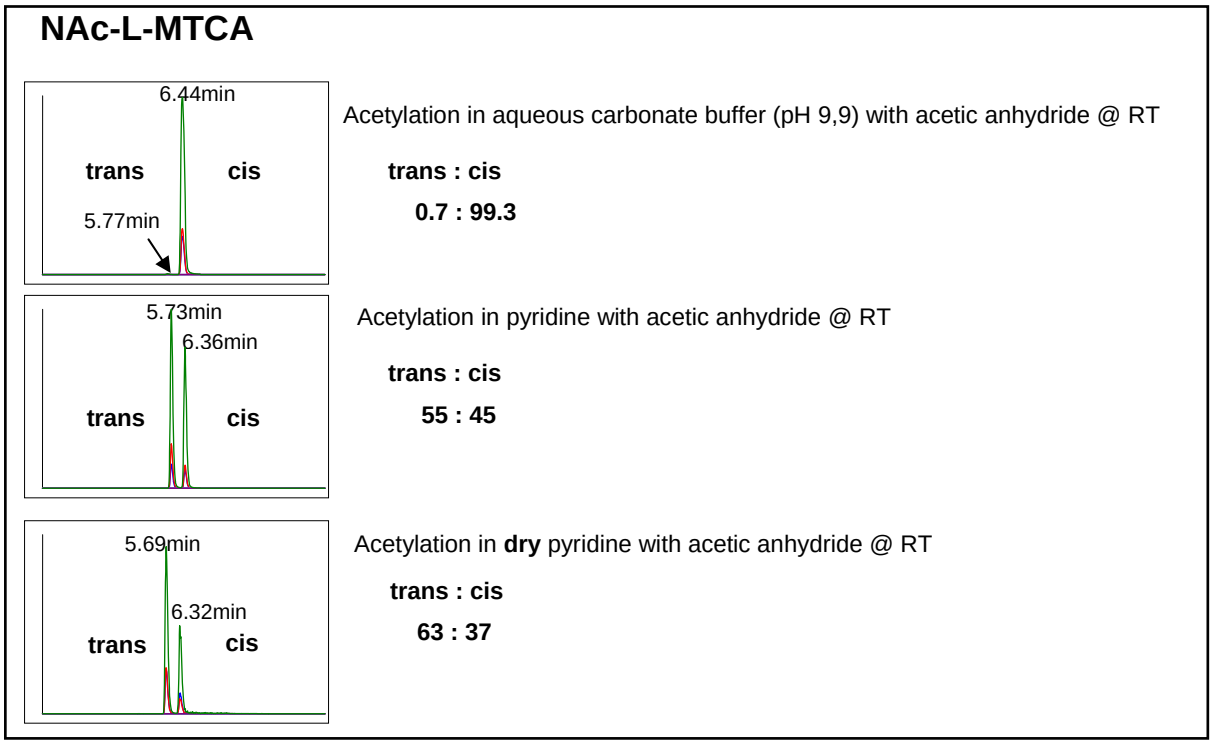

Figure II.7 Impact of the water content in the reaction medium on the relative stereoselectivity of NAc-MTCA formation.

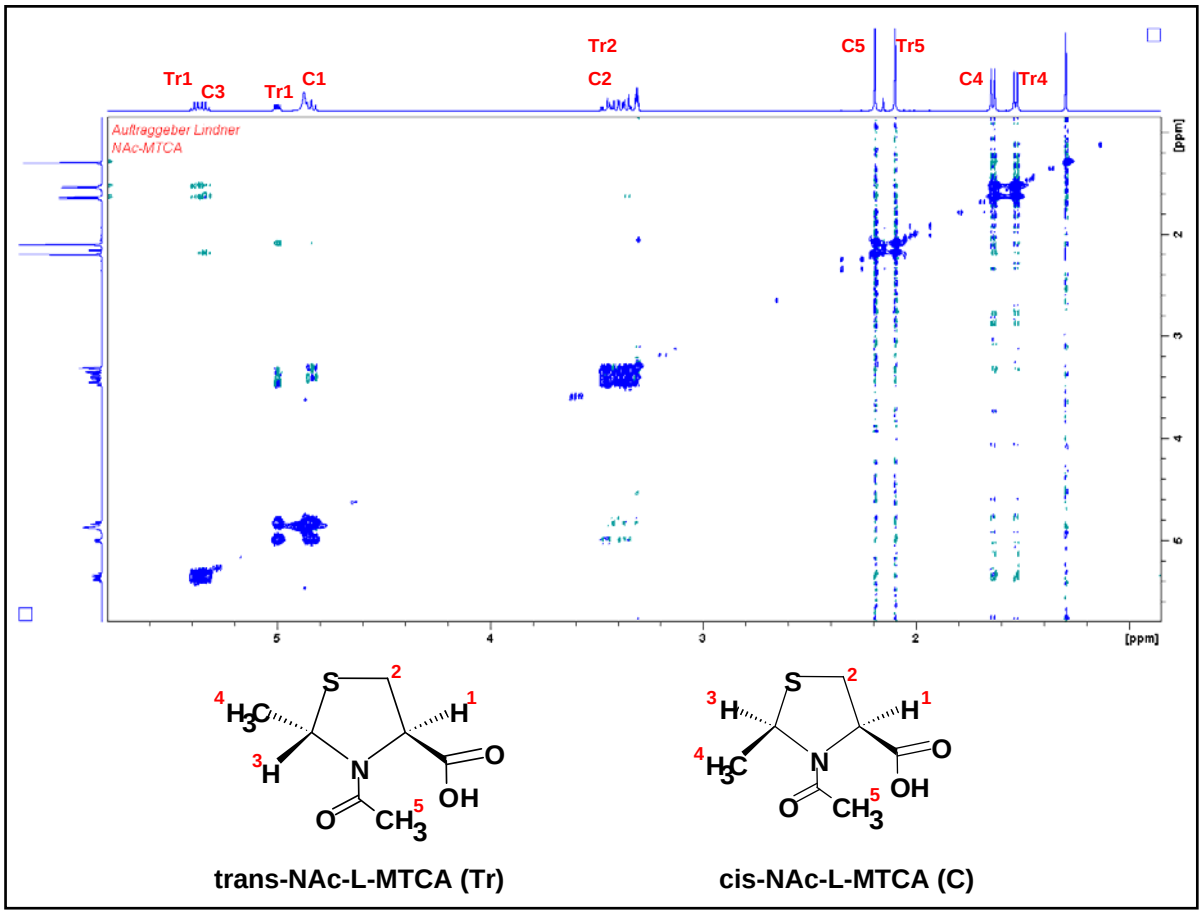

Figure II.8 2-D NMR (HMBC) of NAc-L-MTCA (synthesized from L-Cys) showing a strong direction towards cis – arrangement, sample acetylated under aqueous conditions

III. Cinchona Alkaloid Zwitter Ion Exchangers - ZWIX

Carbamate-type cinchona alkaloid based chiral stationary phases have been applied successfully to the enantioseparation of a broad variety of chiral acidic compounds [11,12]. However, these CSPs have limitations concerning the separation of zwitterionic species, such as free amino acids, which generally are not retained on these phases.. The introduction of acidic functionalities to the quinine and quinidine anion exchangers led to a new family of zwitterionic cinchona-sulfonic acid hybrid chiral selectors. To date, several articles have been published by our research group on the synthesis and the analytical evaluation of the resulting zwitterion exchanger chiral stationary phases ZWIX CSPs [13-15]. In the present study, the chromatographic performance characteristics of the in-house-made stationary phases Tau-QN and Tau-QD were evaluated. These CSPs were derived from quinidine and taurine, with the sulfonic acid being attached via a carbamate linkage at the C9-functionality. To evaluate the impact of the acidic functionality in Tau-QD-ZWIX, its performance was compared under identical chromatographic conditions with the commercial anion exchange QD-AX CSP (Figure III.1).

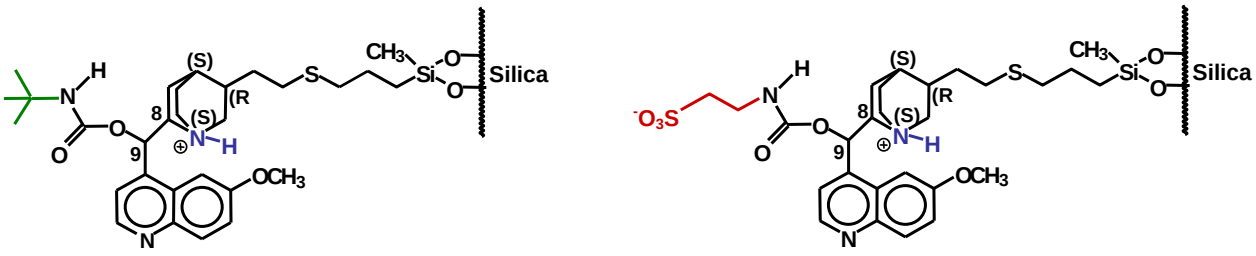

QN-AX
(8S,9R)-Quinine

Tau-QN-ZWIX
(8S,9R)-Quinine-Taurine

Figure III.1 Chromatographic selectors QD-AX and the zwitterionic Tau-QD

Implementing a strongly acidic functional group to a weak anion exchanger has major impact on the retention behaviour of the resulting selector. Evidently, the sulfonic acid functionality acts as an intramolecular counter ion (IMCI) and thereby retention is strongly reduced at comparable additive concentration in the mobile phase.

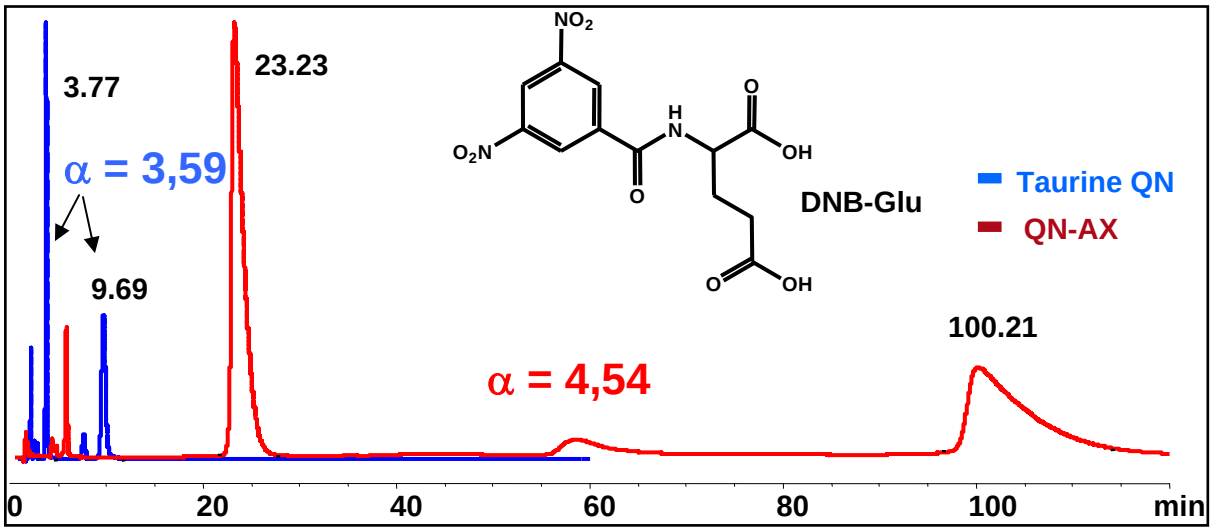

Figure III.2 Bis – acidic DNB-Glu and the strongly reduced retention on the Tau-QN-ZWIX-CSP compared to QN-AX **mob.Ph.:** MeOH 50mM AcOH 25mM NH3, 1mL min^{-1}, **stat.Ph.:** 150mm x 4mm**,** λ_{Det}**:** 254nm

From **Figure III.2** it can be seen that sufficient selectivity for baseline separation was maintained at much faster elution with the same rather low additive concentration in the mobile phase. The dinitrobenzoyl label significantly contributed to the chiral recognition of this analyte and allowed for UV detection at 254nm.

III.1. Enantioselective Exclusion Chromatography

Investigations on the mobile phase-related behaviour of ZWIX CSPs also aimed for the exploration of the pH effects on retention and enantioselectivity. Initially the void time (t_0) was determined to be1.45min by the injection of acetone as non retained marker, indicating that the compound does sample the entire pore space of the CSP. Under acidic mobile phase conditions, such as employed in Figure III.2, retention of the Tau-QN CSP was consistent with chiral recognition mechanisms involving retention of both enantiomers. Surprisingly, upon switching to basic mobile phase conditions, (base excess of the mobile phase additives) the retention characteristics for N-acylated amino acids changed radically. Specifically, certain amino acid derivatives eluted before the void volume, indicating a switch in the retention mode from attractive to repulsive interaction. Usually a complete loss of enantioselectivity was observed; however, in some cases the additive composition could be tuned to result in the exclusion of one enantiomer only, thus causing elution prior to the void volume, while the other isomer was retained. This rather unusual phenomenon

resulted in principally extreme values for the chromatographic selectivity. Figure III.4 shows the elution behaviour of racemic DNB-Leu under varying mobile phase conditions, and the radical shift to elution before t_0, occurring as a consequence of enantioselective analyte exclusion. This phenomenon was observed for several N-acylated amino acid racemates and was particularly pronounced for DNB – amino acids (Figure III.5). The phenomenon of this very early elution can be explained by the assumption that only one acid enantiomer can enter the chromatographic pore, undergoing interactions with the anion exchange site and thereby being retained. The other enantiomer is evidently capable to undergo less secondary attractive interactions and is subject to electrostatic repulsion of the sulfonic acid moiety (Figure III.3). Thereby it remains excluded from the pores of the chromatographic support and is forced to elute even before non retained compounds.

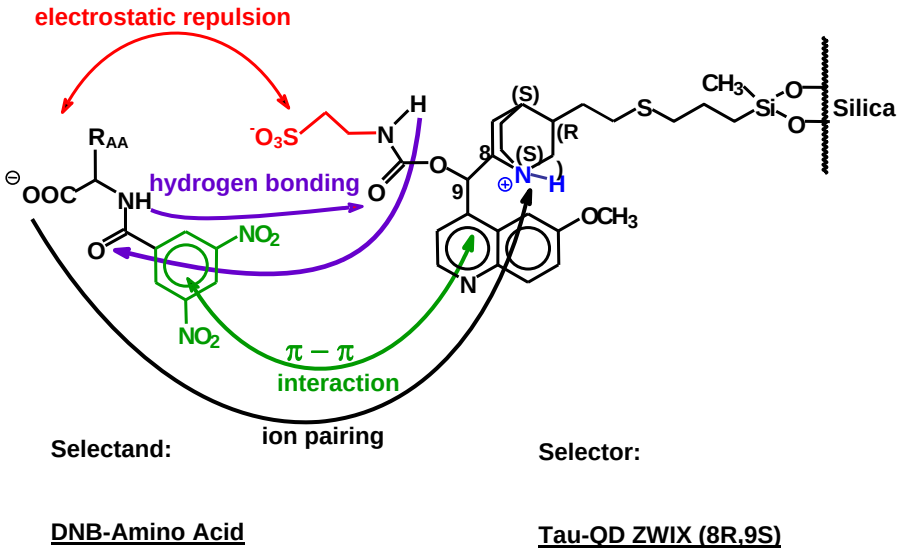

Figure III.3 Proposed selector-selectand interactions between ZWIX selectors and DNB–amino acids

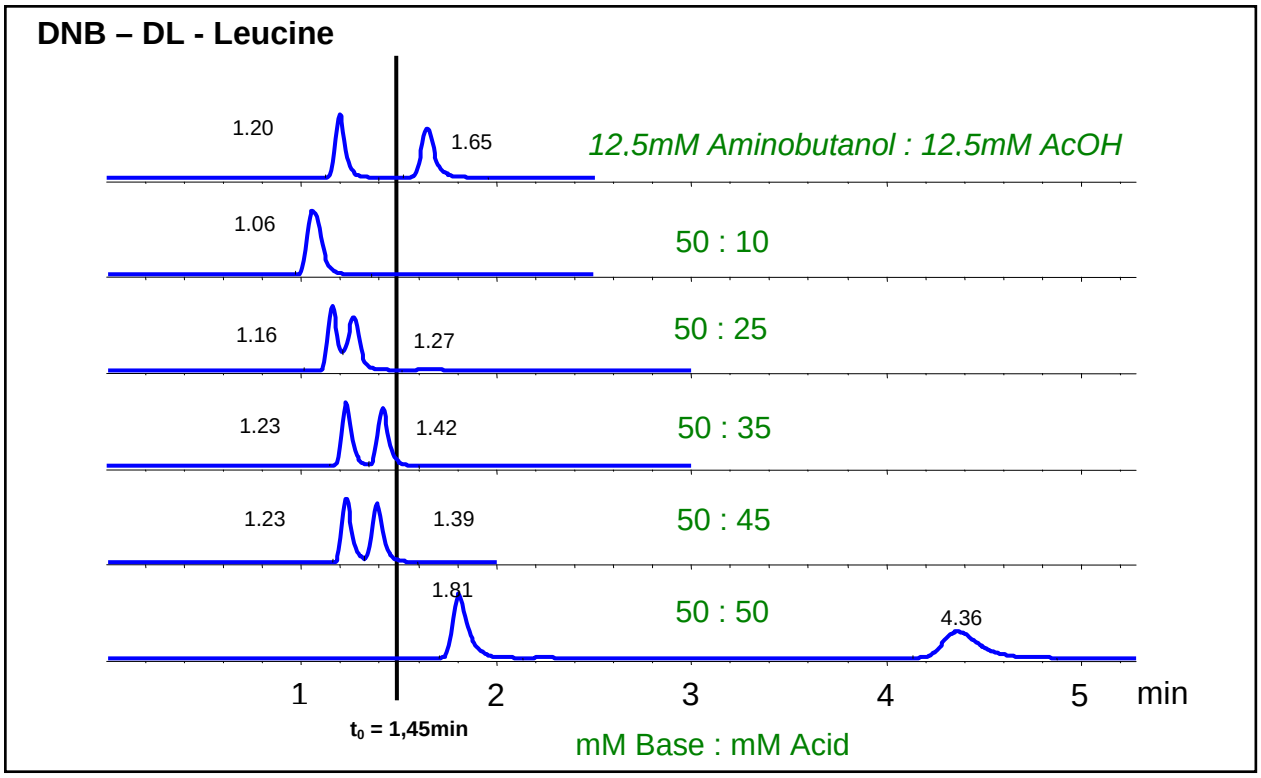

Figure III.4 Variation of the acid to base ratio in the methanolic mobile phase, the black line indicates the void time, **stat.Ph.:** Tau-QD, 150mm x 4mm i.d., 5µm d_p, 210µmol selector per gram silica, **flow:** 1mL min^{-1}, λ_{Det}**:** 280nm, **analyte;** DNB-DL-Leu in MeOH

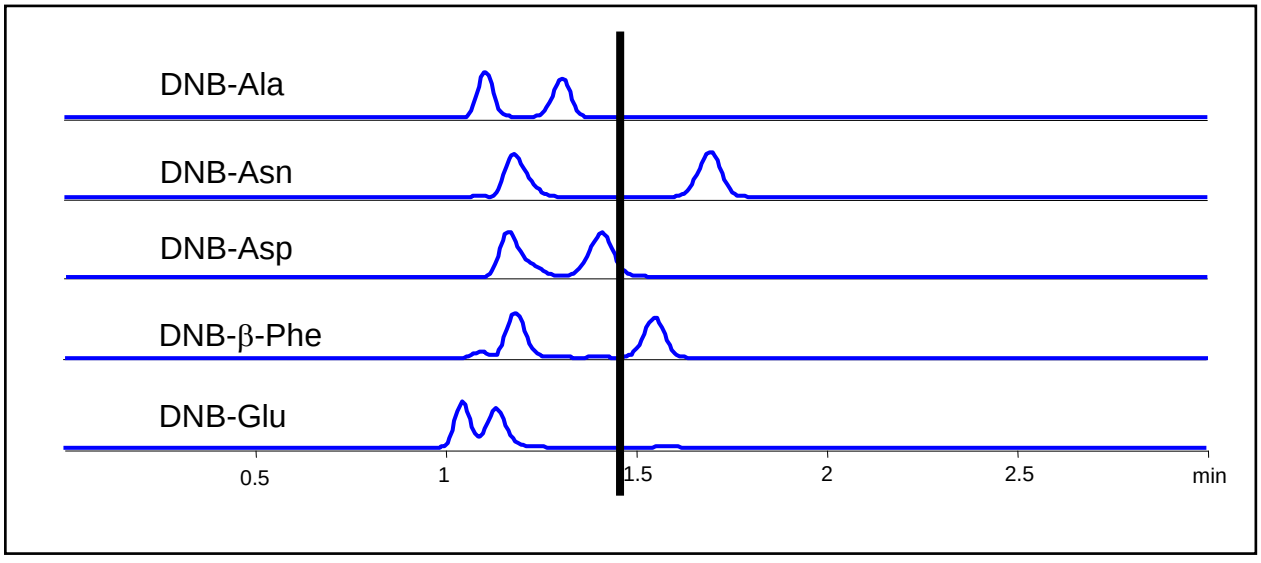

Figure III.5 Exclusion chromatography for DNB-amino acid racemates, the black line indicates the void time, **stat.Ph.:** Tau-QD, 150mm x 4mm i.d., 5µm d_p, 210µmol selector per gram silica, **flow:** 1mL min^{-1}, λ_{Det}**:** 280nm, , **mob.Ph.;** MeOH, 25mM 2-amino-1-butanol, 25mM NH_4Ac

III.2. ZWIX loadability

The loading capacity of a stationary phase for a given compound is a key parameter for any preparative application in terms of compound purification. Theoretically it is limited by several factors like stationary phase surface area, mobile phase composition, charge state of the analyte and solubility of the analyte. Ideally, in analytical chromatography, the linear range of the absorption isotherm will never be exceeded, resulting in constant retention times and Gaussian peak shapes. This is fulfilled in cases where the quantity of the available selector molecules present on the stationary phase surface are in large abundance as compared to the quantity of analyte molecules. In contrast, in preparative chiral chromatography, the loading of the column with selectand is high so that the analyte peaks become distorted, elute with a sharp front and a diffuse tail regions. This phenomenon is also referred to as “tailing”. However, to achieve economic productivity, in preparative chromatography analyte loading is generally increased until peak overlap is realized, even with peak shapes shifting into the no ideal regime.

Critical parameters of a preparative separation are cost, sample throughput and achievable peak purity. Furthermore it is mandatory that the mobile phase and the additives needed are volatile in order to facilitate the isolation of the purified compounds. In this context, ZWIX CSPs appear to be particularly well suited for preparative application due to short retention times and comparably low buffer concentrations required for analyte elution. As illustrated in Figure III.2 the elution of analytes is significantly accelerated through the sulfonic acid moiety of the selector. Consistent with the expectations, employing a mobile phase with an excess of basic additive enantioselective exclusion was observed.

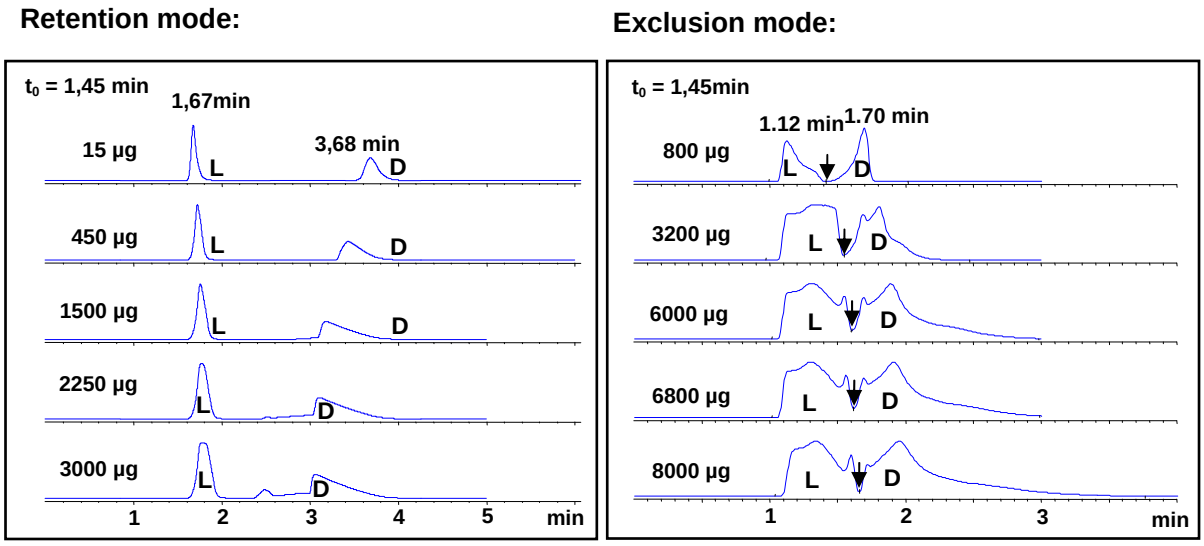

Figure III.6 Preparative separations of DNB-Leu on Tau-QD, 150mm x 4mm i.d., 5µm d_p, 210µmol selector per gram silica, sample injected in mobile phase, **flow:** 1mL min^{-1}, λ_{Det}**:** 360nm, **left:** separation in retention mode, **mob.Ph.;** MeOH 50mM AcOH, 25mM NH_4Ac, **right:** separation in exclusion mode, **mob.Ph.;** MeOH 50mM NH_4Ac, 25mM Aminobutanol, the arrow indicates the cut of the fractions

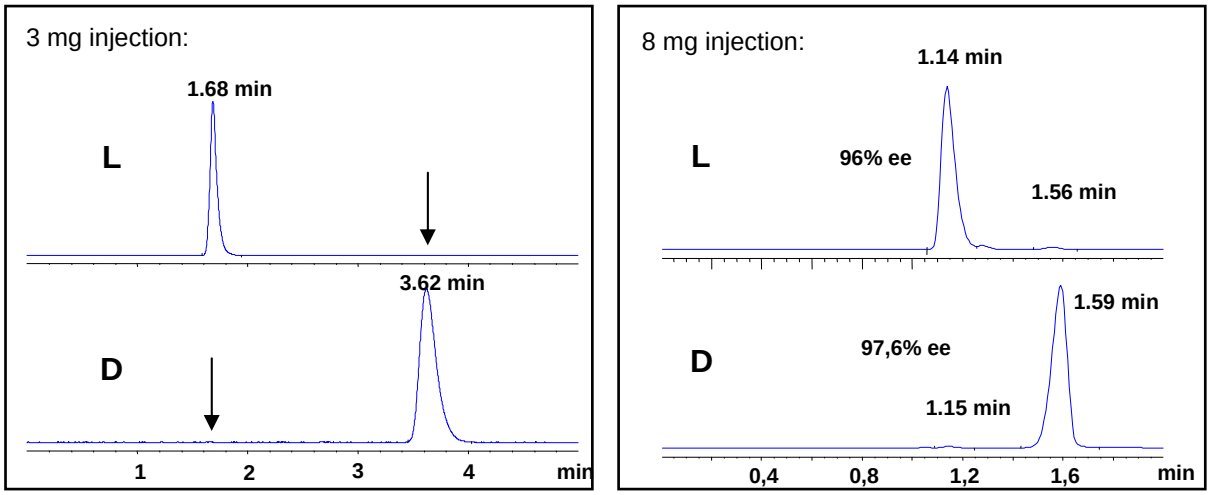

Figure III.7 Reinjection of the fractions cut in **Figure III.6** assessment of peak purity, **stat.Ph.:** Tau-QD, 150mm x 4mm i.d., 5µm d_p**,** 210µmol selector per gram silica, **mob.Ph.: retention mode:** MeOH, 50mM AcOH, 25mM NH_4Ac, **exclusion mode:** MeOH, 50mM NH_4Ac, 25mM Aminobutanol, **flow:** 1mL min^{-1}

In Figure III.6 a preparative loading study of the model analyte DNB-Leu is shown. “Retention mode” describes conventional chromatographic conditions with both analytes being retained, i.e. eluting after a non retained compound (in the present case acetone). For these loading experiments the analyte was dissolved in the mobile phases employed for elution. It is worth noting that for the retention mode experiments the solubility of the analyte in the mobile phase was 30mg mL^{-1}, which was clearly -below the maximum loadability of the stationary phase. For the exclusion mode, the solubility was substantially higher (80mg mL^{-1}) and analyte loading was increased until the maximum injection volume accessible with the employed instrumentation was reached (100µL). From the right chromatograms of Figure III.6 it can be seen that elution was very fast (3min) and that the analytes seem to replace each other from the stationary phase. Baseline separation was fully maintained even at the highest mass loading investigated. Enantiomer fractions were isolated at the time points indicated by the arrows in Figure III.6. Reinjection of the recovered enantiomers demonstrated that the fractions were enantiomerically pure (Figure III.7).

IV. Amino Acid Labelling

The analysis of amino acids remains a demanding field of analytical chemistry. In their native form, all amino acids exhibit zwitterionic behaviour. Furthermore, the side chains of amino acid cover a large range of chemical diversity, including aliphatic, aromatic, acidic and basic functionalities. Moreover, only a few amino acids carry efficient chromophores, and their ionization status varies with the pH of the mobile phase. For these reasons, chromatographic retention and detection of amino acids in generally require derivatization prior to analysis.

The assessment of the enantiomeric purity of chiral amino acid is a frequent requirement in asymmetric synthesis, food and pharmaceutical industry. In particular, the analysis of D-amino acids in biological samples is a rapidly emerging field due to their potential functions as diagnostic biomarkers [16]. Accumulating evidence of seminal studies provided that the presence of D-Ala, D-Asp and D-Ser in tissue samples is indeed related to specific biological functions, such as neurotransmission and endocrine regulation [17,18].

In the framework of this thesis, several strategies for enantioselective amino acid analysis will be investigated, and outlined in the following chapters.

IV.1. Succinimidyl Ferrocenyl Propionate (SFP)

Metalloferrocenes have been employed has tags for the analysis of biogenic amines with LC – ICP –MS [19,20]. The coordinated metal atom was targeted by element specific mass spectrometric detection. The derivatization strategy capitalizes on the introduction of an Fe(II)-ferrocenyl-propionate label via an acyl bond (see Figure IV.1). In this thesis, this strategy was applied to the labelling of chiral amino acids, to introduce chromatographic retention on chiral anion exchanger CSPs. Thereby the chemoselective and enantioselective separation on QD-AX was enabled, with the additional benefit that high detection sensitivity for ESI – MS/MS was obtained.

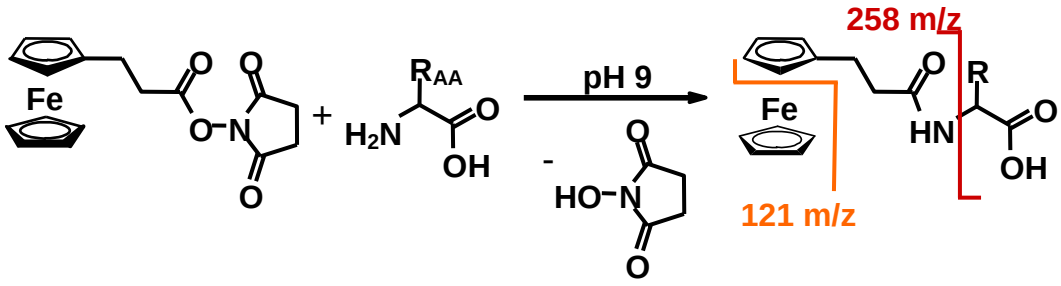

Figure IV.1 Derivatization procedure for amino acids with succinimidyl ferrocenyl propionate and characteristic MS fragments of the label

From Figure IV.2 it can be seen that with the developed analytical method the L–enantiomers of FP- derivatized amino acids generally elute before the corresponding FP-D-AAs on QD-AX. This effect can be readily rationalized by well-established chiral interaction models [11,12] with the FP tag making a significant enantioselective contribution to chromatographic retention.

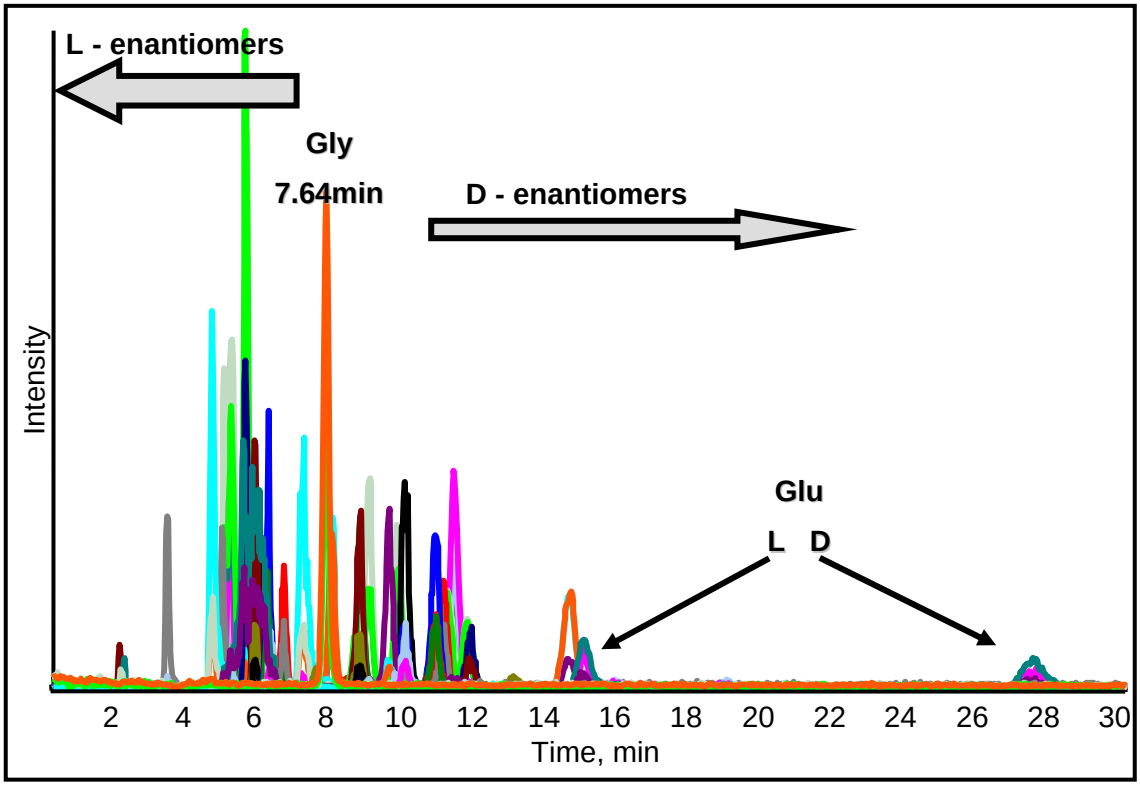

Figure IV.2 FP derivatized D- and L-amino acids generally separated in two elution ranges, Gly amidst. SRM run of 19 derivatized racemic amino acids, 50µmol L^{-1} individual amino acid concentration, **stat.Ph.:** HALO -QD-AX 50mm x 4mm i.d., **mob.Ph.:** 9/1 MeOH/H_2O, 100mM NH_4FA; 0,1% FA, flow 700µl min^{-1}

Chemoselective and enantioselective analysis of proteinogenic amino acids utilizing N – derivatization and 1-D enantioselective anionexchange chromatography in combination with LC MS/MS detection

Roland J. Reischl[a], Lucie Hartmanova[b], Marina Carrozzo[c], Monika Huszar[a], Peter Frühauf[a], Wolfgang Lindner[a,*]

Abstract:

D – amino acid analysis in biological samples still poses a challenge to analytical chemists. In higher developed species trace amounts of D – amino acids have to be detected in vast excesses of the corresponding L - enantiomers. This method utilizes an easy-to-carry-out derivatization step on the amino group with an iron ferrocenyl propionate hydroxy succinimide ester followed by one dimensional enantioselective anion exchange chromatography with cinchona alkaloid based chiral stationary phases (CSPs). MS detection is carried out in the highly sensitive SRM (selected reaction monitoring) mode, which allows a chemoselective differentiation of amino acid derivatives as well as their enantioselective separation in one step. Application of this method allows LOD (limits of detection) in the low µmol L^{-1} range and baseline enantioseparation for all proteinogenic amino acids except for Pro, Arg and His. The D – enantiomers of isomeric Leu and Ile were separated chromatographically and pose an example for the complementary selectivities of LC and MS. A successful application of this procedure to unprocessed human urine indicated the eligibility to analyse biological samples.

[a] Department of Analytical Chemistry, University of Vienna, Währingerstrasse 38, 1090 Vienna, Austria
[b] RCPTM, Department of Analytical Chemistry, Palacky University, 17, listopadu 12, 771 46 Olomouc, Czech Republic
[c] Dipartimento di Scienze Farmaceutiche, Università degli Studi di Modena e Reggio Emilia, Via Campi 183, 41125 Modena, Italy

Keywords: Enantioselective LC MS MS, Amino acid derivatization, Enantioselective amino acid analysis

Received 22 July 2011. Revised 15 September 2011. Accepted 16 September 2011. Available online 21 September 2011

Full length article to be found in Appendix B

IV.2. Methoxychinoline - MQ – labelling

Tagging amino acids has proven to be a powerful method to introduce chemoselectivity and enantioselectivity. Also, the generation of N-acyl derivatives was beneficial for the creation of directed intermolecular interactions such as hydrogen bonding and π–π stacking, further enhancing chiral recognition. The application of the methoxyquinolinoyl tag was an attempt to establish a derivatization reagent incorporating the combined benefits of increased enantioselectivity, pronounced fluorescence activity and improved MS/MS detectability.

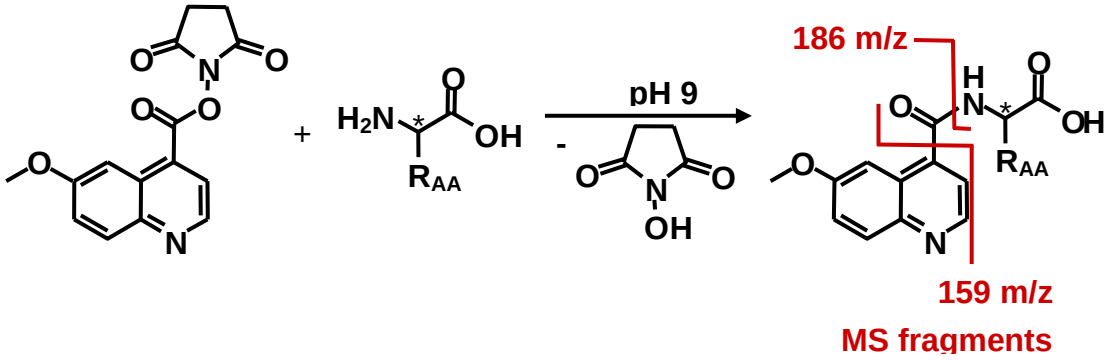

Figure IV.3 Tagging of amino acids with 6-methoxyquinoline-4-carboxylic acid succinimidyl ester

---

Methoxyquinoline labelling - a new strategy for the enantioseparation of all chiral proteinogenic amino acids in 1-dimensional liquid chromatography using fluorescence and tandem mass spectrometric detection

Reischl, Roland J.; Lindner, Wolfgang*

Abstract

The determination of trace amounts of D – amino acids (D-AAs) even in tissue samples of higher developed animals, mammals and humans has opened a wide field of biological questions to be investigated. D-Ala, D-Asp and D-Ser have already been identified to exhibit key functions in cellular regulation processes [21-24]. The abundance of trace amounts of these and also of other D-AAs in various biological fluids and in tissue samples is still being investigated. We herein present a facile derivatization method for amino acids with the 6-methoxyquinoline-4-carboxylic acid-succinimide ester (MQ-OSu) to yield the corresponding stable N-acyl-amino acids (MQ-AAs). Labelling with the MQ tag supports the enantioseparation of all 19 chiral proteinogenic amino acids on anion exchanger type chiral stationary phases, introduces fluorescence activity and particularly promotes sensitive electro spray tandem mass spectrometric detection. LOD values for MQ-L-Ala in water were 1.25µmol L^{-1} with fluorescence detection and 0.015µmol L^{-1} with MS in selected reaction monitoring (SRM) mode. The applicability of this method for the analysis of MQ-D-AAs in biological fluids has been demonstrated.

Journal of Chromatography A, submitted May 15th, 2012, manuscript number: JCA-12-1124

Full length manuscript to be found in Appendix C

V. Protein Crosslinking

The structure of proteins and protein complexes and the localization of protein – protein interaction sites are subject to ever increasing scientific interest. The discovery and elucidation of specific protein interactions is one of the key questions in molecular systems biology that can be favorably addressed by protein cross-linking experiments [25]. This strategy essentially involves the creation of covalent bonds between spatially close amino acid sequences of interacting proteins under physiological conditions, which implements that the chemistry of the cross link formation does not alter the structure of the proteins involved. In a second step proteolytic digest is carried out, resulting mainly in the generation of peptide sequences representing the involved proteins and in a minor fraction of crosslinked peptides. These crosslinks (Xlinks) can either be intra subunit crosslinks, involving spatially close peptides within the same protein; monolinks where only one side of the crosslinking reagent is bound to a peptide; or most desirably it can be inter subunit crosslinks, which actually link vicinal peptide sequences of different proteins. Sophisticated strategies have to be employed to enrich and identify the generated cross links and to maximize their number.

Conventional bottom-up proteomics workflows involve enzymatic protein digests, separation and analysis of peptides (or their amino acid sequences measured by LC-MS^n) followed by data processing in search engines such as MASCOT or Sequest to finally identify the processed protein through comparison with entries in databases such as Swissprot. This procedure is not feasible for cross linked peptides. So far such adducts can only be identified by tailor made software packages, such as XQuest. Crosslinking is a low resolution method for the structural determination of protein complexes, but it can deliver valuable information on the distance between cross linked peptides [26]. Generally, increasing numbers of cross links result in higher structural constraints and therefore narrow down the search space in database searches.

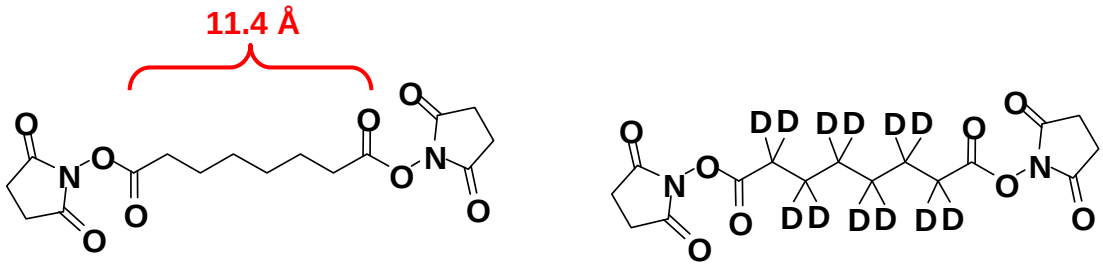

Disuccinimidyl suberate DSS **Heavy DSS, Δm = 12 Da**

Figure V.1 Crosslinking reagent disuccinimidyl suberate

In the framework of this thesis, lysine side chains in model proteins have been crosslinked using N-hydroxysuccinimide esters with defined spacer lengths (in the present case DSS – disuccinimidylsuberate 11,4Å) in 50/50 ratio of light to heavy isotope labeled cross linker. The use of the DSS cross linker led to a specific mass shift between light and heavy isotope chain of 12.075321 Da because of the fully deuterated alkylspacer (Figure V.1).

Thereafter, the cross linked proteins were digested enzymatically, followed by enrichment of thereby generated cross linked peptides via size exclusion chromatography and measurement with LC – MS/MS. High resolution MS^1 was carried out and at a certain signal intensity, unit resolution MS^2 scans were triggered. The choice of inclusion and exclusion criteria for the triggering of MS^2 scans was not trivial and had to be considered carefully during method setup. Maximum sensitivity and analytical performance could only be reached if these parameters were well chosen.

MS^2 spectra were later entered into XQuest search. Since cross linking involved two different proteins the search space expanded exponentially compared to single protein searches and the sequence queries were thus carried out on a multiprocessor cluster computer. The algorithms implemented in the xQuest software first searched for isotope pairs in MS^2 scans with the correct mass shift of 12 m/z and equal signal intensity for the case of the DSS cross linker. If these isotope pairs were found, peptide fragments were identified and database search was carried out. A graphical scheme of the data evaluation workflow is depicted in Figure V.2. The algorithms of xQuest assigned sub scores to the individual peptides and these were summed up to a scoring that enabled the set up of thresholds for cross – link identification. Furthermore xQuest differentiated between inter-protein-crosslinks, intra-protein-crosslinks, loop links (= intra peptide cross links) and

monolinks (= crosslinker only bound at one terminus the second succinimide ester simply hydrolyzed and not bound to an amine). The position of the identified crosslinks was significant for the assessment of structural information and was also part of the xQuest result sheet. Usually measurements were carried out at least in duplicate to enhance data reliability.

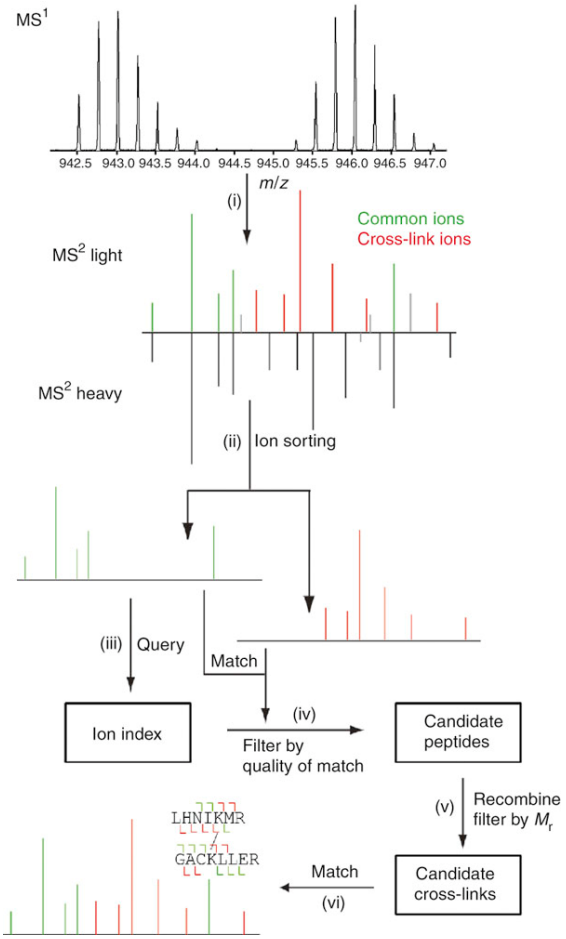

Figure V.2 MS/MS data processing workflow as applied in XQuest searches taken from [27]

When the cross linking workflow consisting of derivatization, digest, enrichment, measurement and data evaluation was completed, the number and position of peptides in amino acid sequences of the involved proteins was obtained. Such data were then further combined with complementary information from other structural protein analyses, such as computational protein simulations, cryo-electron microscopy, or NMR studies to finally yield three dimensional protein structures and structures of protein complexes. In this framework, protein cross linking contributed the irrevocable information of established covalent bonds between protein residues in close spatial proximity.

V.1. Optimization of Protein Crosslinking Protocols

Crosslinking methodolgies involve several sample treatment steps. From the analytical chemistry point of view some of these can be optimized in order to enhance the overall method performance. In the course of the present study the optimization of crosslink yield was carried out with respect to protein digest, increase of MS detection sensitivity through peptide derivatization, improvement of LC separation performance and enhancement of MS mass precision. In all cases, the results were evaluated according to MASCOT scores and numbers of identified sequences or crosslinks.

Crosslinking protein complexes in solution and under physiological conditions had the intrinsic limitation of very low yields. As a consequence the cross linked peptides always occured in highly complex matrices consisting of underivatized native peptides. Using the fact that the covalently linked peptides must have higher molecular weights than average unlinked peptides, size exclusion chromatography (SEC) proved to be a very powerful tool for the relative enrichment of crosslinked peptides compared to native ones.

V.2. Conclusion

Implementing the method optimizations outlined above, the effects of different peptide derivatization procedures on Xlink detection were systematically investigated. Amongst the investigated tagging procedures, only nicotinylation via nicotinic acid NHS resulted in higher Xlink yields but the effects of derivatization were generally not as high as expected. With guanidinylated or imidazolylated samples less sequences and lower sequence coverages were obtained as compared to with native tryptic digests. Therefore derivatization in the case of Xlinked proteins and peptides did not lead to significant improvements with respect to the numbers of detected cross links.

In dedicated enzyme studies the properties and the influence of 5 different enzyme digests (AspN, GluC, LysN, LysC, ArgC) on the cross link outcome were investigated. AspN and GluC showed, as expected, a quite high functional

complementarity to trypsin. Their cleavage sites were amino acids with acidic side chains and therefore the resulting crosslinked peptides were comparatively smaller than those resulting from the cleavage at lysine. Although the overall yield of crosslinked peptides was much lower than the number of cross links from tryptic digest, application of GluC and AspN resulted almost exclusively in previously unseen peptides, and even in new cross liked sites.

The effects of changes in the instrument setup considering chromatography mode, and the use of an internal standard to enhance mass accuracy were only limited and therefore both methods were not applied to further measurements.

Chromatographically, the application of fused core particles and its comparison to fully porous support material was somewhat blurred instabilities of the employed nano electrospray ionizazion, and no conclusive result could be obtained concerning potential advantages of the tested materials. However, it is worth noting that the fused core particles seemed to be more sensitive to higher peptide loadings and that their application to very complex peptide mixtures is therefore not to be recommended.

The complexity of cross linking for the elucidation of protein interactions poses a formidable challenge to analytical chemistry. Generally, comprehensive method optimizations are necessary to work with complex peptide mixtures, especially when separation power of chromatography is pushed towards its limits in cross linking experiments. Additionally there were highest demands to the sensitivity and qualitative information that can be delivered by mass spectrometry. These techniques therefore had to be refined and tuned to their optimal performance. Even after the data acquisition the pipeline was not complete and data evaluation could only be carried out with proper software solutions. Method development and the solution of problems in protein cross linking could only be achieved by a team incorporating competence in molecular biology, LC-MS/MS and bioinformatics.

Expanding the chemical cross-linking toolbox by the use of multiple proteases and enrichment by size exclusion chromatography

Alexander Leitner, Roland Reischl, Thomas Walzthoeni, Franz Herzog, Stefan Bohn, Friedrich Foerster, Ruedi Aebersold

Abstract

Chemical cross-linking in combination with mass spectrometric analysis offers the potential to obtain low-resolution structural information from proteins and protein complexes. Identification of peptides connected by a cross-link provides direct evidence for the physical interaction of amino acid side chains, information that can be used for computational modeling purposes. Despite impressive advances that were made in recent years, the number of experimentally observed cross-links still falls below the number of possible contacts of cross-linkable side chains within the span of the cross-linker. Here, we propose two complementary experimental strategies to expand cross-linking data sets. First, enrichment of cross-linked peptides by size exclusion chromatography selects cross-linked peptides based on their higher molecular mass, thereby depleting the majority of unmodified peptides present in proteolytic digests of cross-linked samples. Second, we demonstrate that the use of proteases in addition to trypsin, such as Asp-N, can additionally boost the number of observable cross-linking sites. The benefits of both SEC enrichment and multi-protease digests are demonstrated on a set of model proteins and the improved workflow is applied to the characterization of the 20S proteasome from rabbit and Schizosaccharomyces pombe.

Received September 8, 2011; Revised December 2, 2011; Published online 2012 January 27.
Mol Cell Proteomics. 2012 March; 11(3): M111.014126; doi: 10.1074/mcp.M111.014126

Full length article to be found in Appendix D

VI. Unpublished Results on Protein Crosslinking

VI.1. Enzyme Studies

In order to further improve the existing crosslinking protocols and to achieve higher sequence coverage for cross-linked proteins new proteases were studied. The application of enzymes with different cleavage sites has lead to a significantly enhanced number of identified peptides compared to the use of only one enzyme [28]. A stock solution of 6 known and preliminarily investigated standard proteins was put together and digested by 6 different proteases.

The proteases were: Trypsin, ArgC, LysC, LysN, AspN, GluC

The analyte proteins: BSA, transferrine (human), ovotransferrin, pyruvate kinase, creatine kinase

Procedure:

Before proteins were further treated the sulfide groups were reduced by dissolving the proteins under highly chaotropic conditions in 8M urea, adding of 5µL 50mM TCEP and shaking for 30min at room temperature. Thereafter, the sulfide groups were alkylated by adding 5µL of 100mM iodoacetamide, mixing and leaving for reaction in the darkness at room temperature. The conditions for the enzymatic digests were chosen according to supplier information. Generally reaction solutions were chaotropic between 1M and 6M urea. Different buffers and pH values as well as digest temperatures had to be chosen. After overnight digest, the digests were stopped by adjusting a concentration of 2% formic acid and peptides were enriched and desalted by C_{18} solid phase extraction (SPE). Analytes were eluted in 50% acetonitrile with 0,1% formic acid. Thereafter evaporation of the solvents was carried out by centrifugation under reduced pressure on a speedvac. Analytes were resuspended in 3% ACN in water with 0,1% FA (=chromatographic starting conditions).

Analysis of the protein digests was carried out by the injection of approximately 1µg absolute amount to a reversed phase capillary column (10,5cm length, 75µm i.d., 3µm particles), flow rate was 300 nL min^{-1} and elution was carried out by using the following gradient: 0-5 min = 5 %B, 5-95 min = 5-35 %B, 95-97 min = 35-95 %B and 97-107 min = 95 %B, where B = (acetonitrile/water/formic acid, 97:3:0.1). MS

detector was a Thermo FT ion cyclotron resonance MS. MS^1 was measured with high resolution (ICR), MS^2 spectra were recorded in the linear ion trap.

After LC-MS analysis the recorded data were converted into mzXML files, then further transformed to .mgf format and submitted to a MASCOT server. Database search was carried out with following parameters:

- Taxonomy: chordata
- Modifications: permanent: carbamidomethylation (C), variable: oxidation (M)
- Missed cleavages: 2
- Instrument type: ESI-Trap
- MS^1: mass error: 15ppm
- MS^2: mass error 0,6 Da
- Decoy mode: on
- Ion score cut-off: 20
- Require bold red checked

The data were filtered and peptides were evaluated in terms of score, number of identified sequences per protein, sequence coverage and specificity for the applied enzyme. The reference was posed by trypsin, which is the standard enzyme used for lysine (K) crosslinked proteins.

Table VI.1 Results from the database search performed for different enzyme digests, specificity gives the fraction of peptides that end with the terminal amino acid defined by the respective enzyme

SUMMARY	MEAN SCORE	Sum of Sequences	Sequence coverage (%)	Specificity
Trypsin	1773	216	60,5	
LysC	794	125	38,7	
LysC + Arg cleavage	672	133	40,8	0,882
LysN	1309	191	53,7	
LysN + Arg cleavage	1093	183	47,5	
ArgC	763	96	35,2	
ArgC + Lys cleavage	1655	274	72,0	0,239
GluC	609	144	43,5	
GluC (Glu+Asp)	453	148	42,5	0,675
AspN	1162	161	55,0	
AspN (Asp+Glu)	921	190	59,7	0,728

The results of Table VI.1 led to the decision to carry out further experiments with all

enzymes except for ArgC which had practically identical specificity as trypsin but was much more expensive.

VI.2. Peptide Derivatization

The altering of side chain basicity in peptides generally leads to a change in ionization behavior, furthermore also the fragmentation patterns change through alteration of the proton mobility at the side chain [29]. In the presented experiments we labeled the basic amino acids lysine (K) and arginine (R) at their side chains. The derivatizations to be carried out were guanidinylation (K), nicotinylation (K), imidazolylation (R side chain and N-terminus) and pyrimidinylation (R/W) (see Figure VI.1). All proteins were digested with trypsin and the results were compared to those achieved by native protein digests with respect to MASCOT scoring, sequence number and sequence coverage.

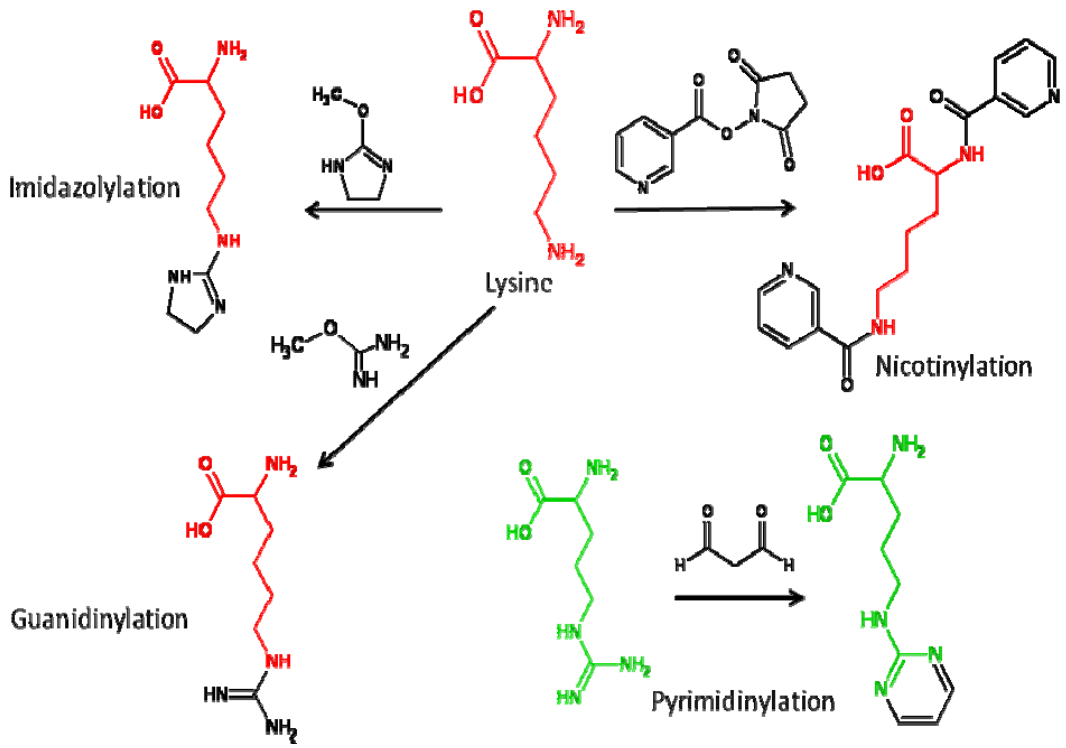

Figure VI.1 Different derivatization strategies carried for lysine

Derivatization procedures :

Guanidinylation:

20µg of tryptic peptides were dissolved in 10µL Na_2CO_3 buffer (1M, native pH), 6µL of O-Methyl - isourea (5M) were added to the solution followed by shaking at 65°C for 30 minutes. Reaction was stopped by adding of 14µL formic acid. Isolation of the derivatized peptides was carried out by C_{18} – SPE. The eluent was evaporated and the peptides were resuspended in 5% ACN with 0,1% FA.

Imidazolylation:

20µg of tryptic peptides in 10µL Na_2CO_3 buffer (1M, native pH), 20µL of 2-methoxy-4,5-dihydroimidazole (2M) were added and the solution was shaken for 3h at 55°C. The reaction was stopped by adding of 5µL 50% HCOOH followed by isolation of the derivatized peptides by C_{18} SPE.

Nicotinylation:

20µg of tryptic peptides were suspended in 5µL of 50% ACN, 25µL Nicotinic Acid N-hydroxy succinimideester (33mg mL^{-1} = 0,15M in DMSO) were added immediately and 3 further portions of 10µL were pipetted to the reaction solution in 15min intervals. After the last portion had been added shaking was carried out at room temperature for 2h. Thereafter formic acid was added to a final concentration of 2% (v/v). Isolation of the derivatized peptides was carried out by C_{18} – SPE. The eluent was evaporated and the peptides were resuspended in 5% ACN with 0,1% FA.

Pyrimidinylation:

This reaction was carried out according to [30]. 20µg of tryptic peptides were dissolved in 50µL 37% HCl and 1,5µL tetrapropoxypropane were added to set free the reagent malondialdehyde. The mixture was shaken for 60min at RT. Thereafter the reaction solution was diluted 1 : 100 and SPE was carried out to isolate the derivatized peptides.

Table VI.2 Starting conditions, scores and coverage given for native underivatized tryptic peptides

Tryptic Digest	Score	Matches	Sequences	sequ. Coverage (%)
BSA	2372	162	44	73
Transferrin	2194	116	46	59
Catalase	1370	96	26	56
Ovotransferrin	1533	94	39	57
Pyruvate Kinase	2054	123	38	69
Creatine Kinase	2054	73	23	49

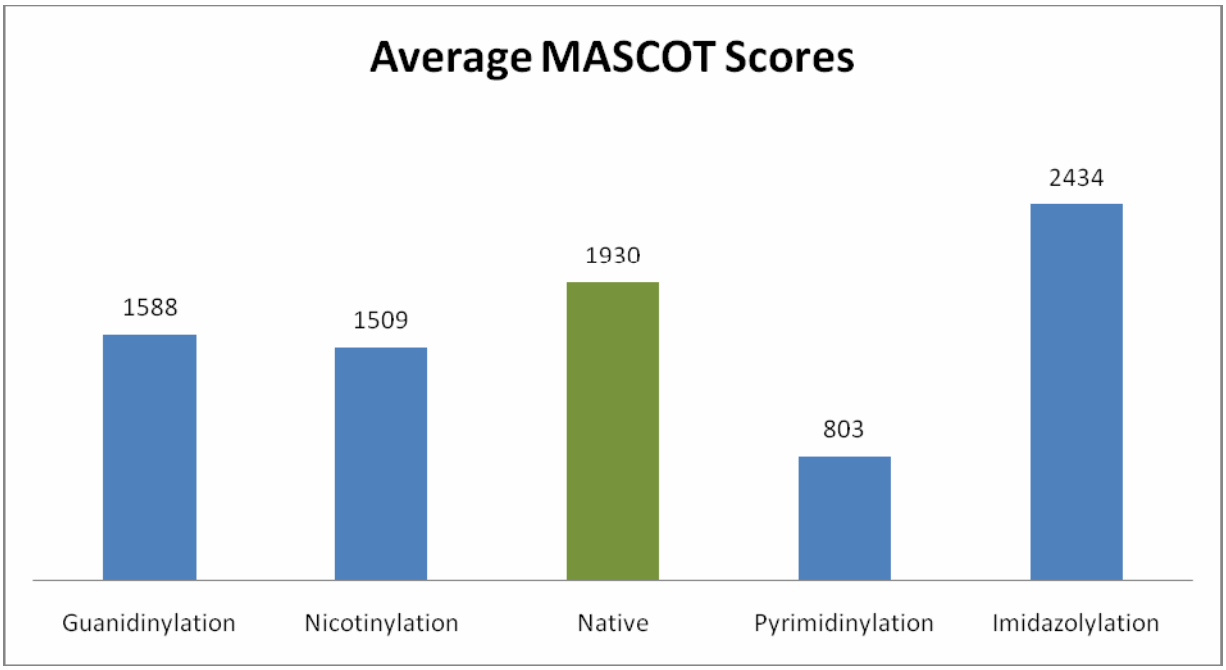

Figure VI.2 Average mascot scores for N – derivatized peptides

Average scores over all derivatized peptides gave a useful measure for the applicability of these derivatizations to analytical proteomic methods (Figure VI.2). In order to apply peptide derivatizations to cross linking protocols, all possible derivatization sites had to be fully derivatized. Otherwise search space in xQuest searches would have increased drastically – as calculation time would have - and thereby analytical reliability would have suffered from severe drawbacks. Therefore the applied reactions were also evaluated with respect to the overall yield of derivatized groups (Figure VI.3).

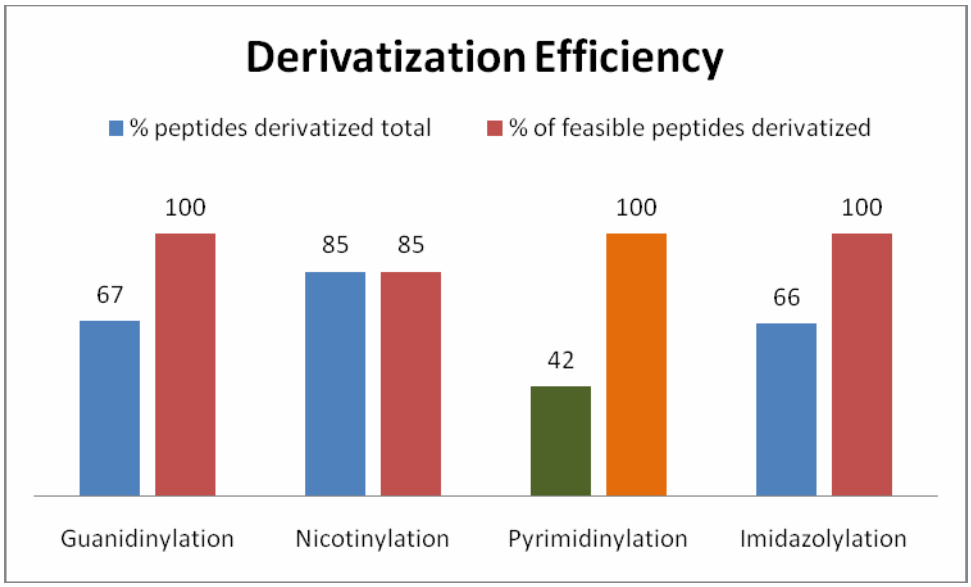

Figure VI.3 Degree of derivatization achieved with different agents

Considering those results the reaction procedures were slightly changed and the effect of those changes was evaluated. The pyrimidinylation reaction also led to chemical side reactions that had to be considered in further method development namely methyl ester formation and derivatizations of tryptophane (W). This was indicated by the evaluation of W containing peptides in the native tryptic digests compared to the derivatized ones. Also esterification was evaluated by modifying the MASCOT search parameters towards methyl esters (N-terminal and on D and E side chains).

Final protocols:

Nicotinylation:

20µg of tryptic peptides were suspended in 5µL of 50% ACN, 25µL Nicotinic Acid NHS (33mg mL^{-1} = 0,15M in DMSO) were added immediately and shaking was carried out at 37°C. Thereafter one further portion of 10µL nicotinic acid NHS was added. After a further 15min of shaking the next 10µL of reagent was added and temperature was increased to 55°C, one further portion of 10µL was added and the reaction continued for 2h to completion. The total reaction time of 2h 45min did not change compared to the initial conditions. Finally formic acid was added to an end concentration of 2% (v/v). Isolation of the derivatized peptides was carried out by C_{18} – SPE. The eluent was evaporated and the peptides were resuspended in 5% ACN

with 0,1% FA. Heating above 55°C could result in increased oxidation of the peptides and therefore was not carried out.

Pyrimidinylation:

This reaction was carried out according to [30]. 20µg of tryptic peptides were dissolved in 50µL 37% HCl and 1,5µL tetrapropoxypropane were added to set free the reagent malondialdehyde. The mixture was shaken for 60min at RT. Thereafter the reaction solution was diluted 1 : 100 and SPE was carried out to isolate the derivatized peptides. In a second reaction step the extracted and dried peptides were redissolved in 100µL of a 50mM pyrrolidine solution and shaken for 2h at room temperature. Thereafter SPE was carried out again.

Imidazolylation:

Since imidazol derivatizations also led to unsatisfying results the reagent was added in two portions the total amount was kept constant.

Results

By applying optimized derivatization protocols the yield of derivatized functional groups was significantly improved (Figure VI.4). When evaluation of the peptide lists was carried out the numbers of derivatized peptides and peptides that could have been derivatized were compared (Figure VI.5). Essentially 100% derivatization yield was achieved for all derivatizations. Nicotinylation has to be mentioned as the one procedure that enabled derivatization of all generated peptides. MASCOT scores were tripled by nicotinylation.

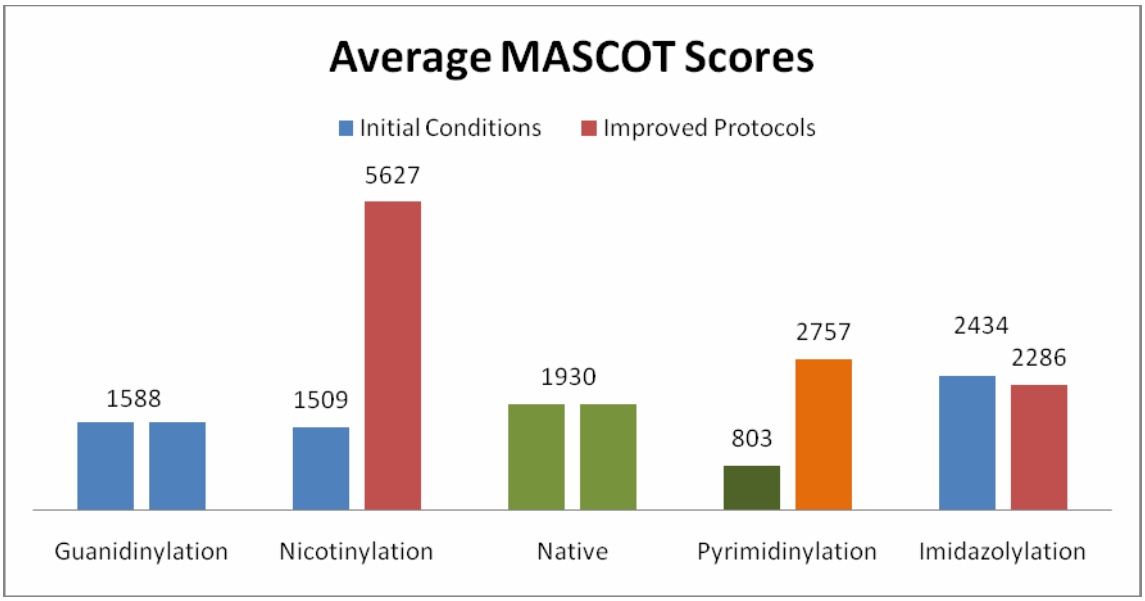

Figure VI.4 Increased MASCOT scores achieved by improvements in the derivatization protocols

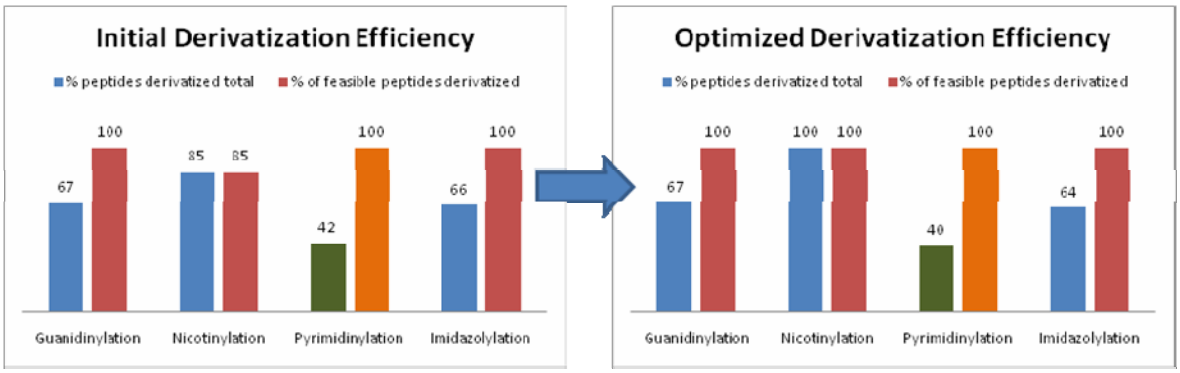

Figure VI.5 Percentages of derivatized peptides nad derivatizable peptides before and after protocol optimization

VI.3. Enzymatic digest of cross linked peptides

As a proof of principle, the results of the enzyme studies led to the conclusion that all new applied enzymes could deliver valuable results except for ArgC that showed cleavage practically indentical with trypsin. Therefore proteins were cross linked and mixed together to yield an 8 protein mix of:

BSA, transferrine (human), ovotransferrine, pyruvate kinase, creatine kinase, lactoferrine, aldolase

The proteins have been cross linked separately, which had the advantage that false positive results could be excluded in xQuest searches i.e. only crosslinks between identical proteins were feasible. This 8 mix had been reduced, alkylated and then digested with the respective enzyme.

VI.4. Fractionation of cross-linked peptides by size exclusion chromatography

Purified samples were reconstituted in 20 µL of SEC mobile phase (water/acetonitrile/TFA, 70:30:0.1). 15 µL were injected on a GE Healthcare Ettan micro system consisting of autosampler, binary pump, UV/pH/conductivity detectors and fraction collector. Peptides were separated on a Superdex Peptide PC 3.2/30 column (300 x 3.2 mm) at a flow rate of 50 µL min^{-1} using the SEC mobile phase. The separation was monitored by UV absorption at 215, 254 and 280 nm. 2 min fractions (100 uL) were collected into 96-well plates over a separation window of 1 column volume (2.4 ml = 48 min). For analysis by LC-MS/MS, fractions of interest were removed and evaporated to dryness.

From the optical absorption (@ λ=280nm) we calculated the dilution with mobile phase A (water/acetonitrile/formic acid, 97:3:0.1) that we had to apply in order to get similar absolute peptide concentration in every fraction. We injected 2µL of every fraction to an LC-MS platform consisting of an Eksigent 1D-NanoLC-Ultra system coupled with a Thermo LTQ Orbitrap XL mass spectrometer with a standard nanoelectrospray source.

Ion source and transmission settings of the mass spectrometer were: Spray voltage = 2 kV, capillary temperature = 200 °C, capillary voltage = 60 V, tube lens voltage = 135 V. The mass spectrometer was operated in data-dependent mode, selecting up to five precursors from a MS1 scan (resolution = 60 000) in the range of m/z 350-1600 for collision-induced dissociation (CID). Singly and doubly charged ions and precursors of unknown charge states were rejected. CID was performed for 30 ms using 35% normalized collision energy and an activation q of 0.25. Dynamic exclusion was activated with a repeat count of 1, exclusion duration of 30 s, list size of 300 and a mass window of ±50 ppm. Ion target values were 1 000 000 (or maximum 500 ms fill time) for full scans and 10 000 (or maximum 200 ms fill time) for MS/MS scans.

After conversion of the .raw files to mzXML, database search was performed with xQuest. For MASCOT search the mzXML files were further converted into the MASCOT generic file, .mgf format. The results of MASCOT searches were compared to those acquired with xQuest. Thereby the distribution between cross

linked peptides and not cross linked ones was estimated in every fraction, which was a measure for cross link enrichment. In order to enable searches with different enzymes the xQuest software had to be adapted to alternative cleavage sites.

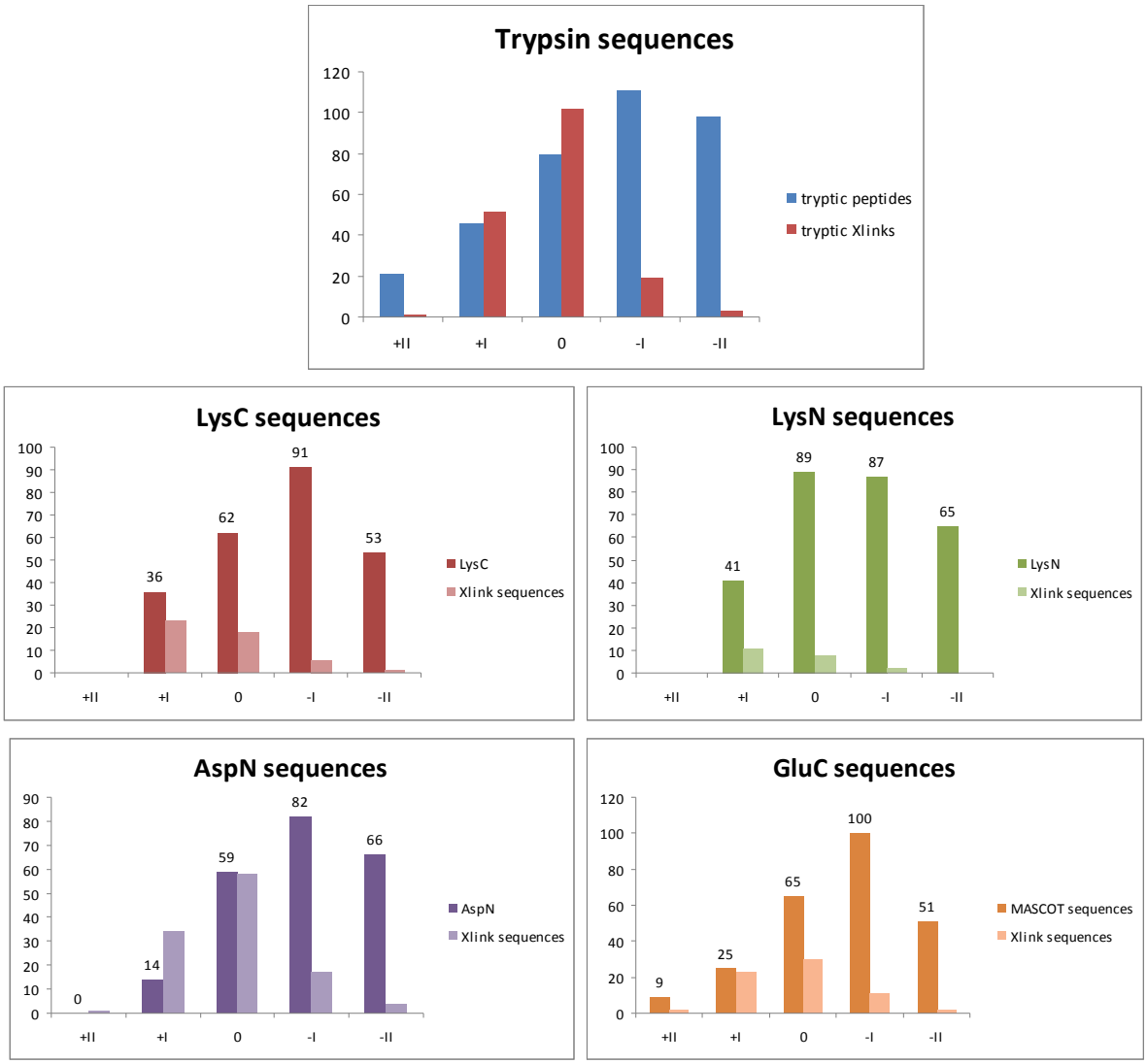

Figure VI.6 SEC fractionation and the number of identified peptide sequences for each applied protease

It has to be mentioned that no database search was performed for the +III fractions that only had very low numbers of MS^2 scans and therefore could not possibly give any good results. Very high molecular masses often suffered from discrimination in MS detection due to bad chromatographic behaviour (broad peaks through poor mass transport properties), low ionization efficiency, bad fragmentation through internal quenching of the fragmentation energy in collision induced decay, CID.

The high molecular weight +II fractions of LysC and LysN delivered very big raw data files of more than 2GB and therefore could not be opened by Excalibur^{TN} instrument software. Later we cut down recording times of the LC-MS/MS measurements and decreased file sizes. Subsequent analysis of the runs showed a very high background that triggered MS^2 scans throughout the whole run but did not deliver any evaluable peptide peaks. As trypsin also LysN and LysC suffered from the fact that cleavage did not take place at cross linked lysines and thereby resulted in high molecular mass fragments with all the detection disadvantages mentioned above. This might explain the comparably low numbers of cross linked peptides compared to non cross linked ones.

AspN and GluC showed maximum numbers of cross linked peptides shifted to the medium molecular weight 0 fraction. Another important aspect was that naturally there was an overlap between the size exclusion fractions and many peptides were found in at least two fractions. For our evaluations considering the total numbers of cross links for every enzyme we only considered non redundant cross linked peptides.

The most important results from xQuest database searches in terms of protease complementarity were indeed the positions of the cross linked lysines. Inherently the peptides yielded have to be different because every enzyme cleaves the (cross linked) proteins at different sites. But xQuest also assigns a number to every amino acid within the primary structure of the protein. We chose a cut off value for the distance between two cross linked lysines that had to be bigger than 20 amino acids in order to yield a structurally relevant cross link site. These cleavage sites have been compared for each separate protein and throughout all enzymes with trypsin being the reference in all cases. In that aspect AspN showed the highest complementarity by yielding a total number of 52 non redundant and 5 redundant cross link sites in all of the eight proteins in the sample mixture giving a gain of 40% in cross link sites compared to the sole application of trypsin as a protease.

VI.5. Cross link derivatization

After the protein 8 – mix had been digested first by LysC, then by trypsin which is the standard procedure, we desalted and derivatized the resulting peptides with the three selected most successful protocols. Namely: Guanidinylation, pyrimidinylation and nicotinylation. The derivatization was carried out prior to SEC and afterwards in the two fractions of interest. These results were compared to get a measure of which step to carry out first. Unfortunately only the guanidinylation and pyrimidinylation could be implemented to xQuest software because the present algorithm does not allow searches for N terminal modification as would be the case for nicotinylation, which was the most successful protocol in preliminary studies. The samples again were measured on the FT-ICR-MS instrument.

MASCOT Results

As in the enzyme studies also here MASCOT searches were performed to be able to compare to the xQuest data. It can be seen that there is a smaller number of detected sequences in all cases compared to native peptides. Considering these data it is also obvious that nicotinylation with the optimized protocols yields derivatized peptides exclusively.

Table VI.3 Numbers of peptide sequences determined in the SEC fractions 0 and 1. Dependence of the peptide identifications on derivatization before or after fractionation.

		unique matches	unique sequences	derivatized peptides
Guanidinylation:	fraction 0	81	21	15
before SEC	fraction 1	24	9	8
	fraction 0	100	25	19
after SEC	fraction 1	28	14	10
Nicotinylation:	fraction 0	94	33	33
before SEC	fraction 1	39	15	15
	fraction 0	111	24	24
after SEC	fraction 1	40	17	17
Pyrimidinylation	fraction 0	44	18	18
before SEC	fraction 1	26	16	15
	fraction 0	51	17	10
after SEC	fraction 1	17	9	5
Negative underivatized control	fraction 0	138	48	0
sample after SEC	fraction 1	45	22	0

xQuest Results

Cross link search has been performed with xQuest software and yielded only limited numbers of new cross linked peptides that had not been detected in the analysis of the untreated, native cross linked peptides. These gains are not representative since they could also stem from missed MS^2 scans in the FT-ICR-MS. Measurements in technical replicate could also result in higher numbers of non redundant cross linked peptides.

Table VI.4 Numbers of derivatized cross linked peptides compared to underivatized cross linked peptides

	Guanidinylation		Pyrimidinylation		Untreated	
sample	**Xlinks**	**mono links**	**Xlinks**	**mono links**	**Xlinks**	**mono links**
pre 0	11	11	0	5	29	13
pre +1	8	1	0	4	12	3
sum	19	12	0	9	41	16
without fraction overlap	15		0		34	
derivat K's	22				40	
new Xlinks	**2**					

post 0	8	10	7	6
post +1	2	4	0	5
sum	10	14	7	11
without fraction overlap	10		7	
derivat K's	14		9	
new Xlinks	**2**		**2**	

VI.6. LC-MS method optimization

In single analyses several changes in MS measurement method were to be investigated and their influence on sensitivity and analysis performance was evaluated.

Chromatography Mode

A very important parameter in information dependent analyses (IDA) is the choice of inclusion and exclusion lists for the triggering of MS^2 scans. If a peak appears in MS^1 spectra the method setup usually triggers fragmentation and an MS^2 scan as

soon as the signal for the respective peak lies above a certain threshold. After a certain number of MS^2 scans / a certain time period the m/z peak is put into the exclusion list in order not to interfere with the detection of other simultaneously eluting peaks. If the time of MS^2 triggering is not well chosen the risk is high to loose a lot of sensitivity or simply not detect many peptides.

The Excalibur™ software offers a so called “Chromatography mode“ where MS^1 masses are monitored in the course of time and MS^2 scans are triggered around the chromatographic peak apex in order to fragment every analyte in the moment of its maximum concentration during elution. One of the drawbacks of this method could come from the high CPU resources it takes to monitor these masses. In our experiments we injected the standard analyte for system performance, namely yeast lysate tryptic digest (1µg injected on column) and the number of identified peptides was very close to the peptide numbers acquired with the standard method. Therefore no further development was carried out with respect to chromatography dependent MS^2 triggering.

Lock Mass Experiments

The key strength of Orbitrap™ MS is its very high mass resolution together with reasonable mass accuracy at relatively short cycle times. These parameters enable cross link searches in the first place because they allow constraints to the huge search space in the case of two proteins involved in one crosslink. The higher these constraints are the faster the database searches could be carried out and the bigger could be the differences in scoring for similar cross linked peptides. In brief: the higher is the overall analytical performance. There are several options how to carry out online mass calibration during LC-MS measurements to enhance the mass precision. The Excalibur™ software offers the possibility to check an “L” button in the method set up. Thereby a lock mass is chosen that is permanently in the chemical noise of Orbitrap™ measurements (this background ion can be detected also with other sensitive ESI-MS). The molecular ion is Polydimethylcyclohexasiloxane (m/z = 445,120025) and it stems from the vapor of the fore vacuum pump oil that is always found in MS labs. It reaches the ESI interface and is constantly ionized. This mass peak is therefore assigned in every single spectrum to its fixed mass. Thereby mass

errors for other peaks should be minimized significantly. Throughout our studies typical mass errors with our weekly calibrated instrument lay in the range of 1-3ppm and in rare cases above 5ppm. Lock mass analysis was performed again with yeast lysate and subsequent MASCOT search was carried out. The mass errors were not significantly improved by the activation of the lock mass mode and on the other hand the electronic demands for this calibration are very high, therefore lock mass was not used in further experiments.

VI.7. Fused core particles in nanoLC-MS

The separation of cell lysate digests with hundreds of peptides that have to be separated in a single RP-LC run with a very shallow gradient poses the highest challenge to the separation power of chromatography. So far analyses have been carried out with full porous sub 3µm silica particles packed into capillary columns with 75µm i.d. Tryptic peptides in general are medium mass molecules and therefore suffer from reduced mass transfer terms during the chromatographic process. Fused core particles only have a porous surface layer and a solid core; thereby diffusion paths are much shorter and have a much sharper statistical path length distribution compared to fully porous particles. The peak broadening that is caused by different diffusion path lengths is limited and thereby mass transfer dependent drawbacks of heavier molecules could be compensated through the application of fused core materials with wide pores adapted to peptide analysis. We packed a capillary column with Supelco Ascentis® Express Peptide ES material with 2,7µm particle size and injected different amounts of digested yeast lysate to investigate chromatographic performance in terms of peak shape and sample loadability of the material. We analyzed the peak width at half maximum and compared it to previously carried out runs with the same sample on the usual fully porous support material. Furthermore also MASCOT searches were performed to investigate potential changes in sensitivity.

Peak width

Initially it has to be mentioned that the spray in the reference measurements with the standard material was not constant and therefore the TIC showed strong variations during all measurements. This is why subjectively observed, the runs carried out

with the porous shell particles seemed better. Three peaks were chosen for our investigations in the low, middle and high range of the reversed phase gradient. We injected 100, 200, 300, 500 and 1000ng in duplicate and always took the second runs into consideration. We observed slightly broader peaks for the fused core material for the lowest loadings and strongly increasing peak widths towards the highest loading. In terms of peak shape full porous particles were superior throughout all runs.

Sensitivity

Sensitivity was measured in terms of MASCOT scores and numbers of peptide identifications and the results were somewhat strange. On one hand the scores are significantly higher for the fully porous particles and on the other hand more peptide sequences have been identified with the fused core material Figure VI.7. This could indicate that low abundant peptides are detectable through narrower and therefore higher LC peaks. In order to get reliable results the reference experiments have to be repeated and evaluated.

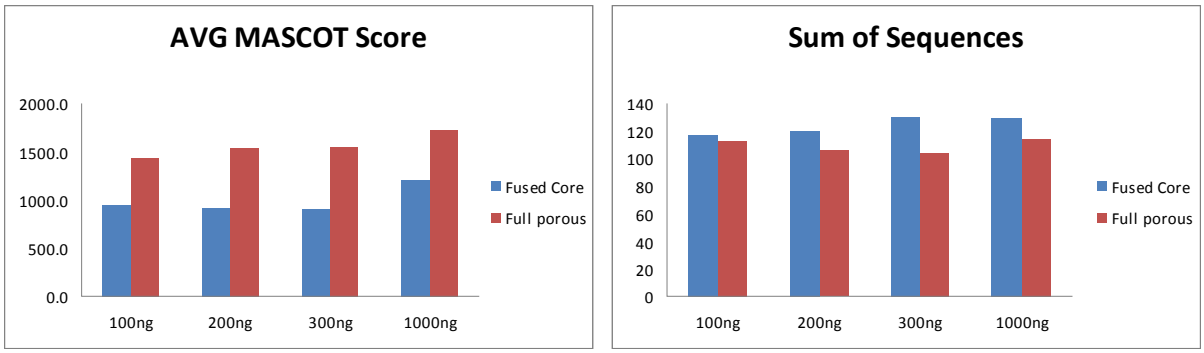

Figure VI.7 Average MASCOT score and sum of identified sequences in dependence of the chromatographic support material and the injected amount of analyte

VII. Conclusion

The present thesis is a compendium of studies, which have in common that they deal with selectivity aspects for LC-MS methods. In all cases, biomolecules were investigated with the challenge to be differentiated from their matrices. The key to success was the introduction of complementary selectivity profiles.

HPLC methodologies have a very high separation performance, which is potentiated by MS detection. Essentially, all separations reported in the present thesis were realized by exploiting differences in molecular size, lipophilicity, and chirality. Additional levels of selectivity were achieved through dedicated analyte derivatization, providing the missing puzzle stone to master these challenges. In other words, the successful methodologies presented in this thesis are based on a combination of selectivity principles from three different origins (see Figure VII.1).

Firstly, selectivity was implemented by using derivatization techniques that exclusively targeted the amino group of the amino acids under investigation, generating more easily separable acidic molecules. Secondly, further improvements in selectivity on the level of liquid chromatography were achieved by prudent choice of the stationary phases, proper selection and optimization of mobile phase systems. Thirdly, ultimate selectivity was obtained by adding mass spectrometric detection methods to this platform, and it was even enhanced by pursuing selected reaction monitoring protocols. This synergistic approach allowed for a highly sensitive and unambiguously selective separation, identification and quantitation of metabolites in biological systems.

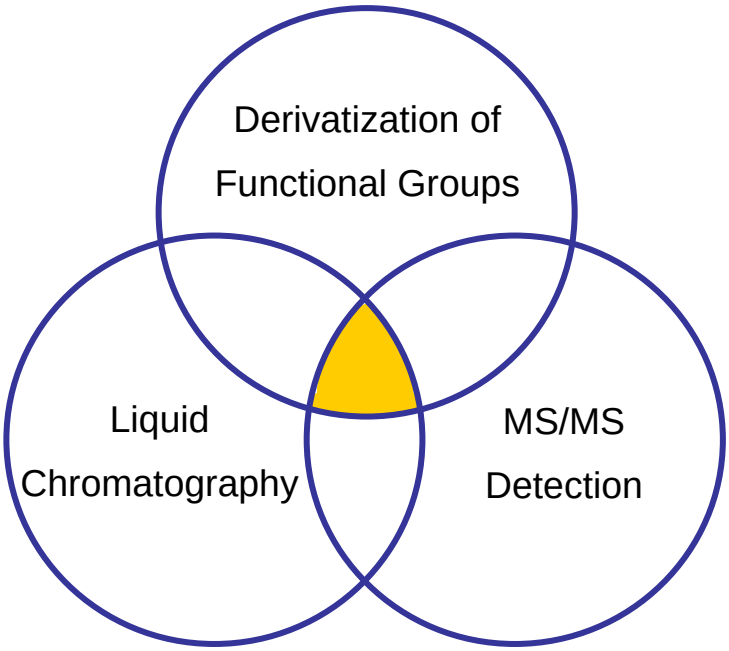

Figure VII.1 Three pillars for the introduction of analytical selectivity. The ultimate goal of all experiments was the golden middle – the overlap of selectivities

Specifically, biologically relevant amino acids and peptides were labelled with acetyl, dinitrobenzoyl, ferrocenylpropionoyl, 6-methoxy-quinolinoyl- and suberoyl tags. Acetylation stabilized the alcohol metabolite under study, MTCA, and avoided its *in-matrix* decomposition; furthermore, it enhanced the lipophilic behaviour of the analyte, and improved reversed phase retention. Dinitrobenzoyl labelling enabled enantioselective ion exclusion chromatography on zwitter ion exchanger chiral stationary phases by particularly promoting chiral recognition. Ferrocenylpropionoyl derivatization facilitated enantioselective separation on QN-AX and QD-AX anion exchange type CSPs; established a predictable enantiomer elution order pattern with L-AAs being less strongly retained than D-AAs on QD-AX; and provided a very characteristic, label-based MS/MS fragmentation. 6-methoxy-quinolinoyl-tagging introduced enantioselectivity for the entire set of chiral proteinogenic amino acids on QN-AX; moreover it enabled fluorescence detection and significantly increased MS/MS detection sensitivity. Finally, the chemical crosslinking with distinctly isotope-labelled suberate and enzymatic digestion of protein complexes generated large peptides amenable to enrichment by size exclusion fractionation. The analyte signals of the emerging crosslinked peptides could easily be extracted from a vast excess of matrix signals due to the characteristic light and heavy isotope pattern introduced by the crosslinking label.

VIII. Literature References

[1] WHO. World Health Organisation, http://www.who.int/substance_abuse/publications/global_alcohol_report/en/, 2011.

[2] M. Comporti, C. Signorini, S. Leoncini, C. Gardi, L. Ciccoli, A. Giardini, D. Vecchio, B. Arezzini, Genes and Nutrition 5 (2010) 101.

[3] Y. Yamada, T. Imai, M. Ishizaki, R. Honda, Journal of Human Genetics 51 (2006) 104.

[4] P.J. Brooks, J.A. Theruvathu, Alcohol (New York, NY, United States) 35 (2005) 187.

[5] F. Tagliaro, G. Lubli, S. Ghielmi, D. Franchi, M. Marigo, Journal of Chromatography, Biomedical Applications 580 (1992) 161.

[6] A.W. Jones, Toxicological Reviews 25 (2006) 15.

[7] W. Bicker, M. Lammerhofer, T. Keller, R. Schuhmacher, R. Krska, W. Lindner, Anal Chem 78 (2006) 5884.

[8] H. Kharbouche, F. Sporkert, S. Troxler, M. Augsburger, P. Mangin, C. Staub, Journal of Chromatography, B: Analytical Technologies in the Biomedical and Life Sciences 877 (2009) 2337.

[9] L. Politi, F. Leone, L. Morini, A. Polettini, Analytical Biochemistry 368 (2007) 1.

[10] H.T. Nagasawa, D.J.W. Goon, F.N. Shirota, Journal of Heterocyclic Chemistry 18 (1981) 1047.

[11] M. Laemmerhofer, W. Lindner, Journal of Chromatography, A 741 (1996) 33.

[12] N.M. Maier, S. Schefzick, G.M. Lombardo, M. Feliz, K. Rissanen, W. Lindner, K.B. Lipkowitz, Journal of the American Chemical Society 124 (2002) 8611.

[13] C.V. Hoffmann, R. Pell, M. Laemmerhofer, W. Lindner, Analytical Chemistry (Washington, DC, United States) 80 (2008) 8780.

[14] C.V. Hoffmann, R. Reischl, N.M. Maier, M. Laemmerhofer, W. Lindner, J. Chromatogr., A 1216 (2009) 1157.

[15] C.V. Hoffmann, R. Reischl, N.M. Maier, M. Laemmerhofer, W. Lindner, J. Chromatogr., A 1216 (2009) 1147.

[16] K. Hashimoto, T. Fukushima, E. Shimizu, S.I. Okada, N. Komatsu, N. Okamura, K. Koike, H. Koizumi, C. Kumakiri, K. Imai, M. Iyo, Progress in Neuro-Psychopharmacology and Biological Psychiatry 28 (2004) 385.

[17] A. D'Aniello, P. Spinelli, A. De Simone, S. D'Aniello, M. Branno, F. Aniello, G.H. Fisher, M.M. Di Fiore, R.K. Rastogi, FEBS Letters 552 (2003) 193.

[18] K. Hamase, A. Morikawa, S. Etoh, Y. Tojo, Y. Miyoshi, K. Zaitsu, Analytical Sciences 25 (2009) 961.

[19] S. Bomke, B. Seiwert, L. Dudek, S. Effkemann, U. Karst, Analytical and Bioanalytical Chemistry 393 (2009) 247.

[20] B. Seiwert, U. Karst, Analytical and Bioanalytical Chemistry 390 (2008) 181.

[21] A. Morikawa, K. Hamase, T. Ohgusu, S. Etoh, H. Tanaka, I. Koshiishi, Y. Shoyama, K. Zaitsu, Biochemical and Biophysical Research Communications 355 (2007) 872.
[22] M. Katane, H. Homma, Journal of Chromatography, B: Analytical Technologies in the Biomedical and Life Sciences 879 3108.
[23] J.E. Thompson, T.W. Vickroy, R.T. Kennedy, Analytical Chemistry 71 (1999) 2379.
[24] H. Wolosker, E. Dumin, L. Balan, V.N. Foltyn, FEBS Journal 275 (2008) 3514.
[25] A. Leitner, T. Walzthoeni, A. Kahraman, F. Herzog, O. Rinner, M. Beck, R. Aebersold, Molecular & cellular proteomics : MCP 9 1634.
[26] A. Leitner, L.A. Joachimiak, A. Bracher, L. Monkemeyer, T. Walzthoeni, B. Chen, S. Pechmann, S. Holmes, Y. Cong, B. Ma, S. Ludtke, W. Chiu, F.U. Hartl, R. Aebersold, J. Frydman, Structure (Oxford, United Kingdom) 20 814.
[27] O. Rinner, J. Seebacher, T. Walzthoeni, L. Mueller, M. Beck, A. Schmidt, M. Mueller, R. Aebersold, Nature Methods 5 (2008) 748.
[28] D.L. Swaney, C.D. Wenger, J.J. Coon, Journal of Proteome Research 9 1323.
[29] A.R. Dongre, J.L. Jones, A. Somogyi, V.H. Wysocki, Journal of the American Chemical Society 118 (1996) 8365.
[30] A. Foettinger, A. Leitner, W. Lindner, Journal of Mass Spectrometry 41 (2006) 623.

IX. Abbreviations

AA	amino acid
Ac	acetyl-
CoA	co-enzyme A
CSP	chiral stationary phase
DNB	dinitrobenzoyl
DSS	disuccinimidylsuberate
ESI	electro spray ionization
FP	ferrocyl propionate
HOPCA	hexahydro-oxopyrimidine carboxylic acid
HPLC	high performance liquid chromatography
IMCI	intra molecular counter ion
mob.Ph.	mobile phase
MQ	Methoxyquinoline
MS	mass spectrometry
MTCA	2-methylthiazolidine-4-carboxylic acid
MTCGly	2-methylthiazolidine-4-carboxyglycine
NMR	nuclear magnetic resonance spectroscopy
QD-AX	tertButyl-Quinidine anion exchanger
QN-AX	tertButyl-Quinine anion exchanger
RP-LC	reversed phase liquid chromatography
SEC	Size exclusion chromatography
SFP	Succinimidylferrocyl propionate
stat.Ph.	stationary phase
Tau-QD	taurine-quinidine
Tau-QN	taurine-quinine
WHO	world health organisation
Xlink	cross link
ZWIX	zwitter ion exchanger
@RT	at room temperature

Amino Acids

Ala	Alanine	Leu	Leucine
Arg	Arginine	Lys	Lysine
Asn	Asparagine	Met	Methionine
Asp	Aspartic acid	Phe	Phenylalanine
Cys	Cysteine	Pro	Proline
Glu	Glutamic acid	Ser	Serine
Gln	Glutamine	Thr	Threonine
Gly	Glycine	Trp	Tryptophan
His	Histidine	Tyr	Tyrosine
Ile	Isoleucine	Val	Valine

X. Abstract

The separation, identification and quantitation of metabolites in biological systems poses an important, yet challenging field of application in analytical chemistry. Generally, monitoring metabolites and biomolecules in biological samples demands for a reduction of sometimes very high sample complexity. Furthermore, the identification of trace amounts of these analytical targets necessitates the introduction of highly selective and highly sensitive analytical techniques.

High performance liquid chromatography (HPLC) is a powerful and versatile method for compound separations utilizing a broad range of selectivity principles. The coupling of HPLC with mass spectrometric (MS) detection combines orthogonal selectivities with very high detection sensitivity. Dedicated analyte derivatization procedures can be synergistically employed to introduce a final advance in both detection selectivity and sensitivity.

Amino acids pose the central analytical targets in the present thesis and they were analysed according to a wide spectrum of their biological roles. Cysteine was investigated as an acetaldehyde scavenger to deliver valuable information on the metabolic pathways of alcohol in humans; moreover it was evaluated as a biomarker for recent ethanol consumption.

In a fundamental scientific approach, new enantioselective zwitter ion exchanger chiral stationary phases for liquid chromatography were studied with respect to their ability of preparatively separating amino acid derivatives.

The detection of trace amounts of D – amino acids in biological fluids was established by different HPLC-MS strategies in combination with selectivity enhancing derivatization protocols. For this reason two different labelling strategies were developed. The introduction of a metalloferrocene tag to amino acids facilitated enantioselective separation of most proteinogenic amino acids and enabled very sensitive mass spectrometric detection. In an attempt to further improve these selectivity and sensitivity promoting properties, a methoxyquinolinoyl tag was employed that allowed for the enantioseparation of all chiral proteinogenic amino

acids, delivered supreme mass spectrometric detectability and moreover introduced fluorescence activity. Thereby this labelling approach additionally offered the applicability to highly sensitive LC methods with fluorescence detection.

Finally, structural information of protein complexes was gathered in approaches involving the covalent crosslinking between the lysine side chains of protein regions in close proximity and consecutive proteolytic digest of the proteins. Due to a very high number of chemically similar matrix constituents, protein crosslinking experiments demanded for ultimate separation capability of liquid chromatography and pushed the performance of MS detection towards its limits. Thus, enrichment of the generated cross linked peptides via size exclusion fractionation and nano – HPLC – high resolution mass spectrometric detection were employed to deliver this analytical peak performance.

Essentially, the successful outcome of the experiments was generally associated with the complementary contribution of chemical derivatization, chromatographic separation and tandem mass spectrometric detection to overall method selectivity and sensitivity.

XI. Zusammenfassung

Die Trennung, Identifizierung und Quantifizierung von Metaboliten in biologischen Systemen stellt eine große Herausforderung für analytisch chemische Methoden dar. Generell, macht die Analytik von Metaboliten und Biomolekülen in biologischen Proben meist eine Reduktion der hohen Probenkomplexizität nötig. Darüber hinaus bedingt die Identifizierung von Analyten im Spurenbereich auch die Einführung hoch selektiver und sensitiver Messtechniken.

Hochleistungsflüssigkeitschromatographie (HPLC) ist unter zu Hilfenahme einer breiten Anzahl an verfügbaren Selektivitätsprinzipien eine sehr vielseitige Methode zur Stofftrennung. Die Kopplung von HPLC und Massenspektrometrie (MS) stellt eine Kombination orthogonaler Selektivitäten mit sehr hoher Detektionsempfindlichkeit dar. Zielgerichtete Derivatisierungsstrategien stellen können synergistisch eine weitere Steigerung sowohl der Selektivität, als auch der Empfindlichkeit der so erstellten Methoden zur Folge haben.

Aminosäuren stellen die zentralen Analyten dieser Arbeit dar und sie wurden mit Hinblick auf eine große Breite ihrer biologischen Relevanz untersucht. Cystein wurde in seiner Funktion als Acetaldehyd Fänger betrachtet und lieferte dabei wertvolle Informationen zum Alkoholstoffwechsel im menschlichen Körper, weiters wurde es als Biomarker für kurzfristigen Alkoholkonsum erforscht.

In einem fundamentalwissenschaftlichen Ansatz wurden enantioselektive Zwitterionenaus-tauscher als stationäre Phasen für die HPLC untersucht. Sie wurden dabei auf präparative Trennungen von derivatisierten Aminosäureenantiomeren angewandt.

Durch die Anwendung diverser LC-MS Methoden in Kombination mit selektivitäts-fördernden Deriviatisierungsstrategien konnten Spuren von D – Aminosäuren in biologischen Flüssigkeiten nachgewiesen werden. Zu diesem Zweck wurden zwei verschiedene Labelling Methoden angewendet. Die Einführung eines Metalloferrocen – Tags erlaubte die Trennung fast aller chiralen, proteinogenen

Aminosäuren und erlaubte eine sehr empfindliche massenspektrometrische Detektion. In einem Ansatz diese Eigenschaften noch weiter zu verbessern, führte die Derivatisierung von Aminosäuren mit Methoxychinolin zur Trennung aller chiralen, proteinogenen Aminosäuren und einer weiteren Steigerung der MS-Empfindlichkeit, darüber hinaus wurde so eine fluoreszierende Funktionalität eingeführt, die zusätzlich HPLC mit hochempfindlicher Fluoreszenzdetektion erlaubte.

Zuletzt wurde Strukturinformation über Proteine und Proteinkomplexe durch chemisches Quervernetzen gewonnen. Bei dieser Methode wurden räumlich nahe Lysin Seitenketten interagierender Proteine kovalent aneinander gebunden. In einem weiteren Schritt wurden die Proteine proteolytisch verdaut und die so gewonnen quervernetzten Peptide mit Größenausschlusschromatographie angereichert. Die nachfolgende nano-HPLC Kopplung mit hochauflösender MS stellte die ultimative Herausforderung für die Leistungfähigkeit sowohl der Chromatographie, als auch der Massenspektrometrie dar.

Letztlich lieferten drei Faktoren komplementäre und essenzielle Beiträge zur Einführung von Selektivität und somit zum erfolgreichen Abschluss der Experimente: chemische Derivatisierung, chromatographische Trennung und tandem-massenspektrometrische Detektion.

XII. Curriculum Vitae

Name: Roland Johann Reischl

Titel: Magister Rerum Naturalium

Geburtstag: 7.7.1982

Geburtsort: Salzburg

4/2008 – 6/2012:	Dissertation in analytischer Chemie an der Universität Wien, Fakultät für Chemie, Arbeitsgruppe Lindner
13.3.2008:	Abschluss des Chemiestudiums mit ausgezeichnetem Erfolg
10/2001 – 2/2008:	Studium der Chemie an der Universität Wien
2001:	Präsenzdienst beim Österreichischen Bundesheer,Gebirgsjäger
1992 - 2000:	Privatgymnasium der Herz Jesu Missionare Salzburg – Liefering (Abschluss mit Matura)
1986 – 1992:	Volksschule Itzling

Chemisch relevante berufliche Referenzen:

2008 – jetzt:	Vollzeitbeschäftigung als Universitätsassistent im Zuge der Dissertation am Institut für Analytische Chemie; Universität Wien
2007: und	Ferialpraktikum bei der Firma Wiberg GmBH, Qualitätssicherung
	Rückstandsanalytik an Gewürzen und Lebensmittelzusatzstoffen
2006:	Ferialpraktikum bei der Agentur für Gesundheit und Ernährungssicherheit (AGES), Salzburg
2003 - 2006:	Studienbegleitende Arbeiten im Labor von Prof. Dr. Erich R. Schmid, Lebensmittel- und Umweltanalytik mittels GC-MS

Lehrtätigkeit:

Betreuung von studentischen Kleingruppen in den Wahlpraktika:

Kopplungstechniken Chromatographie-Massenspektrometrie für die Charakterisierung biologischer Proben

Chromatographische Techniken für bioaktive Verbindungen in Verbindung mit Massenspektrometrie

Praktische Betreuung einer Diplomarbeit und von 4 Studenten in wissenschaftlichen Austauschprogrammen.

Wissenschaftliche Auslandsaufenthalte:

8 / 9 2010:

ETH Zürich, Institut für molekulare Systembiologie, Arbeitsgruppe Aebersold: Arbeiten mit micro- und nano-LC-ESI-MS (Orbitrap XL, und FT-ICR), Proteinstrukturaufklärung mittels chemical crosslinking. Erlernen der Methodik und der Instrumentenbedienung und –wartung inklusive Datenauswertung.

Präsentationen im Fachgebiet:

Posterbeiträge bei Konferenzen:

Anakon 2009 (Berlin), **Euroanalysis** 2009 (Innsbruck), **HPLC** 2010 (Boston), **Anakon** 2011 (Zürich), **HPLC** 2011 (Budapest) mit: „Outstanding Poster Award“

Vorträge:

ASAC Junganalytikerforum 2009:
Determination of 2-Methylthiazolidine-4-carboxylic acid – a reaction product of acetaldehyde and cysteine - in human blood and urine by LC – MS / MS

Lange Nacht der Forschung 2009: Analytik von Alkohol

ASAC Generalversammlung 2010: Phospholipidanreicherung (i.V. Alexander Leitner als Anton Paar Preisträger)

Publikationen im Fachgebiet:

Journal of Chromatography A, 1216 (2009), 1147–1156

Hoffmann, C. V.; **Reischl, R.**; Maier, N. M.; Laemmerhofer, M.; Lindner, W.

Stationary phase-related investigations of quinine-based zwitterionic chiral stationary phases operated in anion-, cation-, and zwitterion-exchange modes

Journal of Chromatography A, 1216 (2009), 1157–1166

Hoffmann, C. V.; **Reischl, R.**; Maier, N. M.; Laemmerhofer, M.; Lindner, W.

Investigations of mobile phase contributions to enantioselective anion- and zwitterions exchange modes on quinine-based zwitterionic chiral stationary phases

Journal of Separation Science, 33 (2010), 3273-3282

Hinterwirth, H.; Laemmerhofer, M.; Preinerstorfer, B.; Gargano, A.; **Reischl, R.**; Bicker, W.; Trapp, O.; Brecker, L.; Lindner, W.

Selectivity issues in targeted metabolomics: Separation of phosphorylated carbohydrate isomers by mixed-mode hydrophilic interaction/weak anion exchange chromatography

Journal of Chromatography A, 1218 (2011), 8379-8387

Reischl, R. J.; Hartmanova, L.; Carrozzo, M.; Huszar, M.; Fruehauf, P.; Lindner, W.

Chemoselective and enantioselective analysis of proteinogenic amino acids utilizing N-derivatization and 1-D enantioselective anion-exchange chromatography in combination with tandem mass spectrometric detection

Molecular & Cellular Proteomics, 11 (2012)
Leitner, A.; **Reischl, R.**; Walzthoeni, T.; Herzog, F.; Bohn, S.; Forster, F.; Aebersold, R.

Expanding the Chemical Cross-Linking Toolbox by the Use of Multiple Proteases and Enrichment by Size Exclusion Chromatography

Analytical and Bioanalytical Chemistry, (manuscript submitted)
Reischl, R.J.; Bicker W.; Keller T.; Lamprecht, G.; Lindner, W.

Analysis 2-Methylthiazolidine-4-carboxylic acid – MTCA – a condensation product of cysteine and acetaldehyde as a consequence of alcohol consumption

Journal of Chromatography A, **(manuscript submitted)**
Reischl, R.J.; Lindner, W.

Methoxyquinoline labelling - a new strategy for the enantioseparation of all chiral proteinogenic amino acids in 1-dimensional liquid chromatography using fluorescence and tandem mass spectrometric detection

Appendix A

Analysis of 2-Methylthiazolidine-4-carboxylic acid – MTCA – a condensation product of cysteine and acetaldehyde as a consequence of alcohol consumption

Roland J. Reischl*, Wolfgang Bicker*[+], Thomas Keller[§], Günther Lamprecht*, Wolfgang Lindner*[#]

* Department for Analytical Chemistry, University of Vienna, Währingerstrasse 38, 1090 Vienna, Austria
[+] Current address: FTC - Forensisch Toxikologisches Labor BetriebsgmbH, Gaudenzdorfer Gürtel 43-45, 1120 Vienna, Austria
[§] IFFB Department of Forensic Medicine and Forensic Neuropsychiatry, University of Salzburg, Ignaz-Harrer-Strasse 79, 5020 Salzburg, Austria
[#] Corresponding author Tel.: +43-1-4277-52300. Fax: +43-1-4277-9523. E-mail: wolfgang.lindner@univie.ac.at

Abstract

Acetaldehyde is a highly electrophilic agent that is endogenously produced as a first intermediate in oxidative alcohol metabolism. Its high reactivity towards biogenic nucleophilic compounds has toxicity and carcinogenicity as a consequence. Acetaldehyde readily undergoes a condensation reaction and a consecutive ring formation with cysteine to form 2-Methylthiazolidine-4-carboxylic acid (MTCA). This reaction product is hydrolytically unstable and can be stabilized by N acetylation. Furthermore N acetylation allows reversed phase chromatography and ESI-MS/MS detection. The LLOQ of MTCA spiked into newborn calf serum was 0,5 mg L^{-1} after acetylation. The measurement of post mortem blood samples showed a very low basal level of our target analyte in alcohol negative patients and strongly enhanced blood levels in patients that were positive in blood alcohol testing. A clear dependency between blood alcohol and MTCA concentration was not determinable. Urinary concentrations of MTCA were much lower and below the LOD in some cases. In a pilot study, the time dependence of MTCA blood levels was analysed after a single per oral dose of 0,5g ethanol per kg bodyweight. The peak concentration of MTCA in blood was determined 250 minutes after the consumption of the alcoholic drink and was still detectable after 780 minutes (13h), in contrast to the corresponding alcohol, which reached a maximum concentration of 0,5 ‰ and levelled off after 7h.

Introduction

Human toxicokinetics and toxicodynamics of ethanol appear to be more intensively studied than for any other xenobiotic compound. Obviously, this comes from the complex and worldwide social, economical, medical as well as forensic dimensions of acute and chronic ethanol intake. The prime metabolic pathway of ethanol is its oxidation by alcohol dehydrogenase. Minor oxidative pathways proceed via katalase and the cytochrome P450 system or the microsomal ethanol oxidizing system (MEOS). These pathways have the intermediate formation of acetaldehyde in common [1]. However, about only 0,1% of all ingested EtOH does not undergo either

of the three described ways and is non oxidatively metabolized to yield ethyl glucuronide and ethyl sulfate, two well established biomarkers for recent alcohol consumption [2-4]. The reactive electrophilic nature of acetaldehyde makes oxidation of ethanol an intrinsically toxifying metabolic step. Acetaldehyde easily reacts with nucleophilic compounds such as nucleobases, proteins, amines and small thiol-containing compounds, as well as amino acids [5-7]. This makes it a potent mutagen and it is classified as a type one carcinogen. Efficient and redundant detoxification routes for acetaldehyde are thus mandatory to prevent local and systemic effects. Acetaldehyde is mainly detoxified by aldehyde dehydrogenase-mediated oxidation to acetic acid, which consecutively enters the citric acid cycle [8]. Polymorphism in aldehyde dehydrogenase activity (like also alcohol dehydrogenase activity) is suggested as a factor of genetically determined interindividual differences in alcohol dependence and adverse effects caused by the accumulation of acetaldehyde [9-11]. On the other hand, reactions with nucleophilic reservoirs such as glutathione may be considered as potent non-enzymatic detoxification routes for acetaldehyde [12,13]. Moreover, acetaldehyde is suspected to exhibit behavioural effects [10] and to thereby take part in the psychoactivity of alcohol.

2-Methylthiazolidine-4-carboxylic acid (MTCA) revisited

Due to the chemical reactivity of acetaldehyde it should conceptually undergo a reaction with cysteine (Cys) thus forming a thiazoldine carboxylic acid instead of a chemically more unstable Schiff base (see Figure 1). Following this route Cys could generally be seen as an aldehyde scavenger. The mechanism for the ring formation has been subject of several studies and it is strongly believed to proceed via a condensation reaction [14-16] (Figure 1). NMR studies revealed a deuterium exchange in the 2-position of the thiazolidine ring when the formation reaction was carried out in D_2O and thereby confirmed an imine intermediate [16-18]. The chemical stability of the resulting thiazolidine-4-carboxylic acids that are substituted in their 2 – position has been addressed and it was found to be dependent on the specific type of substituent (R' in Figure 1) [14,19].

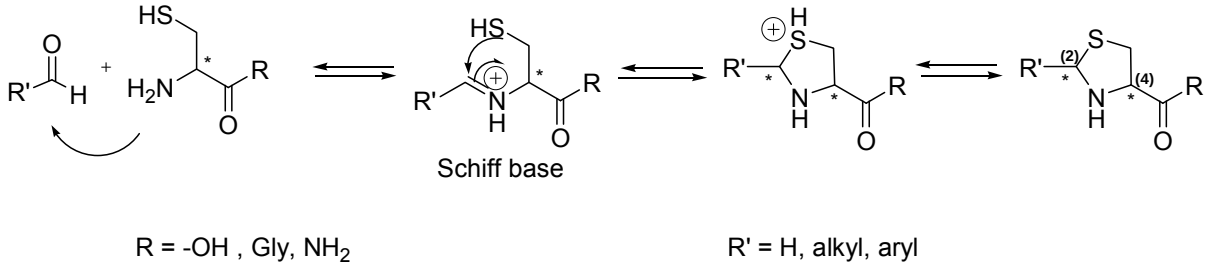

Figure 1 reaction scheme for the formation of thiazoldines as proposed in parts in the literature [16]

The reversibility of this ring formation and thus the chemical instability is successfully employed in the design of cystein-delivering pro-drugs [14,20-22]. Taking into consideration the chemical reactivity of acetaldehyde, literature reports the biogenic formation of adducts with glutathion, cysteamine and penicillamine that only have limited half-life times [12,23,24]. Moreover, also the excretion of condensation products of acetaldehyde with neurotransmitters like dopamin, serotonin and tryptamin was investigated [25].

Concluding, it can be stated that the reactivity of acetaldehyde towards various kinds of endogenous nucleophiles is very pronounced and many studies have been carried out on the reaction mechanism, the stability and the applicability for medical purposes.

In a complementary approach, the dipeptide cysteinyl glycine (CysGly) was subject to studies specifically focussing on the connection between alcohol consumption and the formation of 2-methylthiazolidine-4-carbonyl glycine (MTCG) in the bile of rats [26]. However, this target molecule could not be identified in human plasma after ethanol consumption. While the concentration of CysGly in the bile is relatively high due to its in situ generation from glutathione through gamma glutamyl transferase, it is much lower in the plasma. Free cysteine in plasma is about 10 times more abundant [27-29] than CysGly. Thus, the direct condensation product of acetaldehyde with cysteine, 2-methylthiazolidine-4-carboxylic acid (MTCA), may be hypothesised to be analytically detectable in blood following ethanol consumption.

The aim of the present work follows three lines i.) the reinvestigation of the reactivity of acetaldehyde towards several amino acids and the characterization of the reaction pathway for the formation of MTCA including the chemical stabilization of this product (ii) the determination of MTCA in human blood and urine after controlled ethanol intake employing an optimized LC-MS analysis method (iii) the identification of MTCA in post-mortem blood samples with significant blood alcohol concentrations.

Materials, Methods and Instrumentation

Chemicals

Methanol and acetonitrile (ACN) were of HPLC gradient grade and obtained from VWR (Vienna, Austria). Water was purified in house by a millipore purification system. Formic acid (98–100%, ACS reagent) was purchased from Sigma–Aldrich (St. Louis, MO, USA). Acetic anhydride (ACS reagent, ≥99.0%) was supplied by Fluka (Buchs, Switzerland). Ethanol (LiChrosolv 99,9%) was purchased from Merck, Darmstadt, Germany. Amino acids of analytical grade were obtained from Bachem (Bubendorf, Switzerland) or Sigma–Aldrich $^2D_4$-acetaldehyde with 98 atom % D was purchased from Sigma–Aldrich. D_2O was bought from the Deutero GmbH, Kastellaun, Germany. 2,4-Dinitrophenylhydrazine, KOH and 85% ortho-phosphoric acid were of p.a. grade and supplied by VWR (Vienna, Austria)

Sample preparation

Post mortem blood and urine samples were provided by the Institute for Legal Medicine, Salzburg, Austria. From each patient, both blood and urine had been routinely taken for forensic toxicological examination and were subjected to MTCA analysis.

Alcohol concentrations in blood (BAC) and urine (UAC) were determined by gas chromatography with flame ionization detection (GC-FID) and by complementary GC-MS in the Institute of Legal Medicine. The mean values of these two methods were used in the present study.

Sample preparation for whole blood and serum was carried out through precipitation of proteins by adding 900µL of ice cold ACN to 100µL of sample followed by centrifugation at 12100 x g for 3min. 100µL of the supernatant was taken and 900µL of sodium carbonate buffer (0,1M pH 9,9) was added. N-Acetylation was carried out by adding 10µL of acetic anhydride. Thereafter reaction took place while shaking for 30min at 37°C.Finally, the sample was transferred into an HPLC vial and subjected to LC-MS the measurement.

Urine was acetylated by adding 900µL carbonate buffer to 100µL of urine followed by acetylation with acetic anhydride and shaking at 37°C. After the reaction time of 30min had been fulfilled, the samples were transferred to HPLC vials and measured with LC-MS

Preparation of MTCA

3,0g of L-Cysteine were dissolved in 40mL of N_2 purged deionised water. To the opaque solution 1,8mL of acetaldehyde was pipetted. The reaction was carried out by stirring under nitrogen at room temperature for 1h. Thereafter the reaction solution was strongly reduced under vacuum and the white precipitate was transferred to a glass sinter filter No 4. In there the product was sucked dry, washed with 75% EtOH and then three times with 96% EtOH. The isolated product was finally dried under high vacuum over night. The resulting product is a diastereomeric mixture of cis and trans – MTCA with respect to the methyl group on C -2 and the carboxylic acid function on C – 4. Cis and trans were derived from the NOE experiment. ^{1}H-NMR bands [MeOD] at 400 MHz: diastereomers: **(R)-2-Methylthiazolidine-4-(S)-carboxylic acid (cis):** δ = 1,7ppm (3H, d), 3,5ppm (2H, m), 4,4ppm (1H, T), 5ppm (1H, q) and (**S)-2-Methylthiazolidine-(S)-4-carboxylic acid (trans):** δ = 1,7ppm (3H, d), 3,3ppm + 3,45ppm (2H, 2 d), 4,2ppm (1H, T), 4,8ppm (1H, q)

Preparation of the N – acetyl MTCA reference

1,0 g of MTCA was dissolved in 15mL Na_2CO_3 / $NaHCO_3$ buffer (0,1M carbonate, pH 9) and 1mL acetic anhydride was added. The reaction was carried out by stirring over night and refluxing for 2 hours on the next day. The pH value was controlled by pH indicator strips and still was pH 9 at the end of the reaction. The clear, colourless solution was then extracted 3 times with 25mL ethyl acetate and the unified organic phases were combined, dried over Na_2SO_4, filtered and the filtrate was evaporated. Finally, the yielded clear oil was subjected to preparative C_{18} reversed phase chromatography. ^{1}H-NMR bands [MeOD] at 400 MHz: diastereomers: **N-acetyl-(R)-2-methylthiazolidine-4-(S)-carboxylic acid (cis):** δ = 1,6ppm (3H, d), 2,1ppm (3H, s), 3,3 – 3,5 (2H, m), 4,8 (1H, t), 5,3 (1H q) and **N-acetyl-(S)-2-methylthiazolidine-4-(S)-carboxylic acid (cis):** δ = 1,65ppm (3H, d), 2,2ppm (3H, s), 3,3 – 3,5 (2H, m), 5,0 (1H, t), 5,35 (1H, q)

Preparation of internal standard d_4-MTCA

1,21g (10mmol) of cysteine was dissolved 20mL in deionised and nitrogen purged D_2O. Thereafter, 650µL of d_4 – acetaldehyde was added (= 13mmol) and the mixture stirred under nitrogen for 5 hours at room temperature. For isolation, the reaction mixture was strongly reduced under vacuum resulting in a solid product, which was transferred to a glass sinter filter No 4 and sucked dry. Washing with 75% ethanol

was carried out three times and the clean white powder was dried under vacuum over night. Purity was confirmed through direct injection to the mass spectrometer and full scan measurement as well as after acetylation and reversed phase LC – MS in full scan mode: d_4-MTCA $[M-H]^-$: 150,1 m/z, NAc-d_4-MTCA $[M-H]^-$: 192,1 m/z.

Preparation of acetaldehyde – amino acid adducts

N-acetyl-2-methyl-thiazolidine-4-carbonyl-glycine – MTCG (see Figure 2)

The dipeptide Cysteinylglycine was dissolved in 1mL water in a concentration of 10mmol L^{-1} a 1,5molar excess of acetaldehyde was added and the mixture was incubated at 37°C for 45 minutes. Thereafter 100µL of the reaction solution were diluted with 900µL of carbonate buffer (0,1M, pH 9) and 10µL of acetic anhydride was added. N – acetylation was carried out through shaking for 30 minutes at 37°C (see Figure 2). The product was identified via its molecular mass in LC-MS full scan measurement in negative mode $[M-H]^-$: 245 m/z., as well as MS fragmentation (see Table 1, Figure 3).

Other amino acid acetaldehyde adducts (see Figure 2)

Asparagine and homocysteine were dissolved in water to a concentration of 10 mmol L^{-1} and incubated with acetaldehyde and acetic anhydride as shown above for CysGly (see Figure 2). The resulting products were identified with full scan LC-MS for their molecular mass. Asparagine yielded N-acetyl-hexahydro-oxopyrimidine carboxylic acid (NAc-HOPCA) with $[M-H]^-$: 198.9 m/z. The product of the condensation of homocysteine with acetaldehyde and consecutive acetylation was N-acetyl-2-methy-tetrahydro-1,3-thiazine-4-carboxylic acid (homo-MTCA) with $[M-H]^-$: 201.9 m/z., both were further verified by MS fragmentation experiments (see Table 1, Figure 3).

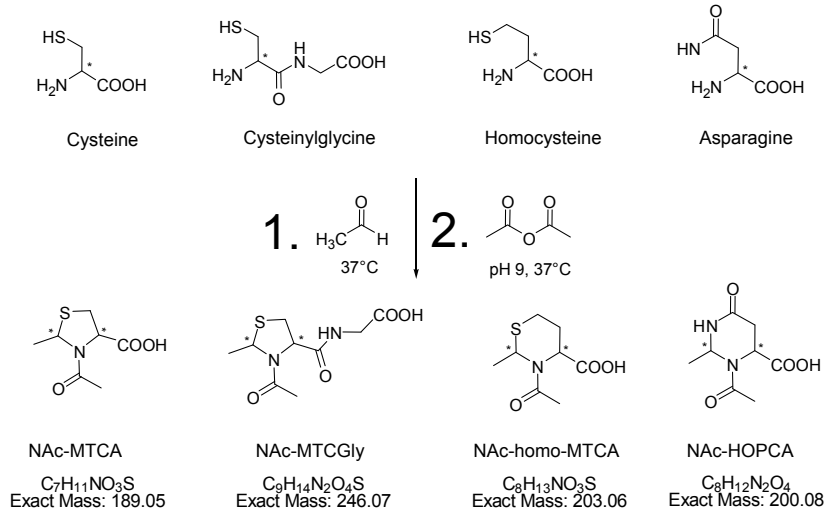

Figure 2 Target analytes and reaction scheme

Liquid Chromatography

All measurements were carried out by using Agilent 1200 series HPLCs with a degasser, binary pump, thermostated autosampler and column compartment, a 6 – port column switching valve as well as a UV detector. All parts produced by Agilent, Waldbronn, Germany.

For the analysis of MTCA we used an Eclipse XDB-C18 column (50mm x 4,6mm) with 1,8µm particle size at a flow rate of 0,75 mL min^{-1} at 20°C. As eluents water (eluent A) and methanol (eluent B) were used with 0,1% (v/v) of formic acid. The gradient method was: 0 – 2 min: 10% B, 2 – 6 min: 10% B to 40% B, 6 – 8,5 min: 40% B to 100% B until 10,5min, followed by reconditioning of the column with 10% B for 1,4min. Injection volume was 5µL and the detection was carried out by ESI – MS.

The determination of acetaldehyde via derivatization with DNPH was carried out with a Brownlee C_8 column (Perkin Elmer, Montreal, Canada) 50 mm x 4 mm i.d., with 7µm particle diameter. The flow rate was 1mL min^{-1} at 20°C. We used a gradient of three eluents: A: water (2mL L^{-1} acetic acid; pH 4,75 with KOH), B: Acetonitrile and C: Methanol with a linear inclination of the organic modifiers from 100% A in 11min to 40% A + 30% B + 30% C. The detection was carried out at 356nm with the UV detector.

Preparative purification of NAc-MTCA was carried out on a Bischoff HPD 200 XL system, equipped with a Lambda 1010 UV detector. The reversed phase column that we used was a Phenomenex Gemini 10µ C_{18} Axia (100mm x 2,1mm i.d., 10µm d_p). Elution was carried out in isocratic mode 90% water 10% acetonitrile and 0,1% formic acid at a flow rate of 10mL min^{-1}. The injection volume was 20µL and the detection wavelength was set to 254nm.

Mass Spectrometer

The MS used during the studies was an Applied Biosystems 4000 QTrap, triple quadrupole mass spectrometer with a linear ion trap being the third quadrupole and the TurboV™ ion source with heated nebulizer gas. Data was evaluated with the Analyst 1.5 software (AB Sciex, Foster City, USA). All analytes were diluted and injected in mobile phase (50% MeOH with 0,1% FA) to optimize selected reaction monitoring (SRM) transitions prior to measurement of the real samples (values in detail are given in Table 1). MS parameters were as follows: curtain, nebulizer and heater gas flow 15, 40, 60 psi. Sprayer voltage: -4500 V, sprayer gas temperature 650°C. Collision induced decay with nitrogen gas (CAD) was set to medium and entrance potential to 10 V. In full scan mode the declustering potential was 40 V and scan range was 75 m/z to 750 m/z in 0.7 seconds (10ms interscan pause). All quantitative runs were carried out with optimized parameters and in SRM mode. The most prominent fragments can be seen in Figure 3 and their proposed structures were deducted from the fragmentation patterns of the structural analogues and of deuterated MTCA (listed in Table 1).

Table 1 optimized MS parameters for SRM measurements (DP: declustering potential, CE: collision energy, CXP: cell exit potential)

	Q1 Mass (Da)	Q3 Mass (Da)	DP (V)	CE (V)	CXP (V)
NAc-MTCA	187.9	58.9	-45	-18	-1
		83.9		-20	-3
NAc-d_4-MTCA	192	83.8	-30	-20	-19
		42.1		-42	-1
NAc-MTCA-Gly	244.8	58.9	-25	-30	-7
		198.8		-10	-13
NAc-Cys	161.9	83.8	-40	-14	-11
		56.4		-32	-5
NAc-homo-MTCA	202.9	159.5	-40	-16	-9
		58.9		-36	-13
NAc-HOPCA	198.9	155	-45	-16	-9
		92.9		-30	-5

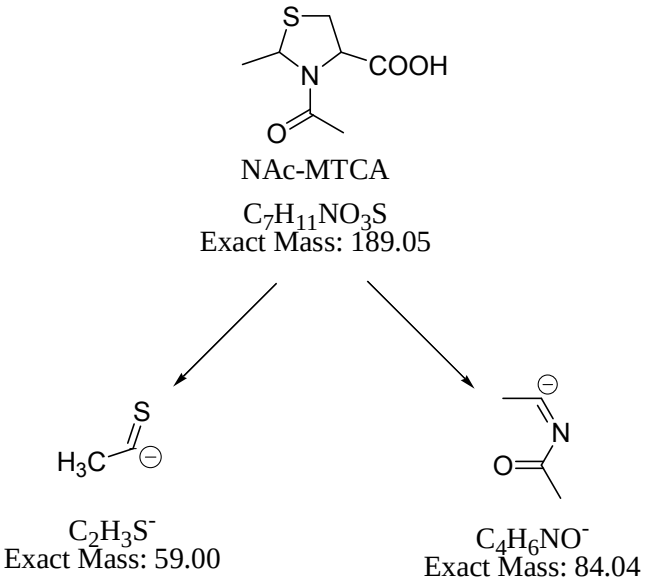

Figure 3 Proposed MS fragments generated from NAc-MTCA and structural analogues

Calibration

Newborn calf serum (NCS) was spiked with underivatized MTCA to concentrations of 0,05 - 0,1 - 0,25 - 0,5 - 1 - 2,5 – 5 - 10 - 25 and 50 mg L^{-1}. These concentrations were achieved by dilution of a stock solution of 10 mg MTCA per mL NCS in not more than four consecutive dilution steps. Also d_4-MTCA was added as an internal standard to yield a concentration of 5mg L^{-1} IS in serum. The samples were consecutively worked up as described above (see sample preparation). Measurements were carried out by LC-MS in SRM mode and manual integration of the analyte peaks. The peak areas were normalized with the internal standard area and the regression function was calculated with the weighting of 1/x in the Analyst 1.5 software.

Reversibility of the MTCA formation

25mg of 2,4-dinitrophenylhydrazine (DNPH) were dissolved in 1mL of 85% o –phosphoric acid the solution was diluted with 3mL of water to yield the derivatization reagent. MTCA was dissolved in NCS to a concentration of 50mg L^{-1}. An aliquot of 0,3mL of the analyte solution was taken and 25µL of the DNPH reagent were added

together with 34µL of KOH (0,3M) to scavenge the free acetaldehyde. The analysis of the sample was carried out by injecting it at various time points over several hours to HPLC - UV (Figure 5). In a follow up experiment another aliquot of the 50mg L^{-1} stock solution was taken that had rested over night at 25°C in absence of the DNPH reagent and the derivatization was carried out in analogy to the previous experiment. An external calibration had been carried out in a concentration range from 1 – 20 mg L^{-1} acetaldehyde in NCS and the concentration of the remaining MTCA was calculated indirectly via the increasing concentration of the acetaldehyde - DNPH in solution.

Exchange of the aldehyde in MTCA

Deuterated MTCA (d_4-MTCA) was dissolved in water, phosphate buffer (100mM, pH 7,4) and newborn calf serum, to yield a concentration of 10mg L^{-1} in each matrix. An about 100-fold molar excess of acetaldehyde over d_4-MTCA was added and the solution was kept at 37°C. At 5 time points (0, 100, 170, 280, 1165 min) aliquots of 100µL were taken, worked up and measured by LC-MS.

Ex vivo formation of MTCA

Undiluted newborn calf serum was spiked with acetaldehyde to yield 25 mmol L^{-1}. Every 60 minutes one aliquot of 100µL was taken, worked up and measured by LC-MS.

Thawing cylces

d_4-MTCA was dissolved in phosphate buffer (0,1M pH 7,4) and NCS. NAc-MTCA was added as a reference, both in a concentration of 5mg L^{-1}. Sample work up procedure was carried out with one aliquot of 100µL in the same way for both chosen matrices prior to the first freezing step. Samples were frozen in a commercial freezer at -22°C and thawed in a water bath at +22°C, as soon as the thawing step was completed the next aliquot of 100µL was taken and prepared for analysis. This way nine thawing cycles were completed and all samples were measured by LC-MS in the same sequence (see Figure 4).

Time Curve

After the uptake of a single per oral dose of 0,5g ethanol per kg bodyweight a healthy, non smoking volunteer with no alcohol consumption for at least 5 days prior to the experiment gave blood and urine with informed consent. The drink of choice was Vodka (40% EtOH v/v) due to its lack of potentially resorption disturbing matrix. It was consumed on an empty stomach. Blood samples were collected in K_3-EDTA vacuum tubes, urine samples in Greiner tubes and frozen immediately. Sample work up was carried out as described above for blood and urine and d_4-MTCA was added before the sample manipulation as an internal standard. The time between the consumption of the alcohol and the sampling was recorded.

NMR

^{1}H NMR spectra of the reference compounds were measured using tetramethylsilane (TMS) as the internal standard and at room temperature on a Bruker DRX 400 NMR spectrometer. Data were evaluated with spin works 3 software and calibrated on the solvent signal.

Results & Discussion

MTCA was acetylated during sample workup; thereby retention on a reversed phase C_{18} column was strongly enhanced. The acetylation of MTCA is the crucial step for analysing this molecule with reversed phase LC-MS. On the one hand it generates retention and on the other hand it hinders the back reaction of MTCA to its educts. Thereby it enables the measurement of a snapshot of the respective MTCA concentration in a sample at a certain timepoint. Moreover it stabilizes the product that can then be kept in solution without significant decomposition over time. Non acetylated MTCA is an ampholytic compound; hence it has zero net charge under given conditions. N acetylation renders the basic amino group into a neutral amide and thereby an acidic analyte is generated. This poses a fundamental improvement for MS detectability.

Calibration

The calibration function over 8 concentration levels between 0,5mg L^{-1} and 100mg L^{-1} in NCS was **y = 0,4907 x + 0,2651** with **R^2 = 0,9999** with weighting (1/x). In water sensitivity was somewhat higher with similar LOD and LLOQ. The function between 0,5mg L^{-1} and 100mg L^{-1} was: **y = 0,5417 x + 0,5693** with **R^2 = 0,9998** weighted (1/x),

Limit of Detection – Limit of Quantitation

Derived from the concentration levels used for the calibration curve, the limit of detection (LOD), defined by a signal / noise ratio of 3:1 was determined to be 0,1mg MTCA L^{-1} NCS. The lower limit of quantitation (LLOQ), which delivered a signal / noise ratio higher than 10:1 was 0,5 mg MTCA L^{-1} NCS.

Thawing cylces

When d_4-MTCA was thawed and frozen, a constant decline in analyte intensity was observed for phosphate buffer pH 7,4 and for newborn calf serum (see Figure 4). On the other hand, the peak area for NAc-MTCA did not change significantly over the 9 cycles in either of the both matrices. This underlines the thesis that the target molecule is stabilized by acetylation and poses an evidence for the hydrolytic instability of native MTCA under physiological conditions.

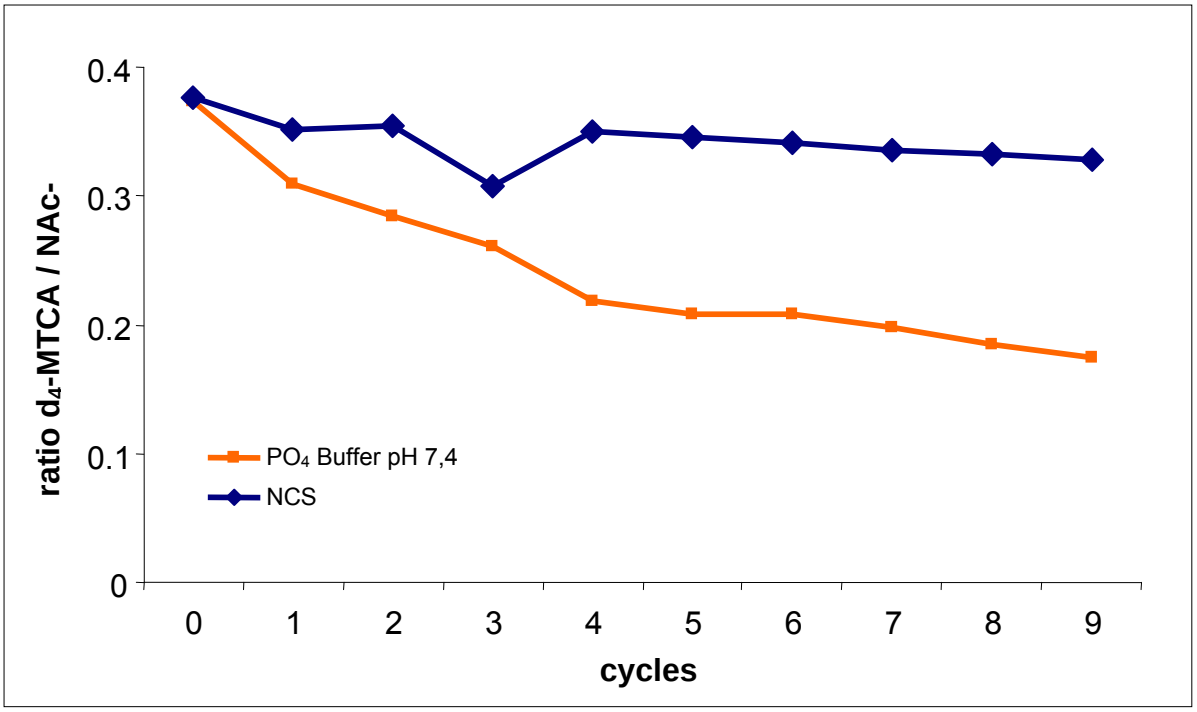

Figure 4 thawing cycles performed with free d_4-MTCA and referenced with NAc-MTCA

Reversibility of the MTCA formation

DNPH derivatization and consecutive LC - UV indicated an increase of the acetaldehyde concentration over time, which we interpreted with the reversibility of the MTCA formation reaction (see Figure 1). With other words the decrease of MTCA concentration was indirectly measured. If DNPH, as an aldehyde scavenger was added after 855 minutes it could be seen that more than 70% of the initial amount of MTCA had remained in solution and that the hydrolysis was strongly accelerated by adding the highly nucleophilic DNPH reagent. This essentially indicates that there is equilibrium between MTCA and the educts cysteine and acetaldehyde that can be shifted towards decomposition by capturing the released acetaldehyde. Moreover this process occurs at biological pH values in aqueous phosphate buffer as well as in newborn calf serum. In this experiment DNPH can be seen as a model – nucleophilic compound that could easily be substituted by other nucleophiles in a biological environment [5].
In an opposite approach, a rise in MTCA concentration with time was observed after spiking NCS with acetaldehyde during ex – vivo formation experiments. Assuming that the pool of Cys is sufficiently high, this points out that MTCA is formed if acetaldehyde is released to the blood stream.

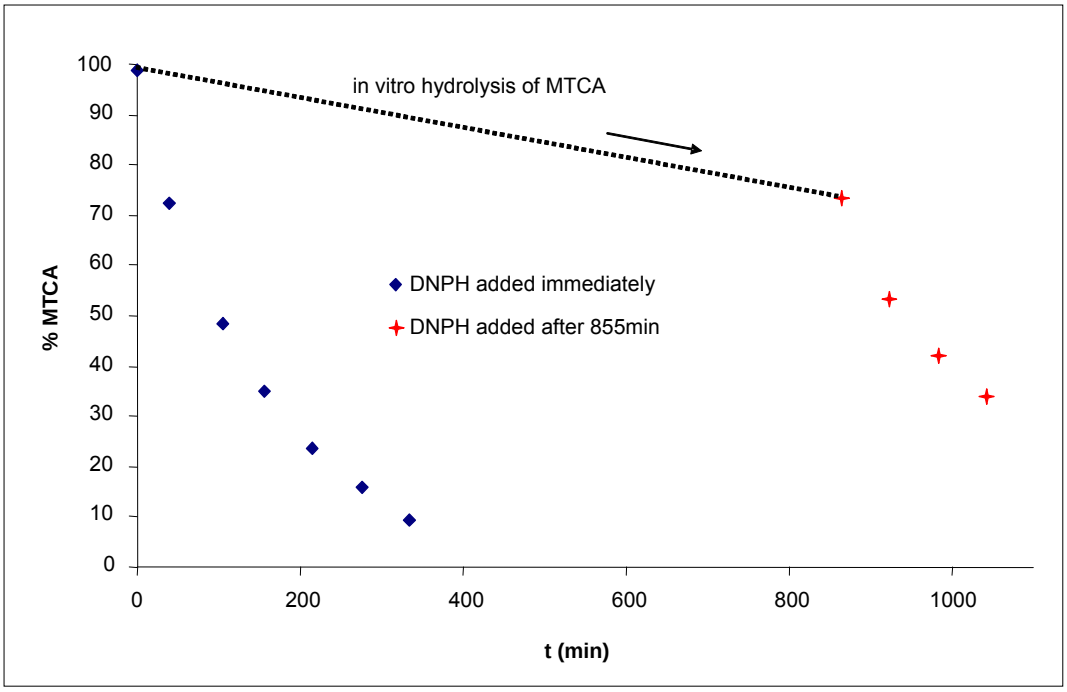

Figure 5 50 mg L^{-1} MTCA dissolved in newborn calf serum at 25°C and excess of DNPH

Exchange of the acetaldehyde in MTCA

When the underivatized stable isotope labelled d_4-MTCA was dissolved in a matrix containing a vast excess of non – deuterated acetaldehyde, a rapid decline in d_4-MTCA concentration could be observed (see Figure 6). In parallel the concentration of non – deuterated MTCA increased. This experiment clearly demonstrates the exchange of the aldehyde part of our target molecule. The cleavage of the MTCA molecule also occurs in phosphate buffer and thus can not be enzymatically mediated. In summary, it strongly suggests a hydrolytic process and poses a further evidence for the reversibility of the formation reaction shown in Figure 1.

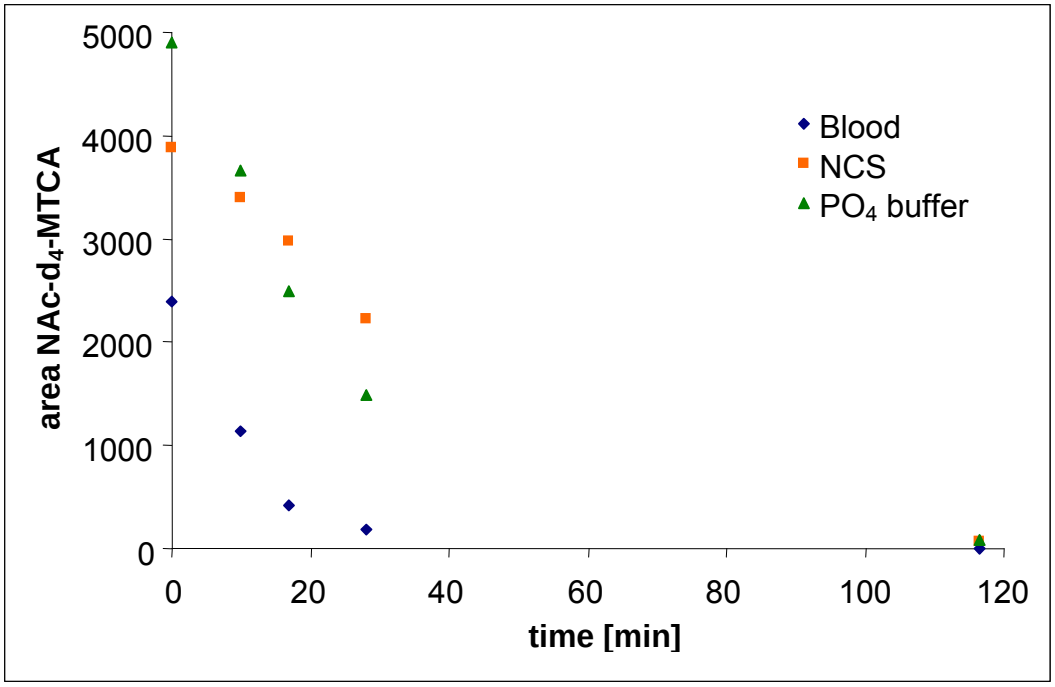

Figure 6 Decline of the d_4-MTCA concentration in 3 matrices blood, NCS, phosphate buffer with time. The analytes were measured after N acetylation

Real samples

To study the biological applicability of our method, initially the MTCA abundance in post mortem blood and urine samples was determined. To each blood sample the corresponding urine sample of the same patient was measured. Two of the three patients were alcohol positive in clinical testing (blood alcohol concentration – BAC: 2,4‰ and 1,7‰), one sample was used as negative control (BAC: 0,00‰). The corresponding urinary alcohol concentrations (UAC) were: 3,25‰ , 3,18‰ and 0,00‰ respectively. Taking into consideration that blood is diluted factor 1:100 during sample workup and urine only factor 1:10, there is a much higher abundance of MTCA in blood than there is in urine (see Figure 7). We assume that this is due to a high rate of MTCA hydrolysis during renal filtration.

Furthermore, it can be seen that MTCA occurs in alcohol positive blood and urine samples. Interestingly, there is a low basal level in alcohol negative blood samples. This was in well accordance with experimental findings in the analysis of other blood samples from alcohol negative patients (data not shown) and it could stem from regular endogenous acetaldehyde occurrence [30,9]. The application of our method to biological samples illustrates that MTCA is not only generated in vitro but can also be observed in vivo. The correlation between BAC and MTCA abundance remains unclear and demands for further investigations on a higher number of patients. Calibration curves showed that we could detect MTCA concentrations as low as 0,1mg L^{-1} in newborn calf serum, which is 680 nmol L^{-1}. This limit is low enough to detect a basal level of MTCA.

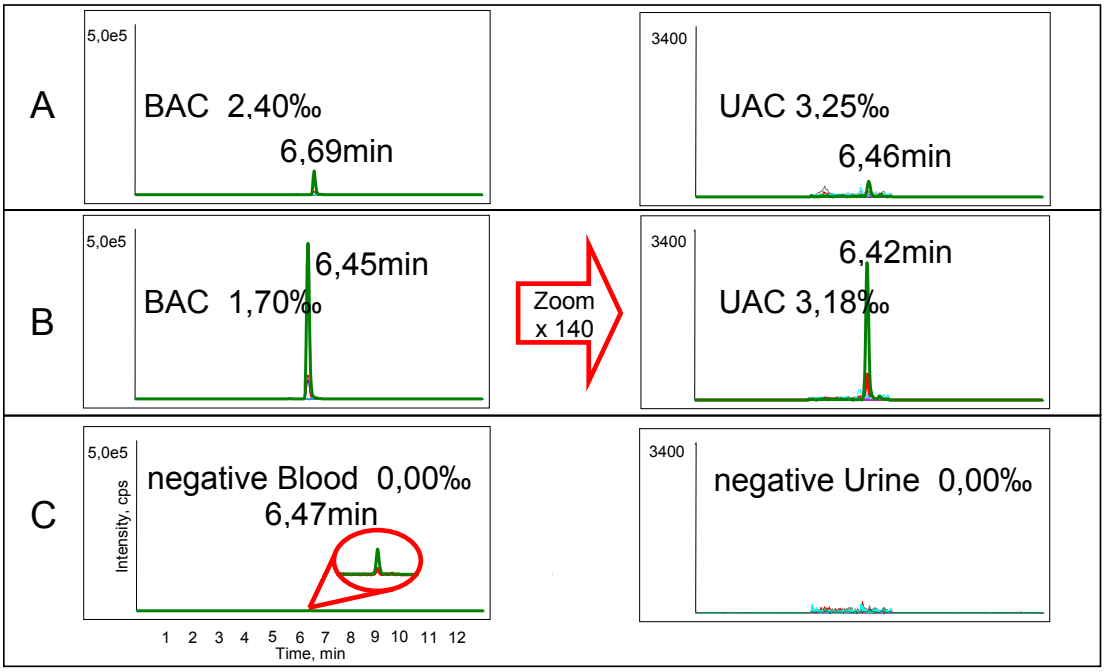

Figure 7 Real samples of patients A, B and C. The left column shows MTCA signals in blood, the right column shows the signals in urine of the respective patient after sample workup including N-acetylation, alcohol concentrations – BAC and UAC - determined by GC-FID, green signal shows most intensive SRM transition 187,9/83,9 Da for NAc-MTCA

Time Curve of MTCA after ethanol intake

In the course of a case study of controlled alcohol consumption and analyzing the appearance and fate of MTCA, we found a sharp inclination of MTCA blood levels after ethanol intake. The maximum blood level of MTCA was measured in the sample taken 250 minutes after the consumption of the alcoholic drink and was 12,6 mg L^{-1} in whole blood. This does not only illustrate that MTCA levels are increased in alcohol positive post mortem blood samples but it also provides data on the time dependence of MTCA blood levels as a consequence of alcohol consumption (Figure 8). In this pilot study it can be seen, that the blood level of MTCA reaches a maximum clearly retarded compared to the blood alcohol level and then decreases. We hypothesise that acetaldehyde that is produced by alcohol dehydrogenase and further being metabolized by aldehyde dehydrogenase may enter a metabolic side cycle. Free acetaldehyde is scavenged by cysteine or any N terminal Cys - peptide and released in an equilibrium reaction. Out of this equilibrium it can be withdrawn by aldehyde dehydrogenase [31]. The ability of cysteine to stabilize aldehyde adducts by ring formation together with its relatively high abundance in vivo make it a main “intermediate” aldehyde scavenger [26,32,6]. As shown recently, the generation of MTCA poses a way for the detoxification of free acetaldehyde [33], always bearing in mind that this molecule only has a limited stability, also in the physiological pH range, as shown by our experiments.

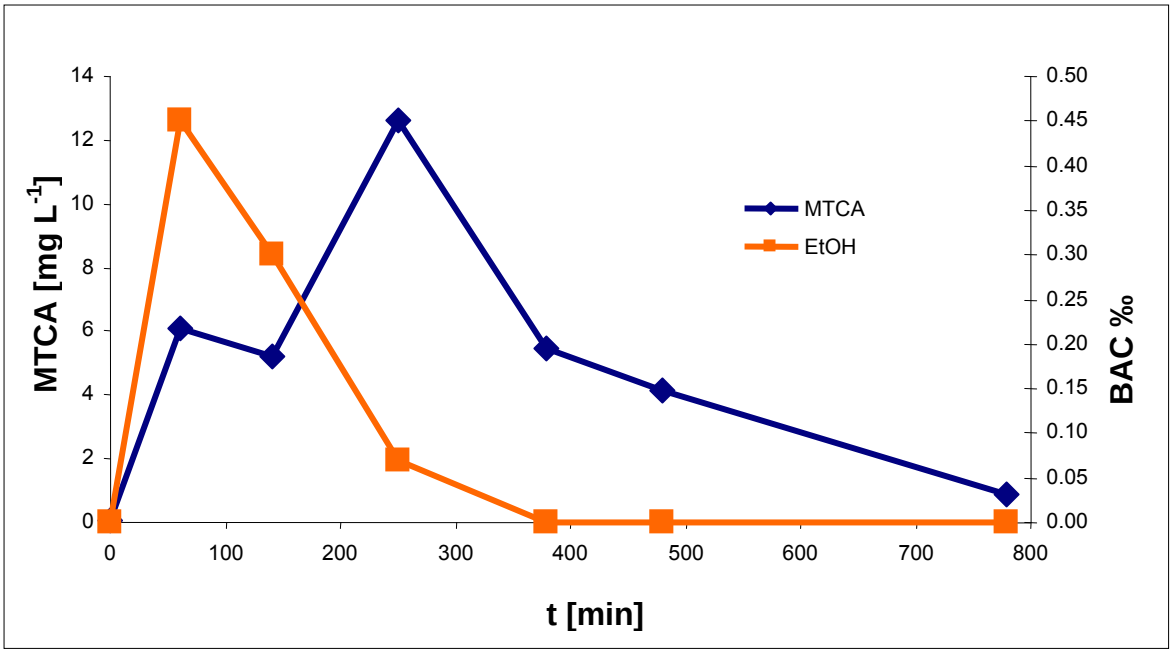

Figure 8 MTCA plasma concentration measured after N – acetylation and calculated from external calibration – all analyte signal areas normalized with the internal standard area

MTCA is not the only known adduct between acetaldehyde and amino acids [6]. In vitro we generated several target molecules and N acetylated them (see Figure 2). Following this assumption, we further optimized the LC-MS instrument for the determination of these targets. However, we could not detect homo-MTCA, nor HOPCA, nor MTCGly in blood or urine by applying our method. We further state that N – acetyl MTCA is not created endogenously and therefore could not be detected in non acetylated biological samples. On the other hand the addition of acetaldehyde to newborn calf serum generated MTCA. This ex vivo formation indicates the non enzymatic generation of this molecule in biological liquids thus corroborating the chemically driven reaction cascade.

Conclusion

We could clearly demonstrate that 2-Methylthiazolidine-4-carboxylic acid (MTCA) is generated by non enzymatic condensation of acetaldehyde and cysteine. This reaction is reversible and the back reaction can be hindered by N acetylation, which also facilitates the LC-MS measurement of this analyte and allows the measurement of snapshots of the MTCA level. Our experiments further indicated that MTCA is also produced endogenously and is an intermediate product in acetaldehyde metabolism. Therefore, it also plays a role in the metabolism of ethanol. However, its low hydrolytic stability in non acetylated state does not make it a suitable marker for intermediate term alcohol consumption. Nevertheless we could detect a significant rise in MTCA plasma levels after ethanol consumption that has a retarded plasma concentration curve compared to ethanol (see Figure 8). We conclude that free cysteine has a pooling function thus acting as a temporary aldehyde scavenger. Via the chemical reversibility of the MTCA formation acetaldehyde can be liberated to further metabolic turnover by aldehyde dehydrogenase. Thereby the concentration of free acetaldehyde can be kept low and MTCA may be seen as a detoxified intermediate. In this context, the determination of the concentration of free acetaldehyde in biological samples remains problematic as, in addition to the various

conjugates acetaldehyde forms with other endogenous molecules, it could be released from MTCA during sample preparation. Thus previously published methods dealing with acetaldehyde analysis may be critically reconsidered. Finally, the application of LC-MS enabled the identification of low basal levels of MTCA in the bloodstream due to its low limits of detection.

1. Comporti M, Signorini C, Leoncini S, Gardi C, Ciccoli L, Giardini A, Vecchio D, Arezzini B (2010) Ethanol-induced oxidative stress: basic knowledge. Genes Nutr 5 (2):101-109
2. Bicker W, Lammerhofer M, Keller T, Schuhmacher R, Krska R, Lindner W (2006) Validated method for the determination of the ethanol consumption markers ethyl glucuronide, ethyl phosphate, and ethyl sulfate in human urine by reversed-phase/weak anion exchange liquid chromatography-tandem mass spectrometry. Analytical chemistry 78 (16):5884-5892
3. Hoiseth G, Bernard Jean P, Karinen R, Johnsen L, Helander A, Christophersen Asbjorg S, Morland J (2007) A pharmacokinetic study of ethyl glucuronide in blood and urine: applications to forensic toxicology. Forensic science international 172 (2-3):119-124
4. Kharbouche H, Sporkert F, Troxler S, Augsburger M, Mangin P, Staub C (2009) Development and validation of a gas chromatography-negative chemical ionization tandem mass spectrometry method for the determination of ethyl glucuronide in hair and its application to forensic toxicology. J Chromatogr, B: Anal Technol Biomed Life Sci 877 (23):2337-2343
5. Brooks PJ, Theruvathu JA (2005) DNA adducts from acetaldehyde: implications for alcohol related carcinogenesis. Alcohol (New York, NY, United States) 35 (3):187-193
6. Park SC, Han JA, Han JG, Kang HS (1995) Asparagine forms a novel adduct with acetaldehyde. Korean Journal of Biochemistry 27 (1):41-45
7. Tsukamoto S, Kanegae T, Nagoya T, Shimamura M, Mieda Y, Nomura M, Hojo K, Okubo H (1990) Effects of amino acids on acute alcohol intoxication in mice--concentrations of ethanol, acetaldehyde, acetate and acetone in blood and tissues. Arukoru kenkyu to yakubutsu izon = Japanese journal of alcohol studies & drug dependence 25 (5):429-440
8. Kuschinsky G, Luellmann H (1984) Short Textbook of Pharmacology and Toxicology. 10th Ed.
9. Otsuka M, Harada N, Itabashi T, Ohmori S (1999) Blood and urinary levels of ethanol, acetaldehyde, and C4 compounds such as diacetyl, acetoin, and 2,3-butanediol in normal male students after ethanol ingestion. Alcohol (N Y) 17 (2):119-124
10. Quertemont E, Tambour S (2004) Is ethanol a pro-drug? The role of acetaldehyde in the central effects of ethanol. Trends Pharmacol Sci 25 (3):130-134
11. Yamada Y, Imai T, Ishizaki M, Honda R (2006) ALDH2 and CYP2E1 genotypes, urinary acetaldehyde excretion and the health consequences in moderate alcohol consumers. J Hum Genet 51 (2):104-111
12. Vina J, Estrela JM, Guerri C, Romero FJ (1980) Effect of ethanol on glutathione concentration in isolated hepatocytes. Biochem J 188 (2):549-552
13. Vogt BL, Richie JP (2007) Glutathione depletion and recovery after acute ethanol administration in the aging mouse. Biochemical Pharmacology 73 (10):1613-1621
14. Riemschneider R, Hoyer GA (1962) Substances protective against ionizing radiation. IV. Synthesis and properties of several 2-substituted 4-thiazolidine-carboxylic acids. Z Naturforsch 17b:765-768

15. Kallen RG (1971) Mechanism of reactions involving Schiff base intermediates. Thiazolidine formation from L-cysteine and formaldehyde. Journal of the American Chemical Society 93 (23):6236-6248
16. Nagasawa HT, Goon DJ, Zera RT, Yuzon DL (1982) Prodrugs of L-cysteine as liver-protective agents. 2(RS)-Methylthiazolidine-4(R)-carboxylic acid, a latent cysteine. Journal of medicinal chemistry 25 (5):489-491
17. Pesek JJ, Frost JH (1975) Decomposition of thiazolidines in acidic and basic solution. Spectroscopic evidence for Schiff base intermediates. Tetrahedron 31 (8):907-913
18. Fulop F, Mattinen J, Pihlaja K (1990) RING-CHAIN TAUTOMERISM IN 1,3-THIAZOLIDINES. Tetrahedron 46 (18):6545-6552. doi:10.1016/s0040-4020(01)96019-3
19. Butvin P, Al-Ja'Afreh J, Svetlik J, Havranek E (1999) Solubility, stability, and dissociation constants of (2RS, 4R)-2-substituted thiazolidine-4-carboxylic acids in aqueous solutions. Chem Pap 53 (5):315-322
20. Sprince H, Parker CM, Smith GG, Gonzales LJ (1974) Protection against acetaldehye toxicity in the rat by L-cysteine, thiamin, and L-2-methylthiazolidine-4-carboxylic acid. Agents and Actions 4 (2):125-130
21. Weber HU, Fleming JF, Miquel J (1982) Thiazolidine-4-carboxylic acid, a physiologic sulfhydryl antioxidant with potential value in geriatric medicine. Arch Gerontol Geriatr 1 (4):299-310
22. Wlodek L, Rommelspacher H, Susilo R, Radomski J, Hofle G (1993) Thiazolidine derivatives as source of free L-cysteine in rat tissue. Biochemical Pharmacology 46 (11):1917-1928
23. Huang T-C, Huang L-Z, Ho C-T (1998) Mechanistic Studies on Thiazolidine Formation in Aldehyde/Cysteamine Model Systems. Journal of Agricultural and Food Chemistry 46 (1):224-227
24. Serrano E, Pozo Oscar J, Beltran J, Hernandez F, Font L, Miquel M, Aragon Carlos MG (2007) Liquid chromatography/tandem mass spectrometry determination of (4S,2RS)-2,5,5-trimethylthiazolidine-4-carboxylic acid, a stable adduct formed between D-(-)-penicillamine and acetaldehyde (main biological metabolite of ethanol), in plasma, liver and brain rat tissues. Rapid communications in mass spectrometry : RCM 21 (7):1221-1229
25. Collins MA (1988) Acetaldehyde and its condensation products as markers in alcoholism. Recent Dev Alcohol 6:387-403
26. Anni H, Pristatsky P, Israel Y (2003) Binding of Acetaldehyde to a Glutathione Metabolite: Mass Spectrometric Characterization of an Acetaldehyde-Cysteinylglycine Conjugate. Alcoholism: Clinical and Experimental Research 27 (10):1613-1621
27. Guttormsen AB, Schneede J, Fiskerstrand T, Ueland PM, Refsum HM (1994) Plasma concentrations of homocysteine and other aminothiol compounds are related to food intake in healthy human subjects. J Nutr 124 (10):1934-1941
28. Parodi O, De Chiara B, Baldassarre D, Parolini M, Caruso R, Pustina L, Parodi G, Campolo J, Sedda V, Baudo F, Sirtori C (2007) Plasma cysteine and glutathione are independent markers of postmethionine load endothelial dysfunction. Clin Biochem 40 (3-4):188-193
29. Yardim-Akaydin S, Ozkan Y, Ozkan E, Torun M, Simsek B (2003) The role of plasma thiol compounds and antioxidant vitamins in patients with cardiovascular diseases. Clin Chim Acta 338 (1-2):99-105

30. Ohata H, Otsuka M, Ohmori S (1997) Determination of acetaldehyde in biological samples by gas chromatography with electron-capture detection. Journal of Chromatography, B: Biomedical Sciences and Applications 693 (2):297-305
31. Kallama S, Hemminki K (1983) Urinary excretion products after the administration of 14C-acetaldehyde to rats. J Appl Toxicol 3 (6):313-316
32. Bird Stephen D, Legge M, Walker Robert J (2004) Formaldehyde scavenging from peritoneal dialysis solutions using reduced aminothiol compounds. Nephrology (Carlton, Vic) 9 (2):65-72
33. Kartal-Hodzic A, Marvola T, Schmitt M, Harju K, Peltoniemi M, SivÃ©n M Permeability and toxicity characteristics of L-cysteine and 2-methyl-thiazolidine-4-carboxylic acid in Caco-2 cells. Pharmaceutical Development and Technology 0 (0):1-6. doi:doi:10.3109/10837450.2012.659253

Appendix B

Journal of Chromatography A, 1218 (2011) 8379–8387

Contents lists available at SciVerse ScienceDirect

Journal of Chromatography A

journal homepage: www.elsevier.com/locate/chroma

Chemoselective and enantioselective analysis of proteinogenic amino acids utilizing N-derivatization and 1-D enantioselective anion-exchange chromatography in combination with tandem mass spectrometric detection

Roland J. Reischl[a], Lucie Hartmanova[b,1], Marina Carrozzo[c,1], Monika Huszar[a], Peter Frühauf[a], Wolfgang Lindner[a,*]

[a] Department of Analytical Chemistry, University of Vienna, Währingerstrasse 38, 1090 Vienna, Austria
[b] RCPTM, Department of Analytical Chemistry, Palacky University, 17, listopadu 12, 771 46 Olomouc, Czech Republic
[c] Dipartimento di Scienze Farmaceutiche, Università degli Studi di Modena e Reggio Emilia, Via Campi 183, 41125 Modena, Italy

ARTICLE INFO

Article history:
Received 22 July 2011
Received in revised form
15 September 2011
Accepted 16 September 2011
Available online 22 September 2011

Keywords:
Enantioselective LC MS MS
Amino acid derivatization
Enantioselective amino acid analysis

ABSTRACT

D-Amino acid analysis in biological samples still poses a challenge to analytical chemists. In higher developed species trace amounts of D-amino acids have to be detected in vast excesses of the corresponding L-enantiomers. This method utilizes an easy-to-carry-out derivatization step on the amino group with an iron ferrocenyl propionate hydroxy succinimide ester followed by one-dimensional enantioselective anion exchange chromatography with cinchona alkaloid based chiral stationary phases (CSPs). MS detection is carried out in the highly sensitive SRM (selected reaction monitoring) mode, which allows a chemoselective differentiation of amino acid derivatives as well as their enantioselective separation in one step. Application of this method allows LOD (limits of detection) in the low μmol L^{-1} range and baseline enantioseparation for all proteinogenic amino acids except for Pro, Arg and His. The D-enantiomers of isomeric Leu and Ile were separated chromatographically and pose an example for the complementary selectivities of LC and MS. A successful application of this procedure to unprocessed human urine indicated the eligibility to analyse biological samples.

1. Introduction

Over the last two decades stereoselective amino acid analysis has increasingly moved into the scope of interest of the scientific community. The importance of amino acids (AAs) as building blocks in all living beings is well accepted and for a long time it has been assumed that in higher organisms only their L-enantiomers are of relevance. But more and more it has become evident that the D-forms of certain AAs are also abundant in highly developed species like mammals. D-Serine (D-Ser) was one of the first D-AAs that was identified to play a crucial role as a neuromodulator in mammalian brain [1]. It is an agonist for the N-methyl-D-aspartate (NMDA) receptor in neuronal synapses of the frontal cerebral cortex in humans [2]. D-Ser was also identified to be endogenously synthesized in mammals by enzymatic racemization from its L-form [3]. Furthermore there is a connection between serum concentrations of D-Ser and neurological implications like Alzheimer's disease and schizophrenia [4,5]. Similarly, D-aspartic acid (D-Asp) was identified in humans in connection with hormonal synthesis and release in the endocrine glands [6]. The enzymatic production of D-Asp and NMDA starting from L-Asp has been described in marine organisms [7,8]. More recently, the occurrence of D-alanine (D-Ala) in mammalian pancreatic cells was assigned to insulin production [9]. The age-dependent degree of racemization of D-Asp in human white brain matter might pose an example for the incidental occurrence of endogenous D-AAs [10]. The occurrence of D-Asp is also a rare example of a D-AA integrated in proteins.

It is now accepted that D-AAs have significant physiological effects. Therefore, the regulation of D-AA levels also has to be ensured in higher organisms. This is accomplished by oxidative deamination through the enzyme D-amino acid oxidase (DAAO). Particularly in the brain DAAO is strongly involved in the regulation of the D-serine concentration [11]. It has to be mentioned that significant concentrations of this enzyme have also been found in liver and kidney of mammals where it is involved into the metabolism of other endogenous and also exogenous alpha amino acids that stem from bacterial metabolism in the intestines or from food and its processing [12–14].

* Corresponding author. Tel.: +43 1 4277 52300; fax: +43 1 4277 9523.
E-mail address: wolfgang.lindner@univie.ac.at (W. Lindner).
[1] On temporary leave.

0021-9673/$ – see front matter © 2011 Elsevier B.V. All rights reserved.
doi:10.1016/j.chroma.2011.09.046

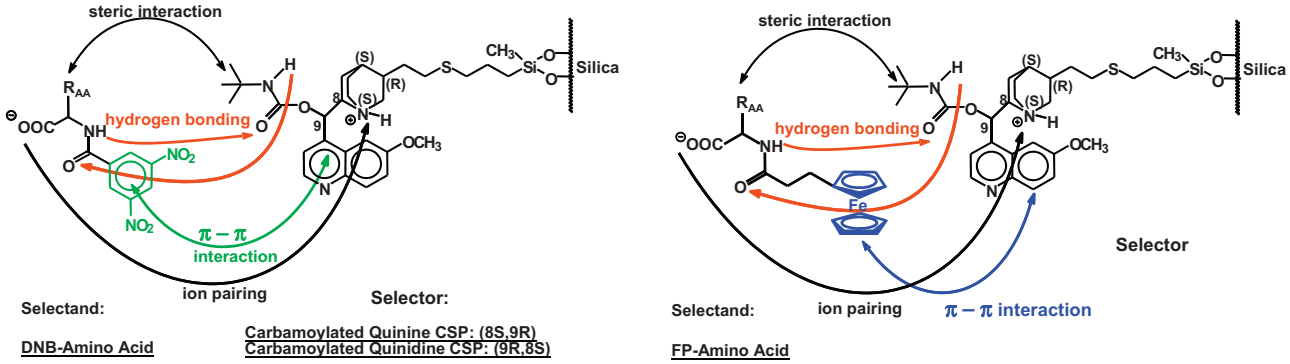

Fig. 1. Proposed stereoselective selector–selectand interactions between cinchona alkaloid modified CSPs, DNB-amino acids and FP-amino acids [43].

Apparently, the development of stereochemical separation techniques together with high performing detectors has enabled scientists to measure trace amounts of D-AAs besides large excesses of their L-enantiomers and even investigate their spatial distribution in tissues [9,15].

The stereochemical separation of amino acids is not trivial and especially in their underivatized and native form it is difficult to achieve satisfying separation performance paired with sensitive detection in all cases [16]. However, recently we have shown that in principle it is possible to stereoselectively analyse free amino acids on low molecular weight zwitterion exchanger type chiral stationary phases-ZWIX CSPs [17,18]. Nevertheless, more common are separation methods that are based on pre-column derivatization. For liquid phase separation techniques like electrophoresis [19] and liquid chromatography, methods involving N-derivatized amino acids are dominant. The introduction of fluorophoric or chromophoric groups is frequently aimed to significantly increase the detection sensitivity paired with altered chromatographic properties.

Gas chromatographic (GC) methods offer the advantage of very high separation efficiencies with commercially available enantioselective capillary columns like Chirasil-Val or cyclodextrin based selectors. The combination of chiral GC with mass spectrometric detection delivers very good separation performance and high detector sensitivity paired with valuable qualitative information [20,21]. The main drawback of GC–MS for enantioselective amino acid analysis is the restriction to evaporizable and non-thermo labile molecules.

In contrary, liquid chromatography offers a wider range of methodologies to separate chiral amino acids and derivatives thereof, respectively.

The techniques and selectors available for chiral amino acid separations span from (i) chiral ligand exchange chromatography (CLEC) via chelation of free α amino acids with Cu^{2+} [22,23] to (ii) chiral crown ethers via their complexation capability for protonated primary amines, amino acid amides and esters [24–26] or (iii) the formation of inclusion complexes with macrocyclic antibiotic type CSPs like teicoplanin and teicoplanin aglycone [27], where hydrogen bonds are dominating the chiral recognition processes [16].

Additionally, ion exchanger type chiral stationary phases (IEX CSPs) are well established and they usually demand for either acidic or basic analytes. As for chiral cation exchangers the amino acids are esterified on their C-terminus and for chiral anion exchangers they are derivatized on their N-terminus leaving the acid function untouched. Another possibility for the enantioselective separation of amino acids is the indirect approach of creating diastereomers by performing reactions with enantiopure derivatizing agents followed by the separation on achiral chromatographic columns [28].

Besides the enabling of an improved chromatographic separation, the introduction of certain labels is also performed for its beneficial influence on the detectability of biogenic compounds. Most of the amino acids do not carry any chromophores, therefore they are often derivatized to enable UV–VIS or fluorescence detection. The latter offers the possibility for laser-induced fluorescence to generate the highest detection sensitivity but therefore the derivatization with appropriate labels is crucial. Diverse reagents like NBD-F (4-fluoro-7-nitro-2,1,3-benzoxadiazole) [29], FITC (fluorescein isothiocyanate) [30], OPA (o-phtaldialdehyde) [31], FMOC (fluorenylmethyloxycarbonyl chloride) [32] or dansyl (5-(dimethylamino)naphthalene-1-sulfonyl chloride) [33,34] have proven their applicability. A multitude of reactions have been described in the literature to introduce UV–VIS absorbance. Besides utilizing above mentioned fluorescent labels sensitive UV–VIS detection can also be achieved by the attachment of phenylic or benzoylic groups like DNP (2,4-dinitrophenyl) or DNB (3,5-dinitrobenzoyl) [35,36].

Concepts of introducing labels that additionally promote chiral recognition of AA derivatives can be exceptionally beneficial. This is the case for DNB derivatized amino acids on cinchona alkaloid selectors. These low molecular weight selectors offer the possibility of distinctive investigations on their enantioselective binding increments. As is depicted in Fig. 1, chiral recognition is achieved by π-donor–acceptor interactions with the π basic chinoline moiety, steric interactions with the tert-butyl group, ion pairing attraction to the tertiary quinuclidine nitrogen and hydrogen donor–acceptor interactions with the carbamate backbone of the cinchona selector [37–39]. The hydrogen bonding event of amide groups is a strongly directed interaction phenomenon and therefore particularly well suited for chiral discrimination processes. These interactions have been studied with NMR by the formation of diastereomeric selector–selectand complexes as well as by X-ray diffraction spectroscopy of a co-cristallizate [40]. By the reaction of amino acids with succinimidyl ferrocenyl propionate an amide group is created and a π–π interaction site is introduced, thereby supporting the present enantiorecognition mechanism. The analogy of FP to DNB protected amino acids is depicted in Fig. 1.

Also for various MS techniques it is useful to introduce chemical tags with special MS fragmentation properties. In tandem MS experiment tags like iTraq™ with easily identifiable fragments that also allow direct quantitation have been established originally for peptide quantitation and are commercially available [41]. It is of eminent importance for enantioselective analysis that, whatever derivatization method is applied, no racemization of the investigated analytes occurs through sample manipulation. The main strength of mass spectrometric detection lies in its high sensitivity in combination with the very valuable information of analyte mass and specific fragmentation pattern.

As indicated above, in liquid chromatographic analysis especially the strategy of N-derivatizing amino acids seems advantageous. To now, several methodologies for amino acid identification and quantitation in biological matrices with individual strengths and drawbacks have been introduced and specific instrumentation and materials for detection and derivatization are commercially available [42]. Recently Karst et al. published on the derivatization of biogenic amines with the newly developed hydroxy succinimidyl esters of various ferrocenes [43–45]. The introduction of an in house synthesized ^{58}Fe containing label was used for LC-ICP–MS and LC-ESI–MS measurements of amino acids, peptides and proteins in biological samples [46].

In the present study we investigated the applicability of iron(II) ferrocenyl hydroxy succinimdyl propionate (SFP reagent) as a non-chiral label supporting (i) the enantioseparation of amide type amino acid derivatives using our cinchona alkaloid based anion exchanger CSPs and (ii) to act as a label for sensitive tandem MS detection that moreover is UV active. Hence, it was the aim of our studies to take advantage of the synergism from the enantioselective separation of the amino acid derivatives and the specific SRM detection principle in MS applying only one single chromatographic dimension.

2. Experimental

2.1. Materials

Methanol was of HPLC gradient grade and obtained from VWR (Vienna, Austria). The water for derivatization and for mobile phase was purified in house by a millipore purification system. The eluent buffer ammonium formate was purchased from Sigma–Aldrich at MS grade (99.995%), as was formic acid (98–100%, ACS reagent). For the derivatization of the amino acids 0.1 molar HCl (Sigma–Alrich) was used. Iodoacetamide was bought from Fluka (Buchs, Switzerland) with purity higher than 98%. The SFP (succinimidyl ferrocenyl propionate) reagent was a kind donation from the research group of Prof. Uwe Karst (Münster, Germany). Amino acids of analytical grade were obtained from Bachem (Bubendorf, Switzerland) or Sigma–Aldrich (St. Louis, MO, USA) in single enantiomer as well as in racemic form and all of them were of analytical grade. The deuterated alanine (L-Ala-2,3,3,3-d_4) was ordered from Cambridge Isotope Laboratories, Inc. (Andover, MA, USA) and its purity was 98 at.%. The chromatographic HALO sub 3 μm silica-based fused core support material was a gift from Advanced Technologies (Wilmington, DE, USA). The particle diameter was 2.7 μm with 0.5 μm porous layer thickness around the 1.7 μm solid core. The mean pore size was 90 Å with 150 m^2 surface area per gram and a selector coverage of 180 μmol per gram.

2.2. LC–MS/MS instrument

All measurements were carried out on an Applied Biosystems (AB Sciex, Foster City, California) 4000 QTrap, a hybrid triple quadrupole mass spectrometer equipped with a linear ion trap as the third quadrupole. ESI source was a Turbo V^{TM} ionspray with an integrated heating device to increase ionisation efficiency. The HPLC system utilized in the LC–MS coupling was an Agilent 1200 system (Waldbronn, Germany) equipped with degasser, binary pump, thermo stated column compartment and thermo stated autosampler. The software used for instrument control and data evaluation was Analyst 1.5.

2.3. LC-instrument

Initial method development was carried out on an Agilent 1200 HPLC system (Waldbronn, Germany) equipped with degasser, binary pump, thermo stated column compartment and a diode array detector. Data evaluation and instrument control were carried out by Agilent ChemStation Rev.B.04.01.

2.4. Selector immobilization on fused core HALO materials

The HALO silica material was modified similarly to our previously published protocol [47]. Accordingly, we modified the HALO silica support with (3-mercaptopropyl)methyldimethoxysilane (1.5 mmol/g silica) in a first step by refluxing overnight in water-free toluene using dimethylaminopyridine (DMAP) as basic catalyst. Consequently, the chiral selector t-butyl-carbamoyl-quinidine (QD) (0.6 mmol/g silica) was exhaustively attached to the thiol groups by nucleophilic addition. This reaction was performed in methanol under reflux conditions for 7 h and in the presence of 2,2′-azobis(2-methylpropionitrile) (AIBN) (10 mol%) acting as radical starter. The resulting chiral stationary phase was packed in house into a 50 mm × 4 mm i.d. column.

2.5. Derivatization procedure of free amino acids

All amino acids were weighed in individually, dissolved in borate buffer (20 mM pH9) and adjusted to a concentration of 1.5 mM. 50 μL of these standard solutions was diluted with 400 μl borate buffer (pH 9) followed by vortex mixing with 50 μl of 5 mM hydroxy succinimidyl ferrocenyl propionate (SFP) solution in acetonitrile resulting in a roughly 4-fold molar excess. The reaction was performed at room temperature and lasted for 60 min. To assure completion the temperature was raised to 40 °C for another 30 min. The pH value was checked by indicator stripes and confirmed to stay pH9 over the reaction period. The reaction progress has initially been studied with leucine by quarter hourly drawing of aliquots of the reaction solution followed by injection to HPLC–UV. No further increase of the product peak area was observed after 60 min of reaction time, which we regarded as quantitative yield. Later studies showed same reaction kinetics also for other amino acids.

Cysteine modification was carried out by protecting first the –SH group with iodoacetamide. Therefore the 50 μL of the 1.5 mM stock solution of cysteine in 0.1 M HCl were mixed with 50 μL of a 15 mM iodoacetamide solution in ACN. After 15 min of shaking at room temperature 400 μL of borate buffer (20 mM, pH 9) was added and the reaction was started by adding of 50 μL of SFP (5 mM in ACN) in analogy to the general derivatization procedure.

For the measurement of amino acids in a biologically relevant matrix 50 μL of unprocessed urine were diluted 1:10 with borate buffer (20 mM, pH 9) and derivatization was carried out according to the procedure for amino acid standard solutions. In order to derivatize naturally occurring cysteine the urine sample was diluted 1:10 with 100 mM hydrochloric acid and 50 μL thereof were mixed with the 50 μL of 15 mM iodoacetamide in ACN. After 15 min of shaking at room temperature 400 μL of borate buffer (20 mM, pH 9) was added and reaction was started by adding 50 μL of SFP (5 mM in ACN). The basic pH 9 was checked by indicator stripes and was constant throughout the complete reaction time of 60 min.

All derivatized samples were diluted 1:100 with mobile phase prior to injection to the LC–MS system.

2.6. LC parameters

Initial HPLC method development was carried out on commercially available QN-AX (quinine based weak chiral anion exchanger) and QD-AX (quinidine based weak chiral anion exchanger) columns with 150 mm length, 4 mm inner diameter and 5 μm fully porous particles with a mean pore size of 120 Å (Chiral Technologies, Illkrich, France). The MS studies were finally carried out on a QD-AX core shell type CSP with 2.6 μm particles and 0.5 μm porous

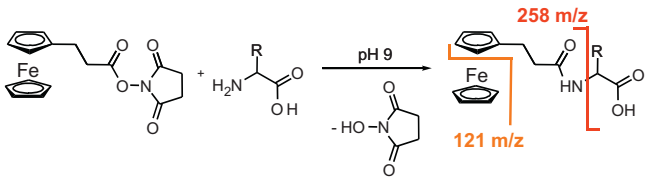

Fig. 2. Reaction scheme for the derivatization of amino acids with succinimidyl ferrocenyl propionate and characteristic MS/MS-fragments.

layer, 150 m^2 surface area per gram and a mean pore size of 100 Å. Column dimensions were 50 mm length with 4 mm inner diameter. The mobile phase composition was 90% methanol with 10% water and 100 mM ammonium formate/formic acid (26.5 mM or 0.1%, v/v) buffer. The flow rate during isocratic elution was adjusted to 700 μL min^{-1} in all cases and the injection volume was set to 5 μL.

2.7. MS parameters

All amino acids were derivatized separately and detection parameters for the reaction products were optimized individually by direct injection to the ESI interface with a syringe pump further utilizing the automated compound optimization function of the analyst software. The conditions for the electro spray ionization were as follows: electro sprayer voltage: +4500 V, curtain gas flow: 10 psi, nebulizer gas flow: 40 psi and drying gas flow 60 psi with a temperature of 650 °C, the entrance potential was set to 10 V for all analytes. The dwell time of every transition was set to 20 ms and including a switching time of 5 ms the overall cycle time was 1.44 s. The analyte specific potentials for the SRM (selected reaction monitoring) measurements are listed in Table 1.

3. Results and discussion

On anion exchanger type stationary phases and using polar organic mobile phases neutral and basic analytes usually elute at the front of the chromatographic run. Thus the N derivatization of amino acids is a common method to enhance the retention of originally zwitterionic amino acids on chiral anion exchangers. Protective groups that offer possibilities for additional interactions with cinchona type selectors (i.e. steric "bulkiness", π–π stacking, hydrogen donor-acceptor) can strongly enhance enantioselectivity. On the other hand the labels of the N-terminus of the amino acids could potentially give characteristic fragments in MS/MS experiments. Thus we carried out initial product ion scans with all the derivatized analytes (Table 2).

3.1. MS detection considerations

Out of all MS optimizations for the different amino acid derivatives two common fragment ions were found to a more or less high extent in all cases: 258 *m*/*z* with a generally higher abundance than 121 *m*/*z*. The 258 *m*/*z* fragment could be assigned to the cleavage of the N-Cα bond and therefore for the cleavage of the whole ferrocenyl propionate (FP) label. The fragment with 121 *m*/*z* most probably stems from the cleavage of one ferrocenyl ring and the central iron atom (view Fig. 2). The subsequently set up method was applied to analyse a mixture of the racemic amino acids alanine, valine, leucine and phenylalanine as shown in Fig. 3. All chromatographic peaks could be identified via the precursor ion mass. Further experiments on the improvement of sensitivity and analytical reliability led to the development of a selected reaction monitoring (SRM) method as can be seen on the right chromatogram of Fig. 3

Table 1
SRM transitions and instrument voltages applied for optimum signal intensities.

	Q1 Mass $[M+H]^+$ (Da)	Q3 Mass (Da)	DP_1	CE_2	CXP_3
Gly	315	232	61	39	18
	315	250	61	35	18
	315	204	61	45	30
Ala	329	73	71	103	12
	329	258	71	35	14
	329	218	71	43	12
Val	357	258	81	35	14
	357	174	81	47	10
	357	274	81	35	16
Leu/Ile	371	258	56	35	14
	371	288	61	37	16
	371	174	51	49	10
Trp	444	258	56	35	14
	444	333	56	47	18
	444	379	56	35	22
Ser	345	262	66	37	14
	345	258	66	37	14
	345	216	66	53	16
Cys + IAM	418	353	60	29	22
	418	218	60	43	54
	418	121	60	103	20
Arg	415	350	51	23	24
	415	332	51	39	28
	415	290	51	39	14
Glu	387	322	61	35	18
	387	193	61	51	10
	387	121	61	89	20
His	396	330	51	25	18
	396	284	51	45	14
	396	199	51	55	10
Thr	359	258	51	35	14
	359	232	51	45	18
	359	204	51	49	16
Tyr	421	309	58	47	20
	421	173	58	59	12
	421	147	58	75	12
Phe	405	340	51	33	22
	405	192	51	47	8
	405	174	51	51	8
Asp	373	258	26	31	14
	373	121	26	89	20
	373	193	26	55	10
Lys-2xFP	627	561	86	33	14
	627	275	86	61	14
	627	495	86	45	12
d4-Ala	333	222	46	45	14
	333	250	46	37	16
	333	194	46	51	10
Gln	386	321	51	31	18
	386	193	51	53	10
	386	258	51	45	14
Met	389	324	56	33	18
	389	258	56	37	14
	389	306	56	37	16
Asn	372	258	56	33	14
	372	307	56	29	18
	372	218	56	49	12
Pro	355	290	96	37	16
	355	244	96	47	14
	355	127	96	25	8

DP, declustering potential; CE, collision energy; CXP, cell exit potential.

Table 2
Chromatographic retention factors and selectivity coefficients for chiral proteinogenic amino acids.

FP amino acid	k (L)	k (D)	α (D/L)
Ala	1.52	2.84	1.87
Val	1.42	4.48	3.15
Leu	1.60	3.58	2.24
Ile	1.60	5.18	3.24
Arg[a]	0.48	0.94	1.96
Asn	1.72	2.82	1.64
Asp	5.44	6.70	1.23
Gln	1.42	2.40	1.69
Glu	2.96	5.78	1.95
CysIAM	2.04	4.08	2.00
His[a]	0.66	1.16	1.76
Thr	1.54	3.68	2.39
Ser	1.76	3.30	1.88
Met	2.54	6.28	2.47
Phe	3.20	7.92	2.48
Tyr	2.58	5.98	2.32
Trp	5.42	14.52	2.68
Pro	1.86	2.32	1.25
Lys	4.48	8.48	1.89
d4-Ala	1.44	2.72	1.89

[a] Partial resolution.

3.2. Chromatographic selectivity

All amino acids have been injected in separate solutions and also in a mix containing all 20 investigated analytes (all proteinogenic amino acids without glycine including deuterated alanine). Comparison of these data sets showed that there is no significant influence of other amino acids being present in the mixture in terms of enantioselectivity. We could achieve enantioselective baseline separation in all cases except for arginine, histidine and proline. Whilst the former two were at least partially resolved, there was no separation at all for proline. It can be explained mechanistically by the lack of any hydrogen donor site on the secondary amide N and therefore this amino acid offers no possibility for the formation of this crucial directed interaction with the quinine/quinidine selector (see Fig. 1).

It can further be seen that on the column with the QD selector the L-enantiomer of the investigated amino acid derivatives was always the first to elute, which would be reversed on QN based CSP. Furthermore, most of the L-AAs elute in the k range of 1.0–2.5, which is well in accordance to previously published data on chiral recognition with cinchona alkaloid selectors [38,40]. There is generally a bigger difference in the k values for the D-enantiomers and therefore the chemoselective separation of the different amino acid derivatives is better. Simultaneously and via enhanced retention times the analyte molecules are separated from potentially interfering matrix components, which may be crucial for ESI-MS detection. This was the rationale for applying the QD related selector rather than QN based CSP for our studies. This seems somewhat in contrast for the analysis of trace amounts of D-AAs where it is preferential to have the minor peak eluted before the largely abundant L-AA peak. For the present case, reversal of elution order can be achieved by the application of the QN selector. In Fig. 4 the original MS measurement that has been evaluated for these data can be seen.

3.3. Control of racemization

Initially the influence of the derivatization reaction was investigated to elucidate very sensitively whether or not any racemization of the amino acids occurs. Therefore samples of L-valine and L-cysteine have been spiked with varying amounts of the corresponding D-enantiomers. We added 5%, 1%, 0.5% and 0.1% of the D-forms and derivatized the mixtures as well as the single L-enantiomers in order to see if any D-peak appears in later measurements. The reaction for valine and cysteine was carried out according to the standard protocols (see experimental part). In no case we could observe an increase of the D-amino acid amount and in the case of pure L-valine and L-cysteine no peak for the respective D-enantiomer could be detected. This indicates also that these two standards were of very high enantiomeric excess and the enantiomeric impurities were lower than the limit of detection for valine and cysteine being 1 and 10 μmol L^{-1}, respectively.

3.4. Calibration of the method

The single amino acids have been weighed in to yield stock solutions and from those a 9-point calibration curve was generated by dilution in no more than three consecutive steps. The concentration range was between 1 μmol L^{-1} and 500 μmol L^{-1} of amino acid in water. To the amino acid solutions $^2D_4$–L-alanine was added as an internal standard in a concentration of 5 μmol L^{-1}. For these solutions derivatization procedure was carried out according to the standard protocol (see above) and after a final 1:100 dilution step with the mobile phase all samples were injected to the LC–MS system and measured with the standard method (including the complete set of 3 SRM transitions for each of the 19 investigated amino acids). Evaluation of the data showed linear dependence of the regression functions for all measured 19 amino acids (glycine was not measured) with linearities ranging from 0.961 (Asp) to 1.000 (Phe). From this calibration curve also lower limit of quantitation (LLOQ) values were determined for all

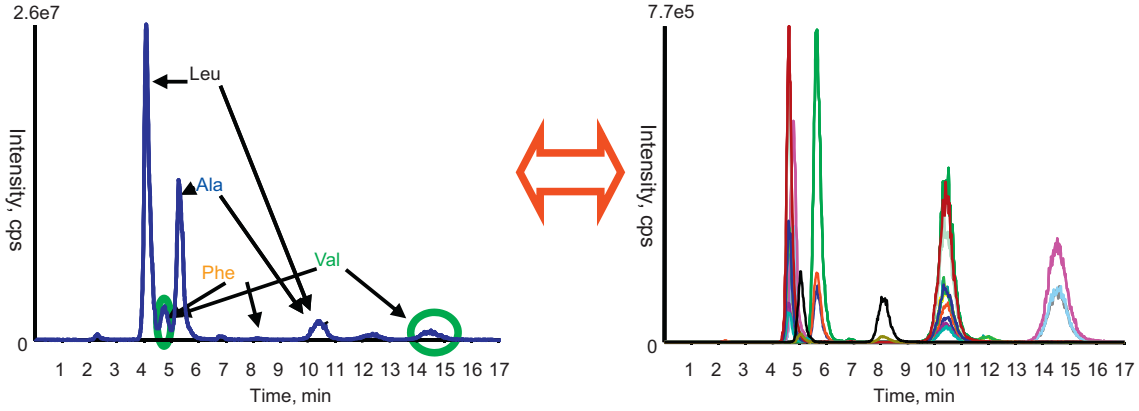

Fig. 3. Amino acid derivatives: precursor ion scan of 258 m/z, positive mode compared to SRM in positive mode, amino acid concentration: 50 μmol L^{-1}, column: HALO-QD-AX, enantiomer elution order: L before D; mobile phase 9/1 MeOH/H_2O, 100 mM NH_4FA, 0.1% FA.

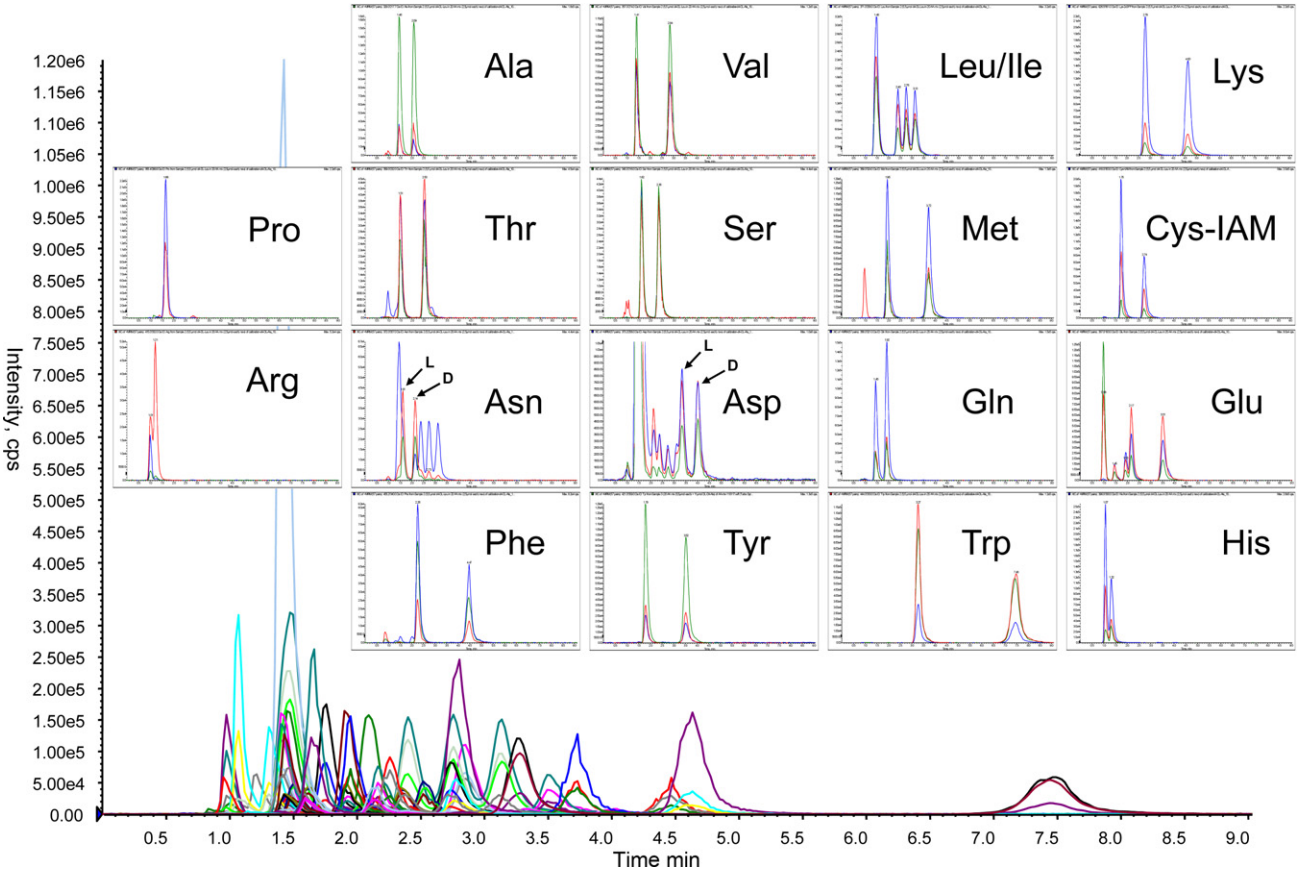

Fig. 4. SRM run of 19 derivatized racemic amino acids, 50 μmol L^{-1} individual amino acid concentration, stat. ph.: HALO-QD-AX 50 mm × 4 mm i.d., mob. ph.: 9/1 MeOH/H_2O, 100 mM NH_4FA; 0.1% FA, flow 700 μl min^{-1}.

analytes, which are listed in Table 3. The minimal requirement for quantitation was a signal to noise ratio of 1:10 and accordingly the limits of detection (LOD) were determined to be one-third of the presented LLOQ values (data not shown). It has to be mentioned, though, that we observed ion suppression phenomena when we injected mixtures of D-amino acids. Typically, the suppression is highest for coeluting amino acids and up to 10% at concentrations of 5 μmol L^{-1} and it is even more pronounced at higher concentrations. Therefore, the use of individual isotope labelled internal standards for each AA enantiomer to be quantified is strongly recommended.

3.5. *Spiking experiments of* L*-AAs with* D*-AAs*

The capability of our chromatographic method in determining minor impurities of D-amino acids in vast excesses of their corresponding L-forms has been investigated. Exemplarily derivatized samples of L-aspartic acid, L-serine, L-cysteine and L-leucine have been spiked with low amounts of the corresponding D-amino acid derivatives. In all cases ratios as low as 0.03% D in 99.97% of L could be detected, if present. The lowest amount of a derivatized D-amino acid absolutely injected on column was calculated for D-cysteine to be 540 femtomol (as can be seen in Fig. 5).

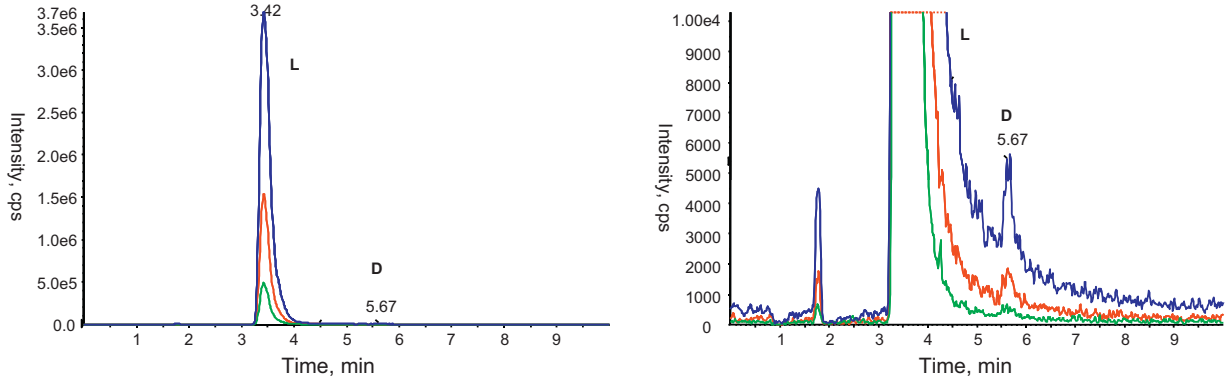

Fig. 5. Separation of iodoacetamido-D-cysteine from its L-enantiomer, Cys concentration: 36 μmol L^{-1}, ratio: L 99.97%: D 0.03%, stat.Ph.: HALO-QD-AX 50 mm × 4 mm i.d., mob. ph.: 9/1 MeOH/H_2O, 100 mM NH_4FA; 0.1% FA, flow 700 μl min^{-1}.

Table 3
Calibration parameters calculated for the 19 AAs as well as lower limits of quantification.

$y = kx + d$	k	d	R^2	LLOQ [μmol L^{-1}]
Ala	0.0383	0.369	0.983	0.5
Val	0.0235	0.082	0.999	1
Leu	0.0282	0.583	0.987	0.5
Ile	0.0300	−0.048	0.998	1
Arg[a]	0.0091	0.017	0.995	2.5
Asn	0.0113	0.022	0.998	2.5
Asp	0.0067	0.039	0.961	5
Gln	0.0600	−0.415	0.964	1
Glu	0.0159	−0.036	0.995	1
CysIAM	0.0061	0.004	0.999	10
His[a]	n.d.	n.d.	n.d.	0.5
Thr	0.0080	0.088	0.977	1.25
Ser	0.0193	0.227	0.930	1.25
Met	0.0262	0.325	0.988	1.25
Phe	0.0141	0.001	1.000	2.5
Tyr	0.0312	0.067	0.998	1.25
Trp	0.0704	0.244	0.987	1
Pro	0.0097	0.009	0.997	1
Lys	0.0640	−0.172	0.992	0.5

[a] Partial separation.

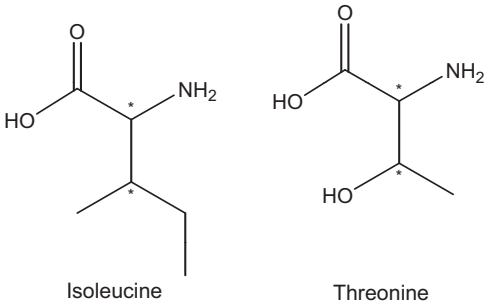

Fig. 6. Molecular structures of Ile and Thr (asterisks indicate the stereogenic centres).

3.6. Analysis of amino acid isomers

Leucine (Leu) and isoleucine (Ile) pose a challenge to chromatographic separation and are indistinguishable through MS detection (Fig. 6). We did not find significant differences in the relative fragment ion intensities; therefore, it is mandatory to separate the analytes prior to MS detection. Using the standard chromatographic conditions we could not separate L-Leu from L-Ile; however, D-Leu

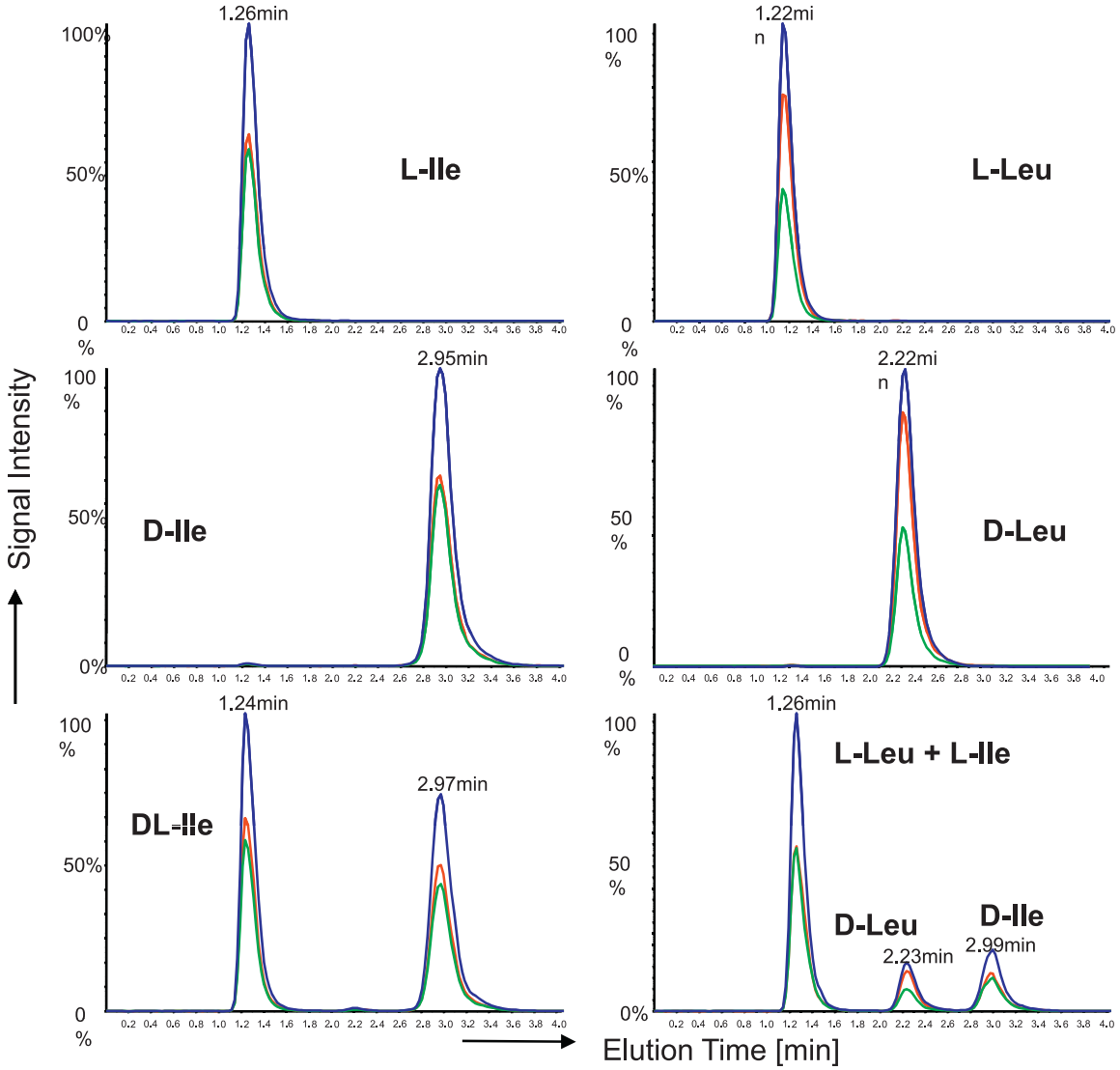

Fig. 7. LC–MS/MS measurements in SRM mode of leucine and isoleucine isomers, stat. ph.: HALO-QD-AX 50 mm × 4 mm i.d., mob. ph.: 9/1 MeOH/H_2O, 100 mM NH_4FA; 0.1% FA, flow 700 μl min^{-1}.

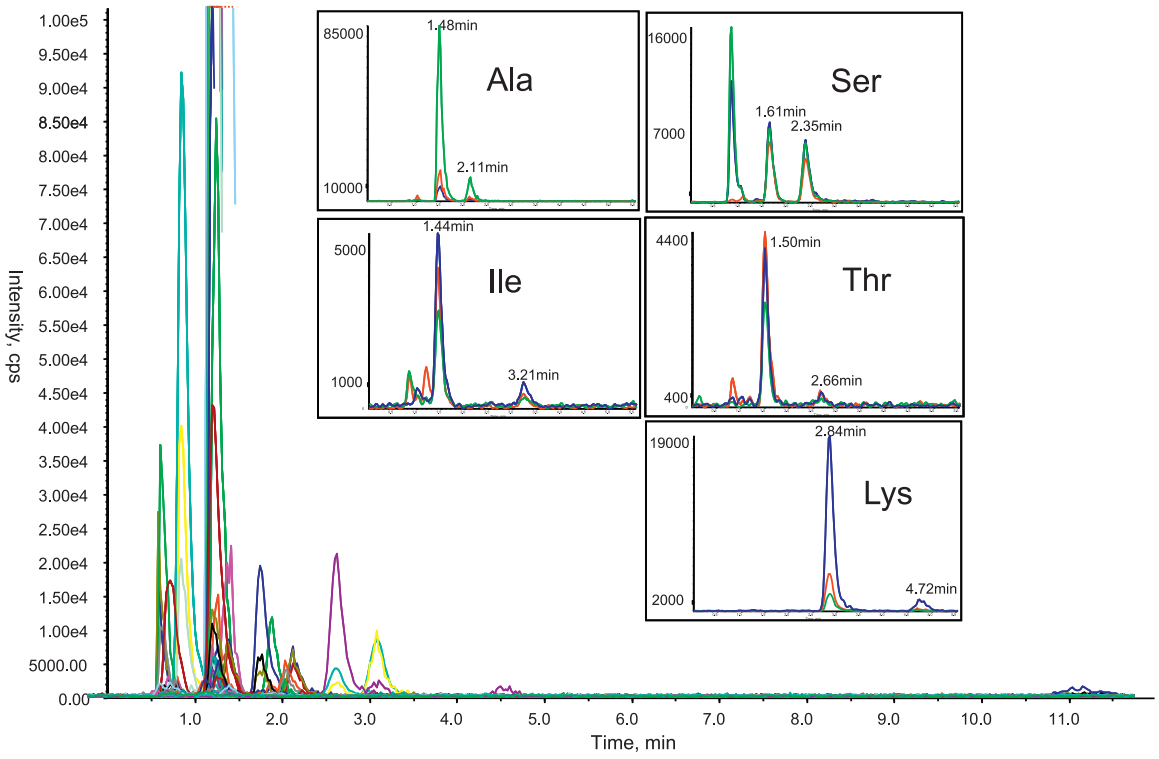

Fig. 8. LC-SRM measurement of human urine after derivatization with SFP, 5 D-amino acids identified, stat. ph.: HALO-QD-AX 50 mm × 4 mm i.d., mob. ph.: 9/1 MeOH/H_2O, 100 mM NH_4FA; 0.1% FA, flow 700 μl min^{-1}.

and D-Ile were resolved (see Fig. 7). To solve this specific problem we applied the home made HALO-QD-AX-CSP, which is based on the identical selector and immobilization protocol as the commercially available QD-AX column but immobilized on highly efficient fused core chromatographic support material. This enabled us to baseline separate the stronger retained D-enantiomers through the chromatographic selectivity. If the same samples were injected to the corresponding HALO-QN-AX-CSP reversal of elution order was observed and the L-enantiomers of Leu and Ile were separated (data not shown). In this case, it can be seen that chromatographic separation offers complementary selectivity where a differentiation via mass spectrometry alone is not possible. However, injecting the allo-form of isoleucine we could only achieve enantioselectivity regarding the chiral centre of Cα and therefore we observed coelution of allo-Ile with D- or L-isoleucine, respectively.

Threonine also possesses a second chiral centre and thus was studied with respect to its chromatographic resolvability. Similar to the observations for Ile we also could not separate D-Thr from D-allo-Thr nor L-Thr from L-allo-Thr with our chromatographic method.

3.7. Application of the method for urine analysis

As a proof of principle and to demonstrate the applicability of the presented method to biologically relevant liquids we carried out the SFP derivatization concept for unprocessed human urine and measured the samples directly without any preconcentration step. By the use of anion exchange chromatography and utilizing polar organic mobile phases uncharged matrix compounds and such with positive charges elute with the front of the chromatographic run and are separated from the acidic and thus stronger retained analytes. In one single measurement the L-enantiomers of 16 amino acids (all proteinogenic AAs except Asn, Asp, Pro, Cys-IAM) could be identified. In the cases of alanine, lysine, serine, threonine and isoleucine also the D-enantiomers were found in significant amounts in urine (as shown in Fig. 8). D-Leucine was not identified. There was an exceptionally high relative amount of D-serine present indicating a peak area ratio of 52% L-Ser to 48% D-Ser.

4. Conclusion

In this contribution we present a one-dimensional chromatographic method that offers good enantioselectivity for most proteinogenic amino acids. The chromatographic resolution power together with MS selectivity and sensitivity pose an efficient symbiosis for analyzing complex mixtures after a simple derivatization procedure. The active ester of hydroxy succinimidyl ferrocenyl propionate reacts readily with different kinds of biogenic amines and forms stable reaction products. Its application as a label for amino acid analysis is firstly beneficial supporting the enantioselectivity on cinchona type chromatographic selectors and secondly it is an outstanding MS tag for fragmentation experiments. We could achieve chromatographic selectivity where a differentiation in MS was not possible due to the same molecular mass (as shown for leucine/isoleucine). Furthermore in most cases the highly selective SRM method allowed us to detect coeluting derivatives of different amino acids side by side. The low limits of MS detection offer the capability of the presented method to determine amino acid concentrations in the low micro mol per liter range. We could also show good linear response throughout the biologically relevant concentration ranges of D-AAs [20]. We herein want to state that this method is adapted for the absolute quantification of D-AAs that is only limited by the MS detection sensitivity and independent of the excess of the corresponding L enantiomers, given that the chromatographic peaks are baseline separated. Finally, the application of our method to urine as a real sample revealed that several D-amino acids are present and can easily be analysed without any prior analyte enrichment step.

Acknowledgements

We want to thank Professor Uwe Karst and Susanne Bomke from the University of Münster, Germany, for the kind donation of their self-synthesized derivatizing reagent. Dr. DeStefano from Advanced Technologies is highly acknowledged for supporting us with the fused core silica material that was the stationary phase support material for the HALO-QD column.

Lucie Hartmanova thanks for the support by the Operational Program Research and Development for Innovations – European Social Fund (CZ.1.05/2.1.00/03.0058, MSMT, Czech Republic) and by Palacky University (PrF_2011_025).

References

[1] A. Hashimoto, T. Oka, T. Nishikawa, Neuroscience 66 (1995) 635.
[2] A. Hashimoto, T. Oka, Prog. Neurobiol. 52 (1997) 325.
[3] H. Wolosker, S. Blackshaw, S.H. Snyder, Proc. Natl. Acad. Sci. U.S.A 96 (1999) 13409.
[4] K. Hashimoto, T. Fukushima, E. Shimizu, S.I. Okada, N. Komatsu, N. Okamura, K. Koike, H. Koizumi, C. Kumakiri, K. Imai, M. Iyo, Prog. Neuropsychopharmacol. Biol. Psychiatry 28 (2004) 385.
[5] K. Hashimoto, T. Fukushima, E. Shimizu, N. Komatsu, H. Watanabe, N. Shinoda, M. Nakazato, C. Kumakiri, S.I. Okada, H. Hasegawa, K. Imai, M. Iyo, Arch. Gen. Psychiatry 60 (2003) 572.
[6] H. Wolosker, A. D'Aniello, S.H. Snyder, Neuroscience 100 (2000) 183.
[7] A. D'Aniello, P. Spinelli, A. De Simone, S. D'Aniello, M. Branno, F. Aniello, G.H. Fisher, M.M. Di Fiore, R.K. Rastogi, FEBS Lett. 552 (2003) 193.
[8] S. D'Aniello, G.H. Fisher, E. Topo, G. Ferrandino, J. Garcia-FernÃ ndez, A. D'Aniello, BMC Neurosci. 8 (2007).
[9] A. Morikawa, K. Hamase, T. Ohgusu, S. Etoh, H. Tanaka, I. Koshiishi, Y. Shoyama, K. Zaitsu, Biochem. Biophys. Res. Commun. 355 (2007) 872.
[10] E.H. Man, G.H. Fisher, I.L. Payan, J. Neurochem. 48 (1987) 510.
[11] L. Pollegioni, L. Piubelli, S. Sacchi, M.S. Pilone, G. Molla, Cell. Mol. Life Sci. 64 (2007) 1373.
[12] M. Friedman, Chem. Biodivers. 7 (2010) 1491.
[13] I. Gandolfi, G. Palla, L. Delprato, F. De Nisco, R. Marchelli, C. Salvadori, J. Food Sci. 57 (1992) 377.
[14] J. Schormueller, J. Weder, Nahrung 6 (1962) 622.
[15] K. Hamase, A. Morikawa, S. Etoh, Y. Tojo, Y. Miyoshi, K. Zaitsu, Anal. Sci. 25 (2009) 961.
[16] A. Berthod, Y. Liu, C. Bagwill, D.W. Armstrong, J. Chromatogr. A 731 (1996) 123.
[17] C.V. Hoffmann, R. Reischl, N.M. Maier, M. Laemmerhofer, W. Lindner, J. Chromatogr. A 1216 (2009) 1157.
[18] C.V. Hoffmann, R. Reischl, N.M. Maier, M. Laemmerhofer, W. Lindner, J. Chromatogr. A 1216 (2009) 1147.
[19] C. Desiderio, F. Iavarone, D.V. Rossetti, I. Messana, M. Castagnola, J. Sep. Sci. 33 (2010) 2385.
[20] H. Bruckner, A. Schieber, Biomed. Chromatogr. BMC 15 (2001) 166.
[21] L. Kirschner Daniel, K. Green Thomas, J. Sep. Sci. 32 (2009) 2305.
[22] V.A. Davankov, Enantiomer 5 (2000) 209.
[23] B. Natalini, R. Sardella, A. Macchiarulo, R. Pellicciari, J. Sep. Sci. 31 (2008) 696.
[24] M. Laemmerhofer, J. Chromatogr. A 1217 (2010) 814.
[25] G. Torok, A. Peter, F. Fulop, Chromatographia 48 (1998) 20.
[26] G. Tan, J.Y. Xue, M.H. Hyun, J. Sep. Sci. 29 (2006) 1407.
[27] N. Grobuschek, M.G. Schmid, J. Koidl, G. Gubitz, J. Sep. Sci. 25 (2002) 1297.
[28] N. Nimura, H. Ogura, T. Kinoshita, J. Chromatogr. 202 (1980) 375.
[29] K. Imai, Y. Watanabe, Anal. Chim. Acta 130 (1981) 377.
[30] K. Muramoto, H. Kamiya, H. Kawauchi, Anal. Biochem. 141 (1984) 446.
[31] R. Hanczko, A. Jambor, A. Perl, I. Molnar-Perl, J. Chromatogr. A 1163 (2007) 25.
[32] S. Einarsson, B. Josefsson, S. Lagerkvist, J. Chromatogr. A 282 (1983) 609.
[33] I. Ilisz, R. Berkecz, A. Peter, J. Pharm. Biomed. Anal. 47 (2008) 1.
[34] Y. Tapuhi, D.E. Schmidt, W. Lindner, B.L. Karger, Anal. Biochem. 115 (1981) 123.
[35] W.H. Pirkle, M.H. Hyun, J. Chromatogr. A 322 (1985) 287.
[36] S. Wongyai, P. Oefner, G. Bonn, Biomed. Chromatogr. 2 (1988) 254.
[37] M. Laemmerhofer, P. Franco, W. Lindner, J. Sep. Sci. 29 (2006) 1486.
[38] N.M. Maier, L. Nicoletti, M. Lammerhofer, W. Lindner, Chirality 11 (1999) 522.
[39] A. Mandl, L. Nicoletti, M. LÃ¤mmerhofer, W. Lindner, J. Chromatogr. A 858 (1999) 1.
[40] N.M. Maier, S. Schefzick, G.M. Lombardo, M. Feliz, K. Rissanen, W. Lindner, K.B. Lipkowitz, J. Am. Chem. Soc. 124 (2002) 8611.
[41] H. Kaspar, K. Dettmer, W. Gronwald, P.J. Oefner, Anal. Bioanal. Chem. 393 (2009) 445.
[42] H. Kaspar, K. Dettmer, Q. Chan, S. Daniels, S. Nimkar, M.L. Daviglus, J. Stamler, P. Elliott, P.J. Oefner, J. Chromatogr. B: Analyt. Technol. Biomed. Life Sci. 877 (2009) 1838.
[43] S. Bomke, B. Seiwert, L. Dudek, S. Effkemann, U. Karst, Anal. Bioanal. Chem. 393 (2009) 247.
[44] B. Seiwert, U. Karst, Anal. Bioanal. Chem. 390 (2008) 181.
[45] B. Seiwert, U. Karst, Anal. Chem. 79 (2007) 7131.
[46] S. Bomke, T. Pfeifer, B. Meermann, W. Buscher, U. Karst, Anal. Bioanal. Chem. 397 (2010) 3503.
[47] M. Laemmerhofer, W. Lindner, J. Chromatogr. A 741 (1996) 33.

Appendix C

Methoxyquinoline labelling - a new strategy for the enantioseparation of all chiral proteinogenic amino acids in 1-dimensional liquid chromatography using fluorescence and tandem mass spectrometric detection

Reischl, Roland J.; Lindner, Wolfgang*

University of Vienna, Department of Analytical Chemistry, Währingerstrasse 38, 1090 Vienna, Austria

* Corresponding author: Tel.: +43 1 4277 52300; Fax +43 1 4277 9523
e-mail: wolfgang.lindner@univie.ac.at

Abstract

The determination of trace amounts of D – amino acids (D-AAs) even in tissue samples of higher developed animals, mammals and humans has opened a wide field of biological questions to be investigated. D-Ala, D-Asp and D-Ser have already been identified to exhibit key functions in cellular regulation processes [1-4]. The abundance of trace amounts of these and also of other D-AAs in various biological fluids and in tissue samples is still being investigated. We herein present a facile derivatization method for amino acids with the 6-methoxyquinoline-4-carboxylic acid-succinimide ester (MQ-OSu) to yield the corresponding stable N-acyl-amino acids (MQ-AAs). Labelling with the MQ tag supports the enantioseparation of all 19 chiral proteinogenic amino acids on anion exchanger type chiral stationary phases, introduces fluorescence activity and particularly promotes sensitive electro spray tandem mass spectrometric detection. LOD values for MQ-L-Ala in water were 1.25µmol L^{-1} with fluorescence detection and 0.015µmol L^{-1} with MS in selected reaction monitoring (SRM) mode. The applicability of this method for the analysis of MQ-D-AAs in biological fluids has been demonstrated.

Keywords: enantioselective chromatography; chiral amino acid analysis; LC-MS/MS; fluorescence labelling; methoxyquinoline tag

1. Introduction

The identification of D - amino acids (D-AAs) in higher developed organisms has led to a paradigm shift in the scientific community. Nowadays it is well accepted that also the D - enantiomers of these fundamentally important biomolecules not only occur, but are even enzymatically produced in humans. The endogenous generation of D-AAs occurs via enzymatic racemization of the corresponding L – amino acids (L-AAs). Currently, two racemases are known to synthesize D–AAs in the human organism: serine racemase and aspartate racemase [5]. For down regulating D–AA levels D – amino acid oxidases have been described [6,7]. Furthermore, D-Ser, D-Ala and D-Asp have been investigated and determined in several mammalian tissues including the brain and the liver [4]. Until now, D – Asp is the only D-AA, which has been identified within proteins and is believed to be formed by deamidation of Asn due to oxidative stress [8,9]. Those D-AAs that are enzymatically synthesized fulfil distinct biological functions, of which some have been described and several others still are under investigation. In this context D-Ser is involved in neurotransmission processes and it is known to be a co-agonist for the synaptic N-methyl-D-aspartate receptor (NMDAR). Its function in the regulation of NMDAR also causes inflictions in neurodegenerative diseases like schizophrenia [4]. D-Ala is reportedly involved in insuline production in rat pancreatic cells [1] and D-Asp plays a key role in the suppression of melatonin excretion and in the promotion of prolactine and testosterone production [2,3]. Still not everything is known about the involvement of other D-AAs in physiological processes and research in this field is strongly connected to methodological advances in analytical chemistry.

In this context the sensitive enantioselective measurement of free amino acids in complex matrices such as biological samples remains a challenge. Therefore, reliable methods were sought, which may combine the simplicity of sample preparation with improved separation performance. Various ways for the chemoselective and enantioselective separation and detection of amino acids in biological samples have been published [2,10,11], multidimensional approaches like comprehensive 2-D-GC [12], 2-D-LC [13] or 2-D-CE [14] and also chip-CE based applications proved particularly promissing [3]. For LC methods, often labelling strategies with fluorescent tags like 4-fluoro-7-nitrobenzo-2-oxa-1,3-diazol (NBD-F)

[15], orthophthal-dialdehyde (OPA) [16] or fluoresceine isothiocyanate (FITC) [17] are applied to enhance detection sensitivity. However, the setup of analysis methods, which include fluorescent tagging and multi dimensional separations can be time consuming and the derivatization reactions require skilful handling, often under light protection.

Laser induced fluorescence (LIF) detection offers striking sensitivity and ESI mass spectrometry usually can not fully challenge the very low limits of detection (LOD). On the other hand, mass spectrometry (MS) has a much broader field of application, very high selectivity and may suffer of only slightly lower sensitivity. This problem can be overcome by the chemical introduction of easily ionizable tags that deliver highly abundant MS/MS fragments like nicotinyl-, dansyl- or quinolinyl-analogues [18].

Besides improving the detectability of analytes, chiral as well as non chiral labelling strategies may be employed to strongly enhance chromatographic chemoselectivity and enantioselectivity. The application of low molecular weight chiral selectors in chromatography facilitates targeted approaches to introduce selectivity propagating molecular tags on the analyte side. Because of their well defined interaction sites cinchona alkaloid based chiral selectors and CSPs acting as enantioselective anion exchangers are particularly well suited for systematic studies of stereoselective interactions [19,20]. In Figure 1 some possible selector – selectand interactions are illustrated. Especially directed interactions such as hydrogen bonding and $\pi - \pi$ stacking have proven valuable for enhancing the enantioselectivity of CSPs like the quinine and the quinidine type anion exchangers (QN-AX and QD-AX). Moreover, the QN-AX CSP and the QD-AX CSP show pseudo enantiomeric behaviour and therefore their affinity for N-acyl amino acid enantiomers is opposed. Thus, under given conditions and with rare exceptions, the D-enantiomers of N-acyl amino acids elute before the corresponding L-congeners on the QN-AX CSP and vice versa L-elute before D – enantiomers on QD-AX CSPs.

<Figure 1>

Along that line, we previously investigated the potential of an N-acyl-bound metalloferrocene tag to promote chemoselective and enantioselective separation of most chiral proteinogenic amino acids and to enhance MS/MS detection sensitivity [21]. The present work focussed on further improvements regarding the labelling concept for all individual chiral proteinogenic amino acids in order to be able to separate and to sensitively quantify them. Therefore we investigated the 6-methoxyquinolinoyl group, as a tag that allowed for combining the simplicity of 1–dimensional chromatography with the sensitivity of inducible fluorescence and the specificity of MS/MS detection.

2. Materials & Methods

2.1 Chemicals

Methanol (MeOH) and acetonitrile (ACN) were purchased from VWR (Vienna, Austria) in gradient grade quality. The water used in our studies was in house purified with a Millipore Milli Q^R Direct purification system and had a resistivity of 18.2 MΩ cm at 25°C. Ammonium formate of MS grade (99.995%) and formic acid (98–100%, ACS reagent) were provided by Sigma–Aldrich. Deuterated alanine (L-Ala-2,3,3,3-d_4) was bought at Cambridge Isotope Laboratories, Inc. (Andover, MA, USA) at a purity of 98 atom%. 6-Methoxyquinoline-4-carboxylic acid was supplied by InnoChemTech GmbH, Braunschweig, Germany. Dichloromethane (CH_2Cl_2) was of technical grade. The silica gel used for flash chromatography was Normalsil (40 – 63µm) from VWR (Vienna, Austria). The plates for thin layer chromatography (TLC) were Silica Gel 60 F254 from Merck (Darmstadt). N-hydroxysuccinimide (97%) and Dicyclohexylcarbodiimide (99%) were from Fluka (Buchs, Switzerland). All amino acids were purchased in analytical quality from Bachem (Bubendorf, Switzerland) and Sigma Aldrich (St. Louis, USA).

2.2 Synthesis of 6-Methoxyquinoline-4-carboxylic acid-N-succinimdylester (MQ-OSu)

An amount of 406mg of 6-methoxyquinoline-4-carboxylic acid (2mmol) was slurried in 50mL of absolute CH_2Cl_2 together with 620 mg dicyclohexyl carbodiimide (3mmol).

350mg of N – hydroxysuccinimide (3mmol) was added and the cloudy yellow mixture was then stirred at 25°C over night with a $CaCl_2$ filled drying tube attached. To remove the precipitated dicyclohexyl urea the mixture was filtrated through a paper filter. The clear solution was applied onto a silica column and purified by elution with 3:1 CH_2Cl_2 : ACN. The fractions containing the product were identified with silica TLC with the same solvent composition (R_f value = 0.43), unified and evaporated to dryness. Thereby a pale yellow, fine powdery product was isolated (440mg, 71% yield). Characterization was done by LC-MS: $[M+H]^+$ = 301 m/z and NMR: ^{1}H-NMR bands [$CDCl_3$] at 400 MHz: δ = 3.0ppm (2 CH_2, s), 4.0ppm (OCH_3, s), 7.50ppm (H^6, q, J^3=9.3 Hz, J^4=2.7Hz), 8.07ppm (H^5, d, J=2.7Hz), 8.11ppm (H^3, d, J=4.5Hz), 8.15ppm (H^7, d, J=9.3Hz), 8.94ppm (H^2, d, J=4.5Hz)

2.3 Derivatization of Amino Acids

Out of amino acid stock solutions (c=1mM in water) 100µL was dissolved in 800µL of 20mM borate buffer (pH 9), 50µL of MQ-OSu (100mmol in ACN) was added and the mixture was shaken for 45 minutes at room temperature. For quantitatively derivatizing all amino groups of the AAs another 25µL of the reagent solution was added, the temperature was then increased to 40°C and the samples were shaken for additional 30min. After the end of the reaction period 20µL of formic acid was added and thereby the sample was prepared to be injected.
In cysteine the –SH group had to be protected prior to N-derivatization with MQ-OSu. Therefore 50µL of a 0.15mM cysteine stock solution was mixed with 50µL of 0.1M HCl, thereafter 50µL of iodoacetamide (c=15mM in ACN) was added. After shaking, the mixture was left to react in the darkness for 15min at room temperature. Thereafter 800µL of borate buffer (20mM, pH 9) and 100µL of the MQ-OSu (100mM in ACN) were added and the derivatization was carried out by shaking 45 minutes at room temperature and 15min at 40°C. Reaction was stopped acidifying with 20µL of formic acid.

2.4 Instrumentation

All HPLC analyses were performed with an Agilent 1200 series HPLC (Waldbronn, Germany) with solvent degasser, binary pump and thermostated autosampler.

The MS detector was an Applied Biosystems 4000 QTrap triple quadrupole mass spectrometer with electrospray ionization and the generated data were evaluated with the Analyst 1.5 software (Applied Biosystems , Foster City, USA). Alternatively to MS an Agilent 1200 series fluorescence detector (FLD) was utilized and data were evaluated with the ChemStation software (B 04.01) from Agilent.

2.5 Chromatographic parameters

The HPLC columns applied in the present study were QN-AX and QD-AX (250mm x 3mm i.d. with 3µm particles).The stationary phase materials were in-house-prepared and had a selector loading between 340 and 350µmol of selector per gram of silica support. The packing of the columns was carried out by Bischoff (Leonberg, Germany). The elution of the analytes was carried out in isocratic mode. Mobile phase composition was ACN/MeOH 1/1 with 25mM ammonium formate and 0.025% (v/v) or 6.6mM of formic acid. The flow rate was adjusted to 700µL min^{-1} and the injection volume was 5µL. Note: QN-AX and QD-AX stationary phases in different column dimensions are available from Chiral Technologies Europe (Illkirch, France).

2.6 MS parameters

The gas flows of the TurboV^{TM} ESI ionization source were as follows: curtain gas 10psi, nebulizer gas 40psi, drying gas 60psi with a drying temperature of 550°C. The electric potentials at the sample inlet were +4300V ionization voltage and 10V entrance potential, all other analyte specific parameters were obtained through direct infusion of the analytes diluted in mobile phase to the MS using a syringe pump and systematic optimization (see Table 1). The resulting cycle time for the measurement of all selected reaction monitoring (SRM) transitions plus switching intervals was 2.04 sec.

<Table 1>

2.7 Fluorescence detection parameters

Excitation and emission maxima were determined online by injecting MQ derivatized alanine and by applying the standard chromatographic method. The full excitation and emission spectra were recorded in the mobile phase. The maxima were determined to be λ_{Ex} = 230nm and λ_{Em} = 430nm. These wavelengths were used throughout all analytical runs.

2.8 Calibration

The LC-MS method was calibrated with aqueous solutions of L-Ala, which were derivatized according to the standard protocol. Calibration function was based on 14 dilutions from 0.01µmol L^{-1} to 100µmol $L^{-1}$and samples were standardized by adding d_4-L-Ala to a final concentration of 100µmol L^{-1}.

Fluorescence calibration was carried out in the same way but with 9 calibration points between 0.625 and 100 µmol L^{-1} L-Ala in water. No internal standard was added.

2.9 Biological samples

2.9.1 Urine

Urine was centrifuged for 3min @ 12100 x g and consequently 100µL of the supernatant was taken and derivatized as described above for amino acid stock solutions.

2.9.2 Newborn calf serum (NCS)

For this application d_4-L-Alanine was used as an internal standard (IS), which was dissolved in water (10mM) and 10µL thereof was added to 100µL of NCS, 900µL of ice-cold MeOH was applied to precipitate the proteins. After 3 min of centrifugation @ 12100 x g. 100µL of supernatant was derivatized as shown above for amino acids.

2.9.3 HT29 cells (human colorectal cancer cell line)

The cancer cells were harvested from a culture plate, an aliquot of 4.5 mio cells was centrifuged and the supernatant nutrient buffer was removed. After resuspension in water, the cell walls were disrupted with a potter at 0°C. 10µL of the IS d_4-Ala (10mM in water) was added to 100µL cell lysate and further centrifugation was carried out for 5min at 12100 x g to remove disrupted cell walls and organelles. Consecutively the supernatant was taken and the proteins were precipitated by the addtion of 200µL of ice-cold MeOH. Following a last centrifugation step (5min @ 12100 x g), the sample was derivatized as described above for AA stock solutions.

3. Results & Discussion

In the following, the various methodological aspects of the methoxyquinolinoyl labelling of proteinogenic amino acids will be discussed with respect to their chromatographic separation, their sensitive determination employing MS/MS or fluorescence detection and the applicability of this method for real world samples.

3.1 Derivatization & MS Fragmentation

All proteinogenic amino acids were successfully derivatized according to the reaction scheme depicted in Figure 2. MS optimization also showed that Lys carried the MQ label on both amino groups. Lys can therefore be used as an indicator for the completion of the derivatization reaction, which can only be assumed if no incompletely derivatized Lys is detectable. Using a 100-fold molar excess of the MQ-OSu over the amino acids, virtually 100% reaction yield is reached in 75min of total reaction time. The aromatic quinoline nitrogen poses a moiety that can easily be protonated; therefore it is highly suitable for positive ESI. Furthermore the aromatic quinoline system delivers energetically stable fragments upon collision induced dissociation and carries the positive charge. Hence, the MQ - labelling strategy contributes to a high ion yield upon ESI ionization and to enhanced detection sensitivity through highly abundant MS / MS fragments as shown in Figure 2. It also allows precursor ion scans of 159 m/z in non targeted approaches.

<Figure 2>

3.2 Chromatographic Aspects

Initially, the enantioselectivity was investigated using the described QN-AX CSP for all 19 MQ labelled chiral proteinogenic amino acids (MQ-AAs). The optimal separation performance was obtained with the polar organic mixture 1:1 ACN : MeOH with a low buffer concentration of 25mM ammonium formate and 6.6mM formic acid. With this mobile phase separation for all 19 chiral MQ-AAs could be achieved (see Figure 3). For 18 racemic MQ-AAs, baseline separation was observed and proline was the one MQ - AA showing only partial separation under these conditions. The general elution order was D enantiomer before the L enantiomer for the respective MQ-AA, which stands in good accordance with previously published data on the separation of N-acyl-amino acids [22,23]. However, opposite elution order for MQ-Asp, -Glu and –Pro was observed. These three candidates had special selector – selectand binding properties in common. MQ-Glu and MQ-Asp carried two acidic groups that interacted additively and competitively with the selector's anion exchanger moiety, thus leading to a strongly increased retention time and also a reversal of elution order. MQ-Pro, with its secondary amine, lacked a hydrogen donor site on its N-acyl group (Figure 5), which also lead to reversed elution.

<Figure 3>

With the applied chromatographic setup all MQ-AAs eluted within 16.5 minutes, except the two bis-acidic analytes MQ-Asp and MQ-Glu (Table 2). The hydrolysis of the MQ-OSu has lead to the formation of 6-methoxyquinoline-4-carboxylic acid (MQ-OH), which was also retained by anion exchange chromatography. Essentially, it eluted in the middle of the k range observed for most amino acids. SRM detection offered the advantage of being able to extract the analyte signals thus minimizing the interference of the label signal.

For MQ labelled amino acids also the fluorescence of the quinoline moiety was used to detect the analytes. By optimizing the chromatographic conditions with respect to the choice between the QD-AX and the QN-AX selector it was possible to elute the

analyte peaks of interest separated from the reagent peak. In Table 2 detailed elution parameters including the separation performance for all MQ-AAs are listed.

<Table 2>

3.3 Chemoselectivity

Due to the high selectivity of the MS / MS detection in combination with chemoselective effects in chiral anion exchange chromatography it was possible to inject a mix of all 20 MQ tagged proteinogenic amino acids and to differentiate between the amino acids and their corresponding enantiomers (see **Figure 4**). The separation performance was only insignificantly changed compared to the injection of single MQ-AA racemates. The baseline separation of MQ-Leu and MQ-Ile as well as the partial separation of the 4 stereoisomers of MQ-Ile (LL, LD, DL, DD) was supported by the lipophilic increment of the cinchona based selector (see Figure 1). The separation of these 6 isomers is highlighted in **Figure 4** and was extracted from a 20 MQ-AA mixture. This illustration demonstrated the high separation performance of the established chromatographic setup. Note that this method is suitable for the gathering of qualitative information on the presence or absence of a target analyte. For quantitative determination it is preferable to introduce additional chromatographic chemoselectivity in order to avoid ion suppression effects, possibly caused by the coelution of analytes into the ESI interface. Ideally, the isotope labelled form of the MQ-AA enantiomer of interest may be employed as an internal standard to compensate for ESI interferences.

<Figure 4>

3.4 Temperature Effects

Cooling the chromatographic column from ambient temperature to 5°C increased the performance of the enantiomer separations of MQ-Arg, MQ-His and MQ-Pro. For MQ-Arg and MQ-His baseline separation was obtained. MQ-Pro exhibited peculiar properties, as can be deduced from Figure 6. Unexpectedly, MQ-Pro showed a distorted peak shape, thus the temperature for this separation was varied to closer

investigate this irregularity. From the plateau between the peaks in Figure 6 it can be deduced that there obviously is equilibrium between two isomeric forms of the analyte molecule and that there may be an interconversion between these isoforms [24]. The interconversion is fast compared to the chromatographic time scale at elevated temperatures and is decelerated towards low temperatures. Effects such as this may be designated to the known rotamers of Pro peptides, which is caused by the rotation around the amide bond (see Figure 5). This phenomenon is also referred to as “cis-trans-isomerism” [25,26]. Especially at 5°C MQ-Pro undergoes a close-to-baseline separation and the two enantiomers are separated from their rotameric forms that seem to co-elute. However, the existence of a not fully resolved rotamer hampers the reliable quantification of the two MQ-Pro enantiomers, but still qualitative information can be provided by the present method.

<Figure 5> <Figure 6>

3.5 Quantitative Aspects

The calibration function for MQ-L-alanine was assessed by LC-MS in SRM mode. Linear regression was obtained by plotting the ratio of MQ-L-Ala peak area normalized with the peak area of the internal standard (MQ-d_4-L-Ala) against the concentration of L-Ala. The function was weighted by 1/x and **y = 0.0123 x + 0.0035** possessing a linearity of **R^2 = 0.9975** between 0.025µmol L^{-1} and 100µmol L^{-1}. The limit of detection (LOD) was 0.015µmol L^{-1} and the lower limit of quantitation (LLOQ) was 0.05µmol L^{-1} for MQ-L-Ala in water. Taken into account that 5µL of sample was injected, effectively an absolute amount of 25 femto mol (= 3.4pg MQ-Ala) was applied onto the column and was quantified. In order to reliably quantitate MQ-AAs in matrix it is highly recommended to analyse and normalize the amino acid enantiomer of interest with its isotopically labelled internal standard.

Since the MQ tag also exhibits high fluorescence activity, measurements were carried out to investigate the applicability of fluorescence detection compared to MS. For this purpose, identical samples were evaluated with LC-MS as well as LC-FLD. In

Figure 7 the representative measurement of racemic alanine is shown. From the calibration function it can be deduced that the obtained LOD and the LLOQ with MS detection are about 100-fold lower than with FLD used in the present study. Moreover, disturbances from the hydrolysis of the MQ-OSu to MQ-OH were observed, which elute before and after the analytes. These chemical interferences can not be prevented by using FLD.
For fluorescence detection, calibration was carried out over nine points, the calibration function calculated via the analyte peak area without internal standard was **y = 1.6746 x + 1.1747** with a linearity of **R^2 = 0.9996**. LOD was 1.25 µmol L^{-1} and LLOQ was 5 µmol L^{-1}. The limits of detection were determined by the lowest detectable calibration point which, exceeded a signal to noise ratio of 3:1 and LLOQ values were measured in the same way and were defined by a signal to noise ratio of at least 10:1.

Since a derivatization step was involved in the analytical concept, the integrity of the analytes had to be investigated. Accordingly, diverse enantiomerically pure proteinogenic amino acids were derivatized using the established protocol, in no case an evidence for racemization was detected. This finding indicated that the N-acylation of amino acids with MQ-OSu employing the optimized conditions fully maintained the stereochemical integrity of these analytes. Also, no significant degradation of crude MQ-AAs in the reaction mixture was determined upon storage at -20°C for several months. Moreover, no sample degradation was observed keeping the sample solution for several days at room temperature in the autosampler tray.

<Figure 7>

3.6 Application to Biological Samples

In order to investigate the presently developed LC-MS method for more complex samples, AAs in biological matrices of various origins were derivatized and analyzed. In a straight forward approach with a very simple sample work up procedure, it was possible to identify besides MQ-L-AAs also several corresponding D-enantiomers. Thus, MQ-D-Ala, MQ-D-Ser and MQ-D-Val were identified in most of the biological

matrices. Also the D – Ile MQ derivative was found in urine, which was the matrix, where the highest number of different D-amino acid derivatives was determined. This was not surprising since many of the water soluble and non metabolized amino acids are excreted via the urinary tract. These amino acids could stem from direct uptake with the food or from bacterial fermentation processes in the gastro intestinal tract. Hence, the biological significance of stereoselective amino acid analysis remains questionable. However, the complex matrix that urine poses is a good general model system for the analysis of L-AA and D-AA in biological fluids. It is worth mentioning that a particularly high relative percentage of MQ-D-Ser (ca. 40%) besides MQ-L-Ser was found in urine.

<Table 3>

4. Conclusion

In the present contribution we demonstrate the successful tagging of all proteinogenic amino acids with the succinimide ester of 6-methoxyquinoline-4-carboxylic acid (MQ-OSu), yielding the corresponding stable MQ amino acid derivatives. This derivatization strategy has lead to an exceptionally high chromatographic selectivity of the MQ-AAs on our chiral anion exchanger columns, allowing the separation of the enantiomers of all investigated 19 chiral proteinogenic amino acids in a single LC-MS run. Additionally to MS selectivity, the chromatographic chemoselectivity also enabled the baseline separation of the two structural isomers MQ-Leu and MQ-Ile. Furthermore, it was possible to inverse the elution order of the D- and L- enantiomers by exchanging the quinine type (QN-AX) for the quinidine type (QD-AX) CSP, thereby facilitating the methodological adaptation to the analytical question. MQ labelling not only promoted chiral recognition, it also enabled sensitive fluorescence detection. Due to the high proton affinity of MQ and its tendency to deliver charged fragments, it posed a particularly suitable tag for ESI – MS/MS detection. For MQ-Ala LODs were determined to be 1.25µmol L^{-1} (fluorescence detection) and 0.015µmol L^{-1} (MS in SRM mode). The here presented analytical method allowed enantioseparation of all chiral proteinogenic amino acids. It enabled the qualitative and quantitative analysis of D-AAs besides large excesses of L-AAs present in biological samples.

Acknowledgement

We kindly thank Professor Doris Marko and her co workers for providing the HT29 cells and for their assistance in cell lysis.

[1] A. Morikawa, K. Hamase, T. Ohgusu, S. Etoh, H. Tanaka, I. Koshiishi, Y. Shoyama, K. Zaitsu, Biochemical and Biophysical Research Communications 355 (2007) 872.
[2] M. Katane, H. Homma, Journal of Chromatography, B: Analytical Technologies in the Biomedical and Life Sciences 879 3108.
[3] J.E. Thompson, T.W. Vickroy, R.T. Kennedy, Analytical Chemistry 71 (1999) 2379.
[4] H. Wolosker, E. Dumin, L. Balan, V.N. Foltyn, FEBS Journal 275 (2008) 3514.
[5] H. Ohide, Y. Miyoshi, R. Maruyama, K. Hamase, R. Konno, Journal of Chromatography, B: Analytical Technologies in the Biomedical and Life Sciences 879 (2011) 3162.
[6] L. Pollegioni, S. Sacchi, Cellular and Molecular Life Sciences 67 2387.
[7] K. Hamase, A. Morikawa, S. Etoh, Y. Tojo, Y. Miyoshi, K. Zaitsu, Analytical Sciences 25 (2009) 961.
[8] E.H. Man, G.H. Fisher, I.L. Payan, Journal of Neurochemistry 48 (1987) 510.
[9] P. Galletti, L. De Bonis Maria, A. Sorrentino, M. Raimo, S. D'Angelo, I. Scala, G. Andria, A. D'Aniello, D. Ingrosso, V. Zappia, The FEBS journal 274 (2007) 5263.
[10] M.C. Waldhier, K. Dettmer, M.A. Gruber, P.J. Oefner, Journal of Chromatography, B: Analytical Technologies in the Biomedical and Life Sciences 878 1103.
[11] H. Bruckner, A. Schieber, Biomedical chromatography : BMC 15 (2001) 166.
[12] M. Junge, H. Huegel, P.J. Marriott, Chirality 19 (2007) 228.
[13] K. Hamase, A. Morikawa, T. Ohgusu, W. Lindner, K. Zaitsu, Journal of Chromatography, A 1143 (2007) 105.
[14] B.Y. Kim, J. Yang, M. Gong, B.R. Flachsbart, M.A. Shannon, P.W. Bohn, J.V. Sweedler, Analytical Chemistry (Washington, DC, United States) 81 (2009) 2715.
[15] K. Imai, Y. Watanabe, Analytica Chimica Acta 130 (1981) 377.
[16] M. Roth, Analytical Chemistry 43 (1971) 880.
[17] K. Muramoto, H. Kamiya, H. Kawauchi, Analytical Biochemistry 141 (1984) 446.
[18] T. Santa, Biomedical Chromatography 25 1.
[19] M. Laemmerhofer, P. Franco, W. Lindner, Journal of Separation Science 29 (2006) 1486.
[20] N.M. Maier, S. Schefzick, G.M. Lombardo, M. Feliz, K. Rissanen, W. Lindner, K.B. Lipkowitz, Journal of the American Chemical Society 124 (2002) 8611.
[21] R.J. Reischl, L. Hartmanova, M. Carrozzo, M. Huszar, P. Fruehauf, W. Lindner, Journal of Chromatography, A 1218 (2011) 8379.

[22] N.M. Maier, L. Nicoletti, M. Lammerhofer, W. Lindner, Chirality 11 (1999) 522.
[23] M. Laemmerhofer, W. Lindner, Journal of Chromatography, A 741 (1996) 33.
[24] I. D'Acquarica, F. Gasparrini, M. Pierini, C. Villani, G. Zappia, Journal of Separation Science 29 (2006) 1508.
[25] J. Jacobson, W. Melander, G. Vaisnys, C. Horvath, Journal of Physical Chemistry 88 (1984) 4536.
[26] A.E. Aliev, S. Bhandal, D. Courtier-Murias, Journal of Physical Chemistry A 113 (2009) 10858.

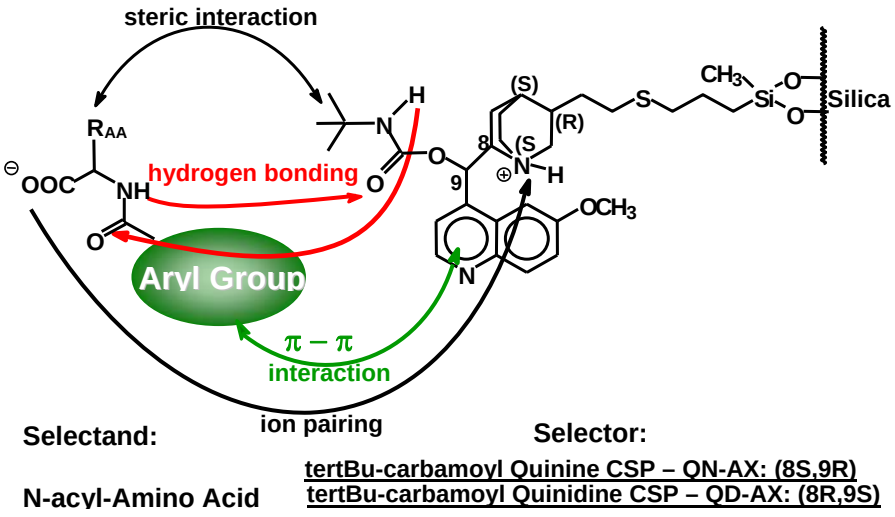

Figure 1 Interactions between cinchona alkaloid type selectors and amino acids derivatized with N-acyl bound aromatic labels (in analogy to [23])

Table 1 Analyte specific MS parameters for SRM measurements, Q1 mass shows the molecular weight of the protonated amino acid derivative, Q3 mass the weight of the correlated fragments. **DP:** declustering potential, **CE:** collision energy, **CXP:** cell exit potential, **MQ:** methoxyquinoline, **IAM:** iodoacetamide

MQ-AA	Q1 mass (Da)	Q3 mass (Da)	Time (msec)	DP	CE	CXP
Ala	275.2	201.0	25	71	37	12
	275.2	229.1	25	71	29	18
	275.2	159.1	25	71	53	12
Arg	360.2	158.0	25	76	55	10
	360.2	186.0	25	76	41	14
	360.2	300.0	25	76	29	18
Asn	318.1	159.1	25	61	59	12
	318.1	186.1	25	61	31	14
	318.1	301.0	25	61	27	18
Asp	319.1	201.0	25	76	41	14
	319.1	159.0	25	76	59	10
	319.1	275.0	25	76	31	16
Gln	332.1	186.0	25	66	31	12
	332.1	158.0	25	66	49	10
	332.1	287.0	25	66	37	16
Glu	333.1	159.0	25	76	59	12
	333.1	259.1	25	76	39	18
	333.1	116.0	25	76	95	6
Gly	261.1	159.1	25	21	45	12
	261.1	116.0	25	21	77	6
	261.1	130.1	25	21	71	8
His	341.1	158.1	25	51	49	10
	341.1	186.0	25	51	33	12
	341.1	110.0	25	51	29	6
Ile	317.2	271.0	25	71	33	16
	317.2	158.9	25	71	53	10
	317.2	116.0	25	71	89	6
Leu	317.1	243.1	25	76	39	14
	317.1	89.1	25	76	115	4
Lys 2 x MQ	517.2	186.0	25	96	45	14
	517.2	158.0	25	96	67	12
	517.2	143.0	25	96	101	8
Met	335.1	159.1	25	81	59	12
	335.1	241.0	25	81	37	14
	335.1	186.0	25	81	33	14
Phe	351.1	159.2	25	81	59	10
	351.1	305.0	25	81	33	16
	351.1	277.0	25	81	39	16
Pro	301.1	257.0	25	71	31	14
	301.1	160.1	25	71	43	10

	301.1	145.0	25	71	57	10
Ser	291.1	159.0	25	76	53	10
	291.1	245.0	25	76	31	14
	291.1	201.1	25	76	33	14
Thr	305.1	159.0	25	76	57	10
	305.1	215.1	25	76	37	16
	305.1	261.0	25	76	29	14
Trp	390.2	159.1	25	86	63	10
	390.2	186.1	25	86	37	14
	390.2	130.0	25	86	77	8
Tyr	367.1	159.0	25	96	55	10
	367.1	321.0	25	96	33	18
	367.1	293.0	25	96	41	8
Val	303.1	257.0	25	86	33	14
	303.1	159.1	25	86	53	12
	303.1	229.1	25	86	39	14
d_4-Ala	279.2	233.0	25	66	31	16
	279.2	159.0	25	66	55	10
	279.2	177.0	25	66	47	10
Cys-IAM	364.0	160.0	25	36	25	12
	364.0	296.1	25	36	13	12
	364.0	186.0	25	36	35	12

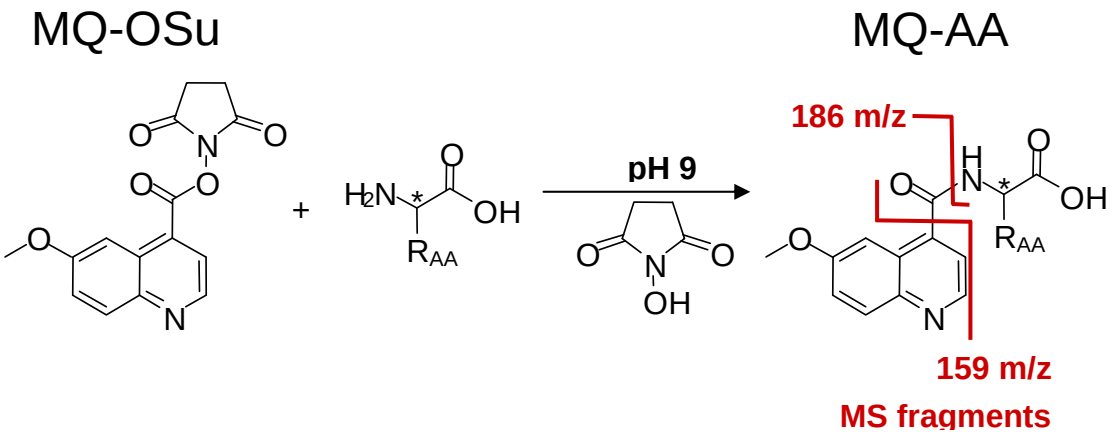

Figure 2 Amino acid derivatization scheme with MQ-OSu and the most prominent MS fragments of the MQ-AA derivatives

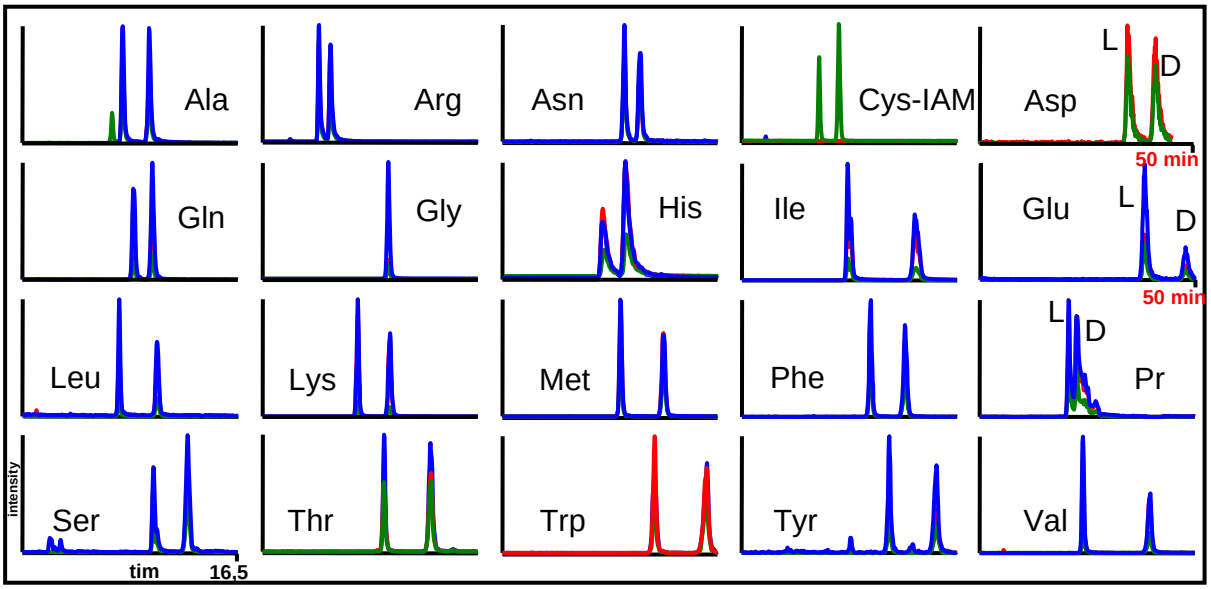

Figure 3 Separation off all MQ tagged chiral proteinogenic amino acids, x – axis scale: 16.5min in all cases except Asp and Glu (50min), general elution order D → L with reversal for MQ-Asp, MQ-Glu and MQ-Pro **stat.Ph.:** QN-AX 250mm x 3 mm i.d., 3µm particle size, **mob. Ph.:** MeOH / ACN 1/1, 25mM NH4FA, 0.025% FA (v/v), **flow:** 700 µL min^{-1}, **T:** 20°C, MS detection in SRM mode, different colors indicate the 3 transitions measured for every analyte, **IAM:** iodoacetamide

Table 2 Chromatographic parameters for all proteinogenic amino acids carrying the 6-Methoxyquinoline (MQ) label

MQ-AA	t 0	t D [min]	t L [min]	k (D)	k (L)	α (DL)	N D [m^{-1}]	N L [m^{-1}]	R (DL)
Ala	1.58	7.67	9.70	3.85	5.14	1.33	15060	16727	3.69
Arg	1.58	4.08	4.97	1.58	2.15	1.36	2174	3226	1.27
Asn	1.58	9.34	10.55	4.91	5.68	1.16	22332	23548	2.30
Asp*	1.58	34.94	41.20	21.11	25.08	1.19	19533	18860	2.85
Gln	1.58	8.50	9.95	4.38	5.30	1.21	14745	23433	2.69
Glu*	1.58	38.10	47.50	23.11	29.06	1.26	8037	13260	2.81
Gly	1.58	9.62		5.09			9254		
His	1.58	7.67	9.41	3.85	4.96	1.29	4172	2519	1.42
Ile	1.58	7.90	13.05	4.00	7.26	1.81	13204	6449	5.57
Leu	1.58	7.21	10.11	3.56	5.40	1.52	16430	18171	5.52
Lys x 2MQ	1.58	7.28	9.76	3.61	5.18	1.44	13568	24386	4.96
Met	1.58	8.85	12.14	4.60	6.68	1.45	24754	31181	6.58
Phe	1.58	9.67	12.30	5.12	6.78	1.33	29553	32008	5.26
Pro*	1.58	6.61	7.24	3.18	3.58	1.13	63408	27386	1.33
Ser	1.58	9.83	12.45	5.22	6.88	1.32	25757	23480	4.60
Thr	1.58	9.23	10.63	4.84	5.73	1.18	26925	14759	2.43
Trp	1.58	11.66	12.70	6.38	7.04	1.10	42969	10323	1.43
Tyr	1.58	11.31	14.93	6.16	8.45	1.37	40428	29114	6.30
Val	1.58	7.90	13.06	4.00	7.27	1.82	15977	25837	8.97
MQ - OH	1.58	11.70		6.41					

*: reversal of elution order: L --> D

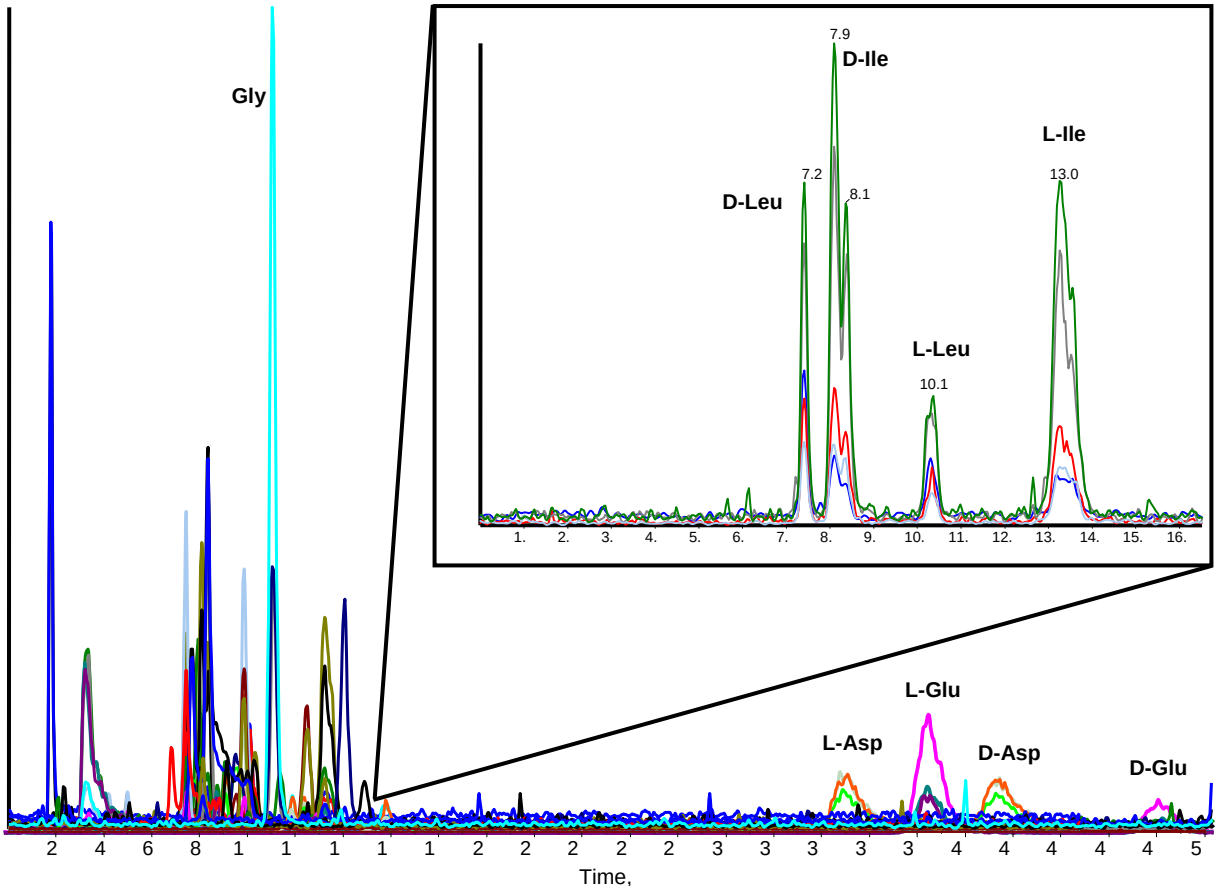

Figure 4 Mixture of 19 proteinogenic MQ-AAs (D and L enantiomers) and MQ-Gly. In the zoom region the extracted ion chromatograms with the enantioseparation and the separation of the structural isomers of Leu/Ile exclusively due to chromatographic selectivity are shown **stat.Ph.:** QN-AX 250mm x 3 mm i.d., 3µm particle size, **mob. Ph.:** MeOH / ACN 1/1, 25mM NH4FA, 0.025% FA (v/v), **flow:** 700 µL min^{-1}, **T:** 20°C, MS detection in SRM mode, different colors indicate the 3 SRM transitions measured for every analyte

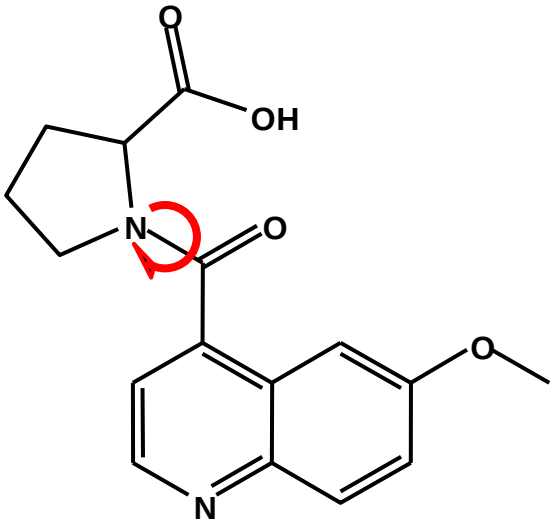

Figure 5 Energetically hindered rotation of the MQ – tag around the amide bond of N-acyl-Pro thus leading to rotamers

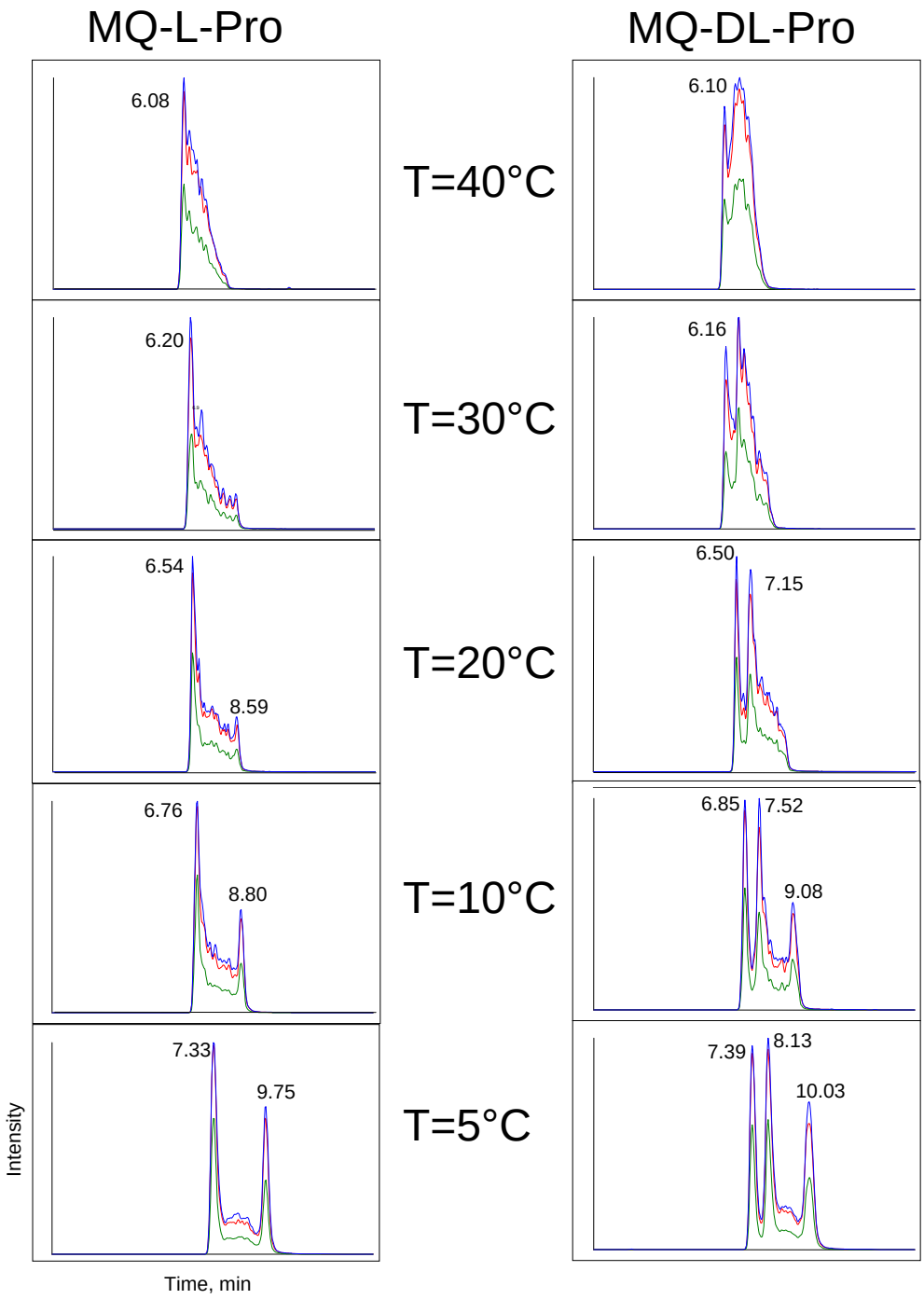

Figure 6 Temperature variation and its influence on the chiral separation of MQ-proline **stat.Ph.:** QN-AX 250mm x 3 mm i.d., 3µm particle size, **mob. Ph.:** MeOH / ACN 1/1, 25mM NH4FA, 0.025% FA (v/v), **flow:** 700 µL min^{-1}, MS detection in SRM mode, different colors indicate the 3 SRM transitions measured for Pro

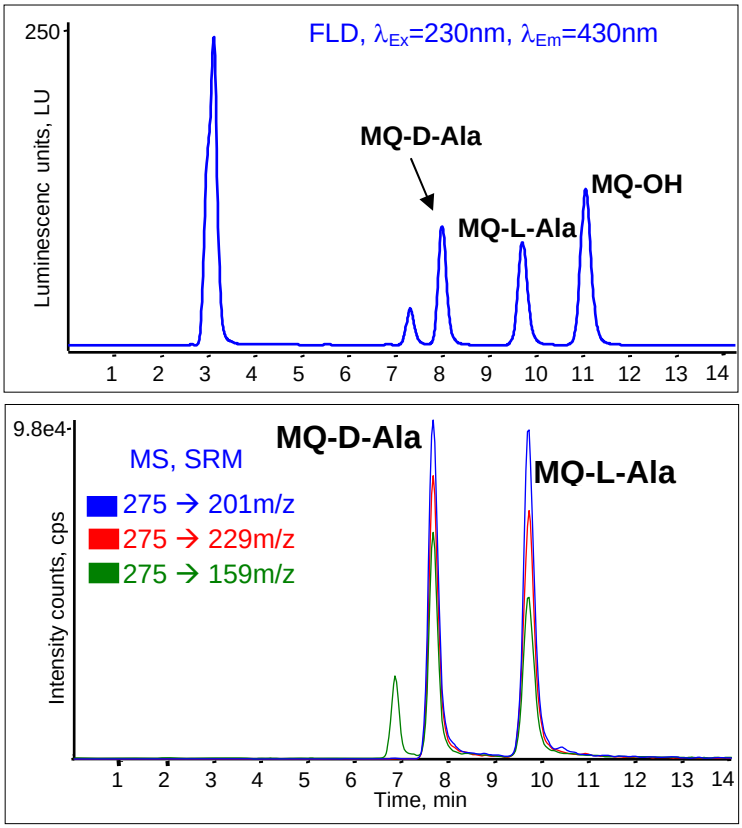

Figure 7 Comparison of measurements of the same sample, above the LC-FLD signal is shown, below LC-MS/MS in SRM mode

Table 3 Peak areas for MQ-L–AAs and the area% for the corresponding MQ-D-AAs in matrix

MQ - AA	α DL	HT29 area L	HT29 % D	NCS area L	NCS % D	urine area L	urine % D
Ala	1.75	6580000		12100000	6.73	8450000	32.35
Arg	1.80	689000		909000	5.97	127000	9.67
Asn	1.77	110000		60900		179000	12.43
Asp	1.19	45700		4390		5070	
Cys-IAM	1.94	26400		9460		178000	
Gln	1.67	4760000		70200		6190000	
Glu	1.91	3120000		3680000		73400	
Gly	1.00	10300000		10500000		66300000	
His	1.77	369000		1070000		5050000	1.18
Ile	2.24	2770000		1730000		367000	5.68
Leu	2.14	3430000	0.31	4140000		845000	
Lys 2xMQ	2.01	2130000		1930000	7.03	1060000	8.57
Met	1.98	855000		590000	<LLOQ	159000	
Phe	1.85	847000		725000	<LLOQ	815000	
Pro	1.00	11100000		13800000		559000	
Ser	1.82	876000	0.61	737000	1.90	1220000	39.57
Thr	2.38	1340000		607000	<LLOQ	739000	9.70
Trp	2.01	309000		492000		1210000	
Tyr	1.92	138000		92800		205000	
Val	2.67	3610000	0.11	6380000	0.17	1270000	6.97

Figure Captions

Figure 8 Interactions between cinchona alkaloid type selectors and amino acids derivatized with N-acyl bound aromatic labels (in analogy to [23])

Figure 9 Amino acid derivatization scheme with MQ-OSu and the most prominent MS fragments of the MQ-AA derivatives

Figure 10 Separation off all MQ tagged chiral proteinogenic amino acids, x – axis scale: 16.5min in all cases except Asp and Glu (50min), general elution order D → L with reversal for MQ-Asp, MQ-Glu and MQ-Pro **stat.Ph.:** QN-AX 250mm x 3 mm i.d., 3µm particle size, **mob. Ph.:** MeOH / ACN 1/1, 25mM NH4FA, 0.025% FA (v/v), **flow:** 700 µL min^{-1}, **T:** 20°C, MS detection in SRM mode, different colors indicate the 3 transitions measured for every analyte, **IAM:** iodoacetamide

Figure 11 Mixture of 19 proteinogenic MQ-AAs (D and L enantiomers) and MQ-Gly. In the zoom region the extracted ion chromatograms with the enantioseparation and the separation of the structural isomers of Leu/Ile exclusively due to chromatographic selectivity are shown **stat.Ph.:** QN-AX 250mm x 3 mm i.d., 3µm particle size, **mob. Ph.:** MeOH / ACN 1/1, 25mM NH4FA, 0.025% FA (v/v), **flow:** 700 µL min^{-1}, **T:** 20°C, MS detection in SRM mode, different colors indicate the 3 SRM transitions measured for every analyte

Figure 12 Energetically hindered rotation of the MQ – tag around the amide bond of N-acyl-Pro thus leading to rotamers

Figure 13 Temperature variation and its influence on the chiral separation of MQ-proline **stat.Ph.:** QN-AX 250mm x 3 mm i.d., 3µm particle size, **mob. Ph.:** MeOH / ACN 1/1, 25mM NH4FA, 0.025% FA (v/v), **flow:** 700 µL min^{-1}, MS detection in SRM mode, different colors indicate the 3 SRM transitions measured for Pro

Figure 14 Comparison of measurements of the same sample, above the LC-FLD signal is shown, below LC-MS/MS in SRM mode

Table 4 Analyte specific MS parameters for SRM measurements, Q1 mass shows the molecular weight of the protonated amino acid derivative, Q3 mass the weight of the correlated fragments. **DP:** declustering potential, **CE:** collision energy, **CXP:** cell exit potential, **MQ:** methoxyquinoline, **IAM:** iodoacetamide

Table 5 Chromatographic parameters for all proteinogenic amino acids carrying the 6-Methoxyquinoline (MQ) label

Table 6 Peak areas for MQ-L–AAs and the area% for the corresponding MQ-D-AAs in matrix

Appendix D

Expanding the Chemical Cross-Linking Toolbox by the Use of Multiple Proteases and Enrichment by Size Exclusion Chromatography*[S]

Alexander Leitner‡‡‡, Roland Reischl§, Thomas Walzthoeni‡, Franz Herzog‡, Stefan Bohn¶, Friedrich Förster¶, and Ruedi Aebersold‡‖‡‡**

Chemical cross-linking in combination with mass spectrometric analysis offers the potential to obtain low-resolution structural information from proteins and protein complexes. Identification of peptides connected by a cross-link provides direct evidence for the physical interaction of amino acid side chains, information that can be used for computational modeling purposes. Despite impressive advances that were made in recent years, the number of experimentally observed cross-links still falls below the number of possible contacts of cross-linkable side chains within the span of the cross-linker. Here, we propose two complementary experimental strategies to expand cross-linking data sets. First, enrichment of cross-linked peptides by size exclusion chromatography selects cross-linked peptides based on their higher molecular mass, thereby depleting the majority of unmodified peptides present in proteolytic digests of cross-linked samples. Second, we demonstrate that the use of proteases in addition to trypsin, such as Asp-N, can additionally boost the number of observable cross-linking sites. The benefits of both SEC enrichment and multiprotease digests are demonstrated on a set of model proteins and the improved workflow is applied to the characterization of the 20S proteasome from rabbit and *Schizosaccharomyces pombe*. *Molecular & Cellular Proteomics 11: 10.1074/mcp.M111.014126, 1–12, 2012.*

The analysis of the three-dimensional structure of proteins and the spatial arrangement of subunits within protein complexes is of great importance to study their biological function (1). Historically, methods such as x-ray crystallography and NMR spectroscopy, together with a variety of other spectroscopic techniques have been used, each with their own drawbacks. Obtaining diffracting crystals still remains a challenge, especially for large protein assemblies, and the application of NMR is predominantly limited to smaller proteins. Lower resolution methods based on electron microscopy have revealed interesting insight into the structure of large macromolecular assemblies. However, their use for smaller complexes remains limited. In recent years, mass spectrometry has contributed a number of emerging approaches that deliver low-resolution structural information on proteins that can provide complementary data to the above-mentioned methods. Among the most established of these are hydrogen/deuterium exchange (2), oxidative footprinting (3), and—for the analysis of intact protein complexes—native MS techniques (4).

In addition, various forms of cross-linking have been employed to study protein structure and protein interactions in combination with mass spectrometry (5–7). In its simplest form, noncovalent interactions in protein complexes can be stabilized, for example using the rather unselective formaldehyde as reagent. In such studies, proteins co-isolated using affinity purification are cross-linked during the isolation step and interaction partners are identified without deriving dedicated information about the exact cross-linking sites. Different forms of cross-linking strategies may be employed that are either based on the introduction of photoreacive amino acids at specific sites into target proteins or, alternatively, cross-linking reagents containing photoreactive groups are used. In both cases, covalent links with interactors are formed upon UV irradiation.

In contrast to these studies where relatively unspecific cross-linking reagents have been used to stabilize complexes, studies attempting the precise localization of cross-linking sites by mass spectrometry—using chemically selective cross-linkers—have proven more challenging, but also more rewarding (5–7). The thus obtained "distance restraints" provide direct information about the spatial proximity of the reactive sites, taking into account the spacer length of the reagent and the length of the amino acid side chains. Such restraints can be used for computational purposes or in combination with other low-resolution techniques such as electron

From the ‡Institute of Molecular Systems Biology, Eidgenössische Technische Hochschule (ETH) Zurich, Wolfgang-Pauli-Strasse 16, 8093 Zurich, Switzerland; §Department of Analytical Chemistry, University of Vienna, Währinger Strasse 38, 1090 Vienna, Austria; ¶Max Planck Institute of Biochemistry, Am Klopferspitz 18, 82152 Martinsried, Germany; ‖Faculty of Science, University of Zurich, Zurich, Switzerland; **Competence Center for Systems Physiology and Metabolic Diseases, Zurich, Switzerland

Received September 8, 2011, and in revised form, December 2, 2011

⌘ *Author's Choice*—Final version full access.

Published, MCP Papers in Press, January 27, 2012, DOI 10.1074/mcp.M111.014126

microscopy and small angle x-ray scattering. For structural studies, chemical cross-linking reagents that target specific functional groups within the protein(s) of interest are used, most commonly amine-reactive succinimide esters such as disuccinimidyl suberate (DSS)[1] or bis(sulfosuccinimidyl) suberate, which cross-link primary amino groups on lysine residues and protein N termini.

Recently, the concept of chemical cross-linking/mass spectrometry has seen a noticeable increase in attention and is becoming more widely adopted. New cross-linking reagents (6) and software tools (8) for data analysis have been introduced, and advances in MS instrumentation have enabled lower detection limits and improved mass accuracy. However, fundamental limitations in the workflow remain. The yield from a cross-linking experiment is typically low. In the case of succinimide esters, hydrolysis of the cross-linking reagent in aqueous solution is a competitive reaction, and using a large excess of reagent might impede further sample processing, *e.g.* because of the reduced efficiency of enzymatic digestion in highly cross-linked samples. Therefore, enrichment of cross-linked peptides is essential when more complex samples are analyzed.

To this end, various strategies have been proposed. They include the use of reagents containing affinity tags (9–11) or the use of strong cation exchange chromatography (SCX) (12–14). Although affinity tagged reagents have been used successfully to some extent, most notably by the Bruce laboratory in the Protein Interaction Reporter concept (15–17), their synthesis is challenging and many studies reported in the literature remain proof-of-principle only. SCX enrichment makes use of the fact that when two peptides are connected via a cross-link, they are more highly charged in solution than their linear counterparts because of the presence of a higher number of protonation sites (usually N- and C termini when proteases such as trypsin or Lys-C are used). This strategy, originally introduced by Rinner *et al.* (12), has recently been applied to larger complexes such as RNA polymerase II (13) or the ribosome (18).

Most of the cross-linking studies to date have used trypsin as the proteolytic enzyme. This protease is widely used in proteomic research because of its robustness and its tendency to produce peptides with advantageous properties (length, charge, and fragmentation behavior) for MS and tandem MS (MS/MS) analysis. However, this may not necessarily be the case for the analysis of cross-linked peptides, because in this case it is required that both connected regions of the protein(s) yield peptides of suitable length. Cross-links with short peptides typically yield only few informative fragment ions, whereas excessively long peptides might cause several other problems—such peptides begin to deviate from the common fragmentation model where amide bonds within the peptide backbone are more or less randomly cleaved, leading to incomplete fragmentation. This issue appears to be further exacerbated in cross-linked peptides, where little general information about their fragmentation behavior is known (19).

To overcome suboptimal fragmentation in conventional collision-induced dissociation, alternative strategies such as the use of electron transfer dissociation (20) or gas-phase cleavable reagents (15–17, 21) have been introduced, although both techniques come with their own drawbacks such as low fragmentation efficiency and reduced scan speeds because of the requirement of performing MS3 scans.

Moreover, long peptides, especially when present in cross-links, are difficult to separate efficiently by reversed-phase chromatography, leading to peak broadening because of poor mass transfer in solution, and might also exceed the optimal mass range for MS analysis, causing a decrease in sensitivity. Therefore, the use of multiple proteases might be advantageous to enhance the yield of cross-linking data. Up to now, no systematic study of the use of different proteases for cross-linking/mass spectrometry has been reported. For conventional proteomics approaches, however, Swaney *et al.* have recently found a clear benefit in the use of additional proteases to increase both proteome and protein sequence coverage (22).

We have shown previously that computational modeling approaches require a considerable amount of low-resolution restraints (such as those from cross-linking experiments) to provide a noticeable benefit (5). To restrain the conformation of interaction partners in protein complexes, the yield of cross-linking experiments should therefore be maximized. To achieve this, the development of more sophisticated and powerful sample preparation strategies is one of the most promising strategies. We introduce peptide size exclusion chromatography (SEC) as a novel chromatographic technique for enriching cross-linked peptides, and thereby expand the yield of structural information from cross-linking experiments. Although not very frequently used for proteomics applications, peptide-level SEC has recently been employed by Quadroni and coworkers to select large tryptic peptides for secondary digestions using complementary enzymes (23). Although most of the peptides resulting from an enzymatic digest have a molecular mass below 2000 Da, the majority of cross-link identifications resulting from the combination of two peptides plus the cross-linker mass result from precursor masses above this level. Therefore even a relatively crude chromatographic separation—as can be expected from a low-efficiency technique such as SEC—should result in appreciable depletion of unmodified peptides and peptides carrying the partially hydrolyzed cross-linker as a modification (designated as "mono-link" according to our nomenclature (5)).

Here, we show that SEC can indeed be used to fractionate digests of cross-linked proteins and complexes and that the

[1] The abbreviations used are: DSS, disuccinimidyl suberate; CP, (proteasome) core particle; RP, (proteasome) regulatory particle; SEC, size exclusion chromatography.

technique enriches for cross-linked peptides in higher mass fractions. The use of multiple proteases (Asp-N, Glu-C, Lys-C, and Lys-N in addition to trypsin) provides complementary distance restraints, therefore extending the amount of information that can be used for computational purposes. The methods are first discussed in detail using a set of model proteins and applied to the cross-linking of the 20S proteasome as an example for a protein complex of high biological relevance. For the model proteins, a total of 240 nonredundant Lys-Lys contacts were covered by combining data from five enzymes. The concept was also found to be applicable to small sample amounts as demonstrated by the proteasome data where the number of cross-links was expanded by 20–50% with the use of a second enzyme (Asp-N) for digestion.

EXPERIMENTAL PROCEDURES

Cross-linking of Model Proteins—Individual stock solutions of the eight model proteins (bovine catalase, rabbit creatine kinase, rabbit fructose-bisphosphate aldolase, bovine lactoferrin, chicken ovotransferrin, rabbit pyruvate kinase, bovine serotransferrin, bovine serum albumin; all obtained from Sigma-Aldrich Buchs, Switzerland) were prepared at concentrations of 5–10 mg ml^{-1} in 20 mM HEPES/KOH buffer (pH 8.2). Samples were diluted for each protein separately to a final concentration of 2 mg ml^{-1} in the same buffer, and 4 μl of the cross-linker solution (25 mM each of DSS-d_0 and DSS-d_{12} (Creative Molecules, Canada) in anhydrous DMF) were added per 100 μl protein solution. Samples were incubated for 30 min at 37 °C in an Eppendorf Thermomixer (mixing speed 750 rpm). Remaining cross-linking reagent was quenched by adding aqueous NH_4HCO_3 solution to a final concentration of 50 mM, followed by incubation for further 20 min. Aliquots of the individually cross-linked protein solutions were then combined and evaporated to dryness in a vacuum centrifuge before further processing.

Cross-linking of 20S Proteasome Samples—The 20S proteasome from rabbit (*Oryctolagus cuniculus*) was obtained from Sigma-Aldrich and cross-linked at a concentration of ~0.8 mg ml^{-1}. *Schizosaccharomyces pombe* proteasome was prepared following a protocol from Saeki *et al.* (24) with modifications as described in (25). The sample was concentrated by ultrafiltration to a final concentration of 0.2 to 0.3 mg ml^{-1}. The cross-linking reaction was carried out as described above for model proteins, with the amounts of cross-linking reagent adjusted according to the lower protein concentrations. Cross-linked samples were split in half and digested with trypsin and Asp-N in both cases, as described below.

Enzymatic Digestions—Dried cross-linked samples were resuspended in 8 M urea solution to a final concentration of 1 mg ml^{-1} (0.2 mg ml-1 for *S. pombe* proteasome). Five microliters of a 50 mM tris(carboxyethyl) phosphine stock solution in water were added and the samples were incubated at 37 °C for 30 min. Subsequently, 5 μl of a 100 mM aqueous iodoacetamide stock solution were added and the samples were incubated for 20 min at room temperature and protected from light.

Trypsin—Following reduction and alkylation, the sample was diluted with 50 mM NH_4HCO_3 to 1 M urea and trypsin (proteomics grade; Promega, Charbonnières, France) was added at an enzyme-to-substrate ratio of 1:50. The solution was incubated at 37 °C overnight.

Lys-C—Following reduction and alkylation, the sample was diluted with 150 mM NH_4HCO_3 to 4 M urea and lysyl endopeptidase (mass spectrometry grade; Wako Chemicals, Richmond, VA) was added at an enzyme-to-substrate ratio of 1:100. The solution was incubated at 37 °C overnight.

Lys-N—Following reduction and alkylation, the sample was diluted with 150 mM NH_4HCO_3 to 6 M urea and endoproteinase Lys-N (gift from Albert J. R. Heck, University of Utrecht) was added at an enzyme-to-substrate ratio of 1:100. The solution was incubated at 37 °C overnight.

Glu-C—Following reduction and alkylation, the sample was diluted with 50 mM NH_4HCO_3 to 2 M urea and endoproteinase Glu-C (sequencing grade, Sigma-Aldrich) was added at an enzyme-to-substrate ratio of 1:100. The solution was incubated at 25 °C overnight.

Asp-N—Following reduction and alkylation, the sample was diluted with 50 mM sodium phosphate buffer, pH 8, to 1.6 M urea and endoproteinase Asp-N (sequencing grade, Roche Diagnostics Rotkreuz, Switzerland) was added at an enzyme-to-substrate ratio of 1:100. The solution was incubated at 37 °C overnight.

After overnight digestion, all samples were acidified to 2% formic acid and purified by solid-phase extraction using 50 mg Sep-Pak tC18 cartridges (Waters, Milford, MA). The eluate (water/acetonitrile/formic acid, 50:50:0.1) was evaporated to dryness in a vacuum centrifuge.

Fractionation of Cross-Linked Peptides by Size Exclusion Chromatography—Purified samples were reconstituted in 20 μl of SEC mobile phase (water/acetonitrile/trifluoroacetic acid, 70:30:0.1). 15 μl were injected on a GE Healthcare Äkta micro system consisting of autosampler, binary pump, UV/pH/conductivity detectors and fraction collector. This corresponded to total protein amounts of 200 μg of standard proteins, 50 μg of rabbit proteasome, and 10 μg of *S. pombe* proteasome, respectively. Peptides were separated on a Superdex Peptide PC 3.2/30 column (300 × 3.2 mm) at a flow rate of 50 μl min^{-1} using the SEC mobile phase. The separation was monitored by UV absorption at 215, 254, and 280 nm. Two-minute fractions (100 μl) were collected into 96-well plates over a separation window of one column volume (2.4 ml = 48 min). For analysis by liquid chromatography (LC)-MS/MS, fractions of interest (retention volumes 0.9–1.4 ml) were removed and evaporated to dryness. For the proteasome samples, only the two main fractions (1.0–1.1 and 1.1–1.2 ml) were analyzed.

Liquid Chromatography-Tandem Mass Spectrometry—LC-MS/MS analysis was carried out on an Eksigent 1D-NanoLC-Ultra system connected to a Thermo LTQ Orbitrap XL mass spectrometer equipped with a standard nanoelectrospray source. SEC fractions were reconstituted in mobile phase A (water/acetonitrile/formic acid, 97:3:0.1). The injection volume was chosen according to the 215 nm UV absorption signal from the SEC separation.

A fraction corresponding to an estimated 1 μg (if available) of the total recovered peptide amount was injected onto a 11 cm × 0.075 mm I.D. column packed in house with Michrom Magic C_{18} material (3 μm particle size, 200 Å pore size). Peptides were separated at a flow rate of 300 nl min^{-1} using the following gradient: 0–5 min = 5% B, 5–95 min = 5–35% B, 95–97 min = 35–95% B, and 97–107 min = 95% B, where B = (acetonitrile/water/formic acid, 97:3:0.1).

The mass spectrometer was operated in data-dependent mode, selecting up to five precursors from a MS^1 scan (resolution = 60,000) in the range of *m/z* 350–1600 for collision-induced dissociation. An intensity threshold of 150 counts was chosen for triggering fragmentation, and singly and doubly charged precursor ions and precursors of unknown charge states were excluded from fragmentation. Collision-induced dissociation was performed for 30 ms using 35% normalized collision energy and an activation *q* of 0.25. Dynamic exclusion was activated with a repeat count of 1, exclusion duration of 30 s, list size of 300, and a mass window of ±50 ppm. Ion target values were 1,000,000 (or maximum 500 ms fill time) for full scans and 10,000 (or maximum 200 ms fill time) for MS/MS scans, respectively. Fragment ions were detected at low resolution in the linear ion trap.

TABLE I

Model proteins used in the 8-protein mix. Shown are UniProt/SwissProt accession numbers, molecular mass (excluding modifications), and the relative content of relevant amino acids, Lys as potential cross-linking and cleavage site and Arg, Asp and Glu as cleavage sites. All parameters were calculated from the processed forms of the proteins, after cleavage of initiator methionines and signal peptides as assigned in UniProt

Protein name	Accession number	Molecular mass (kDa)	% Lys	% Arg	% Asp	% Glu
Catalase, bovine	P00432	59.8	5.3	6.1	7.0	4.9
Creatine kinase, rabbit	P00563	43.1	8.9	4.7	7.3	7.1
Fructose-bisphosphate aldolase A, rabbit	P00883	39.2	7.2	4.1	3.9	6.6
Lactoferrin, bovine	P24627	76.1	7.8	5.4	5.2	5.8
Ovotransferrin, chicken	P02789	75.8	8.6	4.4	6.7	6.6
Pyruvate kinase, rabbit (isoenzyme 1)	P11974	57.9	7.0	5.8	5.7	7.0
Serotransferrin, bovine	Q29443	75.8	9.3	3.4	6.9	6.4
Serum albumin, bovine	P02769	66.4	10.1	3.9	6.9	10.1

Data Analysis—For data analysis, Thermo Xcalibur .raw files were converted into the open mzXML format using ReAdW, version 4.0.2, using the default settings. mzXML files were directly used as input for xQuest searches, while they were further converted into the .mgf (Mascot generic file) format using the tool MzXML2Search, part of the Trans-Proteomics Pipeline (26). MzXML2Search was executed with the option "-T10000" to export precursors with a mass above the default value of 4200 Da.

Mascot Search—Unmodified peptides from the eight-protein mix were identified by database search using an in-house Mascot (27) server, version 2.3.0, against the Uniprot/SwissProt database (version 51.6, 257964 entries). Search parameters were as follows: Maximum number of missed cleavages = 2, taxonomy = chordata, fixed modifications = carbamidomethyl-Cys, variable modification = Met oxidation, MS^1 tolerance = 15 ppm, MS^2 tolerance = 0.6 Da, instrument type = ESI-TRAP, decoy mode = on. For validation, the peptide probability was set to $p < 0.05$, additional filters used were require bold red = yes and peptide score = > 20.

xQuest Search—Cross-linked peptides and peptide mono-links were identified using an in-house version of the dedicated search engine, xQuest, using the same scoring model as described in (12). Tandem mass spectra of precursors differing in their mass by 12.07532 Da (difference between DSS-d_0 and DSS-d_{12}) were paired if they had a charge state of 3+ to 8+ and were triggered within 2.5 min of each other. These spectra were then searched against a preprocessed .fasta database as described in the following.

For the eight-protein mixture, the database contained the UniProt/SwissProt entries of the target proteins. Two separate entries were created for the two isoenzymes of pyruvate kinase, and known signal peptides as annotated in UniProt were removed from the primary sequence. Rabbit proteasome data was searched against all 35 human 26S proteasome subunits retrieved from UniProt because only two probable rabbit subunit sequences are available. *S. pombe* data was searched against a database of all 32 *S. pombe* 26S subunits in UniProt/SwissProt supplemented with the sequence of rabbit creatine kinase (P00563) and YLK1_SCHPO (Q9P7H8), two known contaminants. (No cross-links from contaminants were identified.)

xQuest search parameters were as follows: Maximum number of missed cleavages (excluding the cross-linking site) = 2, peptide length = 4–40 amino acids, fixed modifications = carbamidomethyl-Cys (mass shift = 57.02146 Da), mass shift of the light cross-linker = 138.06808 Da, mass shift of mono-links = 156.07864 and 155.09643 Da, MS^1 tolerance = 15 ppm, MS^2 tolerance = 0.2 Da for common ions and 0.3 for cross-link ions, search in enumeration mode (exhaustive search). Search results were filtered according to the following criteria: MS^1 mass tolerance window = –3 to +7 ppm (–4 to +7 ppm for proteasome samples), %TIC explained ≥ 0.1, xQuest score ≥ 16 for trypsin, Lys-C and Lys-N and ≥ 18 for Glu-C and Asp-N. Finally, all spectra were then manually validated. Identifications were only considered for the final result list when both peptides had at least four bond cleavages in total or three adjacent ones, respectively, and a minimum length of six amino acids (see also Results and Discussion section).

RESULTS AND DISCUSSION

Design of the Study—To evaluate the use of SEC for enrichment purposes and of multiple proteases for obtaining complementary digestion patterns, we first optimized the method on a well-defined set of model proteins (Table I). They range in size from ~40 kDa to 80 kDa, thereby offering sufficient potential cross-linking sites, and are quite diverse in their amino acid composition. The model proteins were cross-linked individually using a mixture of two differentially isotope-coded forms of the amine reactive disuccinimidyl suberate, d_0- and d_{12}-DSS, before mixing (12). This way, all observed interprotein cross-links can be easily assigned as false positive identifications acting as a control for the estimation of false discovery rates. Cross-linked samples were then digested in parallel by five different proteases as described in the Experimental procedures, and analyzed by liquid chromatography-tandem mass spectrometry. Following the assessment of the data from this pilot study, we then applied the optimized workflow to the proteasome, a protein complex currently extensively studied by our group.

Establishing Peptide Size Exclusion Chromatography for the Fractionation of Digests of Cross-link Samples—We used a polymeric FPLC size-exclusion column suitable for a separation range of 1000 to 7000 Da, according to the manufacturer's specifications. We first evaluated the efficiency of the SEC column by analyzing a peptide mixture consisting of insulin (5.7 kDa), oxidized insulin A chain (2.5 kDa), and angiotensin II (1.0 kDa). Careful optimization of the mobile phase was required as symmetric peaks were only observed in the presence of an acidic aqueous/organic mobile phase. The use of 30% acetonitrile and 0.1% trifluoroacetic acid resulted in acceptable separation of the three analytes, particularly in the range of 1–3 kDa that is most relevant for cross-linked peptides, as shown in Fig. 1*A*. This volatile mobile phase composition also ensured direct compatibility with downstream

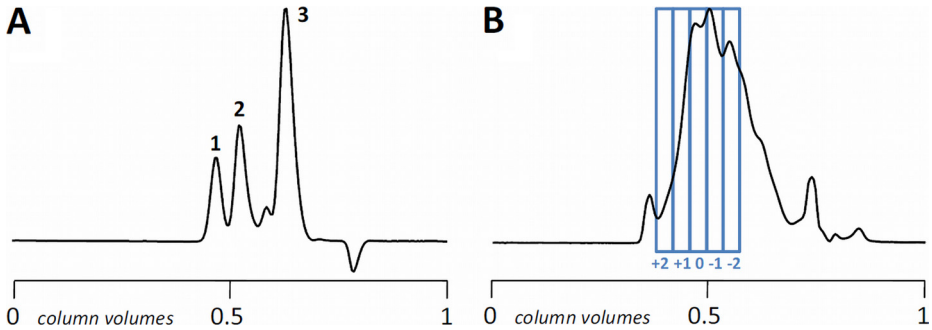

FIG. 1. **Peptide separations by size exclusion chromatography.** UV traces at 215 nm are shown. *A*, Separation of a model peptide mixture (1 μg per peptide injected) consisting of insulin (1; 5.7 kDa), oxidized insulin A chain (2; 2.5 kDa), and angiotensin II (3; 1.0 kDa). *B*, Separation of the eight-protein mix cross-linked with DSS and digested with trypsin as the protease (100 μg total protein digest injected). The fractions collected for LC-MS analysis are highlighted. Elution profiles using other proteases are shown in the supplemental Material Fig. S1.

LC-MS analysis, requiring only an evaporation step and, in contrast to SCX fractionation, no further sample clean-up.

We next used the optimized conditions to analyze a tryptic digest of the eight-protein mixture cross-linked with DSS. The resulting UV chromatogram is shown in Fig. 1*B*. Based on the elution profile, we collected five individual 100 μl-fractions (corresponding to 2 min windows) as shown (elution volumes 0.9–1.4 ml). Preliminary experiments showed that the fraction from 1.1 to 1.2 ml gave the highest number of cross-link identifications and was labeled fraction "0." Higher mass fractions were termed "+1" and "+2" and lower mass fractions "–1" and "–2," respectively, to label their positions relative to the main fraction.

To assess the distribution of different types of peptides over the SEC elution, we analyzed the individual fractions by LC-MS/MS on a linear ion trap-Orbitrap hybrid instrument. MS/MS spectra were analyzed using two software platforms. *Unmodified peptides* were identified with the widely used search engine, Mascot (27), whereas *cross-linked peptides* and single peptide chains carrying a hydrolyzed cross-linker modification (*mono-links*) were assigned with the dedicated cross-linking software, xQuest (12). For this purpose, modified peptides can easily be discerned because they appear as doublets in the MS^1 spectrum, separated by 12/z Da, corresponding to the mass shift of the cross-linking reagent.

We assumed that because of the increase in molecular mass upon cross-linking, cross-linked peptides would appear in earlier fractions and can therefore be enriched to some degree. Fig. 2 shows the distribution of three classes of peptides over the five SEC fractions that were examined. As expected, the maximum number of cross-link identifications is shifted to higher mass fractions compared with unmodified peptides and peptides carrying mono-links. In particular, most of the cross-link identifications were observed in only two fractions (0 and +1). The majority of the linear peptides, unmodified peptides or mono-links, eluted in later fractions (–1 and –2). The actual numbers of unmodified peptides are expected to be even higher as data was obtained from samples where only precursors of charge states three and higher

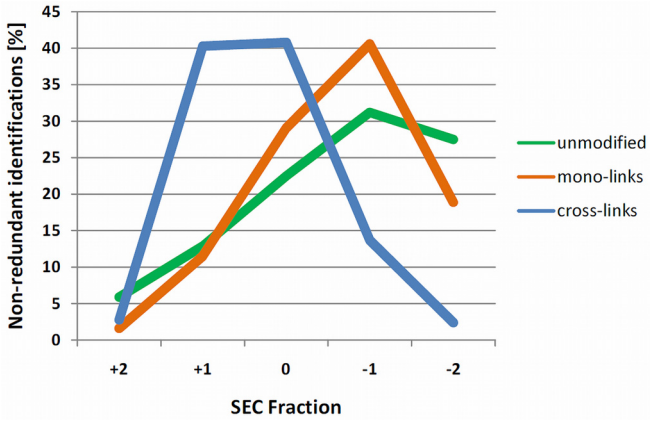

FIG. 2. **Relative distributions of three classes of peptides (unmodified peptides, green; mono-links, orange; and cross-links, blue) among the SEC fractions from a trypsin digest of the eight-protein mix.** Data points are normalized so that for each peptide class, the sum of identifications in all five fractions is set to 100%. Distributions for other proteases are shown in supplemental material Fig. S2.

were selected for fragmentation. This means that likely a considerable number of peptides in the lower molecular weight fraction were excluded from sequencing because they were only present in lower charge states. According to a rough estimate based on UV absorption, these low molecular weight fractions cover ~80% of the total peak area, corresponding to substantial depletion of peptides that are not directly relevant to cross-linking studies. On the other end of the elution window, the number of identifications in the highest MW fractions was quite low. This is most likely a result of the combination of lower abundance and unfavorable analytical properties in this region.

These very promising initial results led us to conclude that an acceptable degree of separation between the subpopulation of cross-linked peptides and the rest of the peptide pool was possible.

Using Different Proteases for the Digestion of Cross-link Samples—To further expand the number of cross-links that can be recovered in combination with SEC fractionation, we

evaluated other commonly used proteases for enzymatic cleavage in addition to trypsin: Asp-N and Glu-C for cleavage at acidic residues and Lys-C and Lys-N for exclusive cleavage at lysine residues.

Evaluating Enzyme Specificity—Preliminary studies were carried out on noncross-linked peptides to evaluate the specificity of the proteases under typical conditions. This was important to keep the search space to a minimum while at the same time using realistic cleavage settings for xQuest. Both Lys-C and Lys-N were found to be highly specific, exhibiting negligible unspecific cleavage at other residues. In contrast, the endoproteinases Asp-N and Glu-C were not exclusively specific for their expected cleavage site: Asp-N was also found to cleave on the N-terminal side of Glu residues, and Glu-C exhibited cleavage also C-terminal to Asp. Specificity was found to be slightly higher for Glu-C, but we decided to consider cleavages at aspartic and glutamic acid for xQuest analysis in both cases, because both peptides connected in a cross-link need to adhere to the defined specificity, and thus even a single deviation in the required four cleavage events would preclude identification of the cross-link.

SEC Fractionation of Cross-linked Samples—Sample preparation for the four additional proteases was carried out as for the trypsin treatment. Proteins individually cross-linked with DSS (the same samples as for the trypsin data set) were digested using procedures as recommended by the manufacturers or, in the case of Lys-N, according to a protocol supplied by the Heck laboratory. SEC fractionation was performed as described above and the same five fractions were collected and analyzed by LC-MS/MS. As shown in supplemental Fig. S1, elution profiles were highly similar for Lys-C, Lys-N, and Glu-C, whereas the Asp-N profile resembled the trypsin chromatogram. The first three enzymes also exhibited a significant peak at the void volume (~0.3 column volumes), pointing to the generation of very large peptides and/or incomplete digestion under the conditions used.

Redundancy and Orthogonality of the Cross-linking Data Sets for Standard Proteins—We next set out to compare the cross-linking identifications from the fractionated digests of the five proteases and to assess the benefit of using additional proteases. In order to comprehensively profile the sample, we first analyzed all five SEC fractions per protease in duplicate. Thus, in total, 50 LC-MS/MS runs were performed for the model protein samples as part of this study. Using the xQuest software pipeline, scan pairs corresponding to light/heavy pairs with a mass shift of 12.07532 Da were detected. Depending on the enzyme used, up to more than 2000 of such scan pairs were detected in a single fraction and submitted to the database search. Results from the technical replicates were then combined before further analysis and manually validated.

Fig. 3 gives an overview of the distribution of nonredundant cross-link identifications in each SEC fraction for the five proteases investigated; and supplemental Fig. S2 compares the distribution of different classes of peptides as shown for trypsin in Fig. 2 above. In all cases, the majority of cross-link identifications are again confined to two fractions; additional fractions yielded much lower numbers of identifications that were also partially overlapping with the set from the two main fractions. Mono-links and unmodified peptides show an elution pattern that is shifted by at least one SEC fraction, which is comparable to the trypsin data set. The separation of cross-linked peptides appears to be somewhat less pronounced for the Asp-N and Glu-C samples, which can be attributed to the fact the cross-linking reaction does not result in missed cleavage sites for these enzymes.

Focusing on the identification of cross-linked peptides, when collapsing all identifications from the five SEC fractions per enzyme, trypsin yielded by far the highest number of nonredundant identifications (Fig. 4). In total, 150 different intraprotein cross-links were identified from this digest, which is a substantial improvement compared with previously reported methods. For comparison, we also analyzed in duplicate an unfractionated sample of the tryptic digest directly by LC-MS/MS. In this case, only 44 intraprotein cross-links were identified. The difference can be explained both by the reduction in sample complexity and the proportional increase in loading for cross-linked peptides because of the partial enrichment.

The second highest number of cross-link identifications, 95, was observed for Asp-N, with Glu-C, Lys-C, and Lys-N following. Fig. 4 shows also the contribution of the two SEC fractions richest in cross-links, demonstrating that the majority of cross-links identifiable with the current approach (88–100%) fall within two fractions for all proteases.

To obtain this comprehensive data set, preliminary results were initially filtered according to the achievable mass tolerance (± 5 ppm, an asymmetric search window was used as no recalibration of the raw data was carried out) and multiple identifications corresponding to the same peptide sequences and the same cross-linking sites ("cross-link topologies") within the peptides were collapsed into single hits. Only the highest scoring identifications were kept. As explained above, because of the experimental design, all putative interprotein cross-links can be confidently classified as false positives. Despite the stringent filtering criteria, the number of these false identifications was still considerable (above 10% in some cases) at the level of unique nonredundant cross-links. Using interprotein cross-link assignments as a guide, we performed additional filtering steps to reduce the number of random hits. We excluded cross-link identifications that contained a peptide shorter than six amino acids as they were found to contain a disproportionally high number of false positives. Furthermore, the acceptable xQuest score threshold needed to be raised from 16 to 18 for the Glu-C and Asp-N data sets, because in these cases, the search space is more than three times larger than for trypsin as a consequence of the higher abundance of acidic residues as cleavage sites.

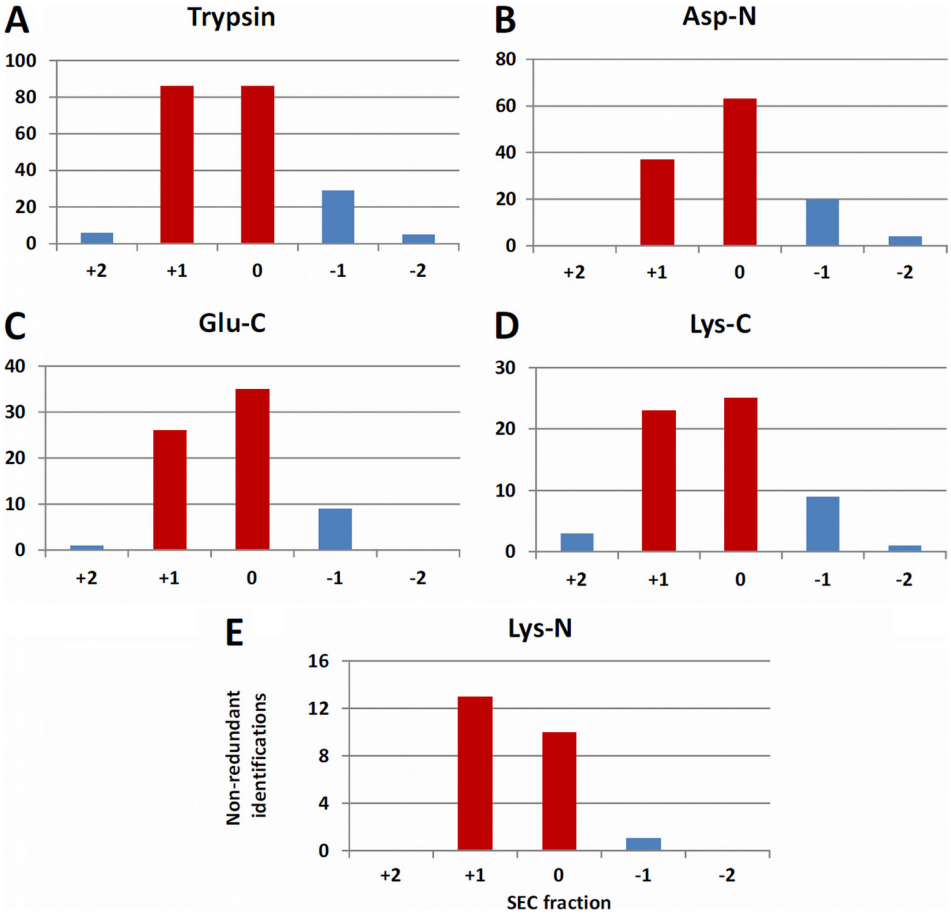

FIG. 3. **Distribution of cross-link identifications in different SEC fractions.** Shown are nonredundant cross-linked peptides in five individual SEC fractions per enzyme, with the two main fractions highlighted in red. (*A*) Trypsin, (*B*) Asp-N, (*C*) Glu-C, (*D*) Lys-C, (*E*) Lys-N.

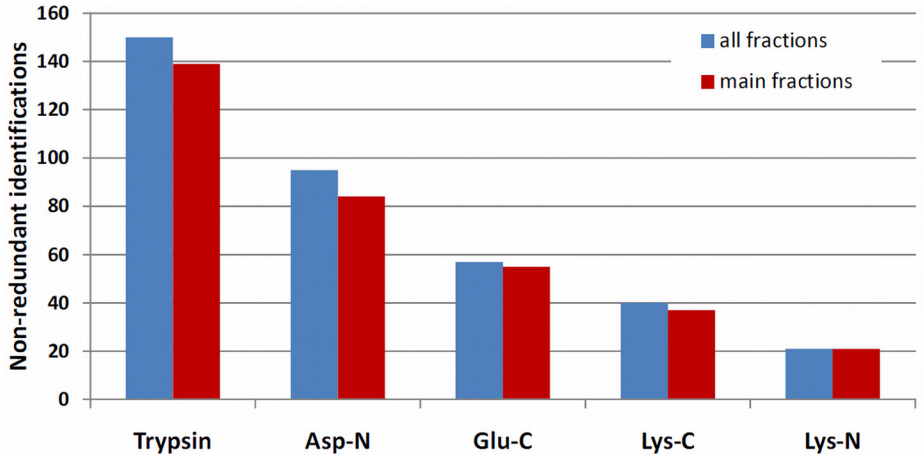

FIG. 4. **Comparison of cross-link identifications with five different proteases.** Shown are nonredundant cross-linked peptides combined over all SEC fractions (in blue) and found in the two main fractions (in red), respectively.

Finally, the remaining spectra were all manually examined for the number of observed bond cleavages in each peptide. We found that many of the assigned interprotein cross-links had only poor sequence coverage in one peptide. Similar to the classification scheme reported by Rappsilber and coworkers (13), we excluded all identifications with less than four bond cleavages in total or three consecutive bond cleavages in both peptides. The final refined data sets are expected to yield FDRs of below 5%, which was also confirmed by structural validation (see below). During preparation of the manuscript, Lauber and Reilly reported similar observations and developed their own filtering criteria for xQuest results (18).

These results already clearly demonstrate that SEC is a powerful tool for cross-linking analysis. However, we cannot

TABLE II
Non-redundant Lys-Lys contacts at the individual protein level for each single protease and combined. Numbers in parentheses show contacts not observed in the trypsin data set

Protein name	Trypsin	Asp-N	Glu-C	Lys-C	Lys-N	Total
Catalase, bovine	3	2 (2)	0	3 (1)	0	6
Creatine kinase, rabbit	12	6 (4)	4 (4)	3 (2)	1 (1)	19
Fructose-bisphosphate aldolase A, rabbit	12	6 (4)	2 (1)	7 (2)	1 (0)	19
Lactoferrin, bovine	21	11 (8)	1 (1)	2 (1)	1 (1)	31
Ovotransferrin, chicken	19	13 (12)	2 (2)	9 (4)	4 (2)	38
Pyruvate kinase, rabbit (isoenzyme 1)	8	7 (6)	2 (2)	1 (1)	1 (1)	15
Serotransferrin, bovine	28	21 (14)	13 (12)	6 (3)	4 (2)	57
Serum albumin, bovine	34	12 (9)	20 (10)	9 (4)	7 (4)	55
TOTAL	137	78 (59)	44 (32)	40 (18)	19 (10)	240

exclude at this stage that different instrumental set-ups and refined software would facilitate the identification of additional cross-links, especially in the higher molecular mass fractions. This could especially be the case for enzymes such as Lys-C and Lys-N, which cleave less frequently and yielded comparably fewer identifications.

Improvement in Cross-link Coverage on the Protein Level—Breaking down the identifications according to the individual proteins presents a very interesting picture. Table II lists the identified unique cross-linking sites observed with the different enzymes for all eight proteins. Here, cross-linking topologies that were identified in different peptides because of the use of different enzyme cleavage specificities or to the presence of missed cleavage sites were combined as they all provide the same spatial information. Although all proteins are relatively comparable in size, the number of distance restraints differs by nearly an order of magnitude (compare serum albumin, 66 kDa, and catalase, 60 kDa). Most apparent is a trend that the number of cross-links observed for a given protein in the trypsin data set is proportional to its lysine content. Although this may not come as a surprise because a lysine-specific cross-linking reagent was used in the study, the connection is still relevant. It shows that for proteins with a disproportionally high lysine content (*e.g.* 10.1% for BSA), unusually high numbers of cross-links are achievable whereas the information that is recoverable for proteins with average lysine content is probably less extensive. Such trends are not as apparent for the enzymes that yield smaller numbers of identifications, such as Lys-C and Lys-N. Interestingly, Glu-C and Asp-N cross-links differ substantially for some proteins (lactoferrin, serum albumin) despite an overall quite similar content of acidic residues for all proteins. This may be connected to the dominant cleavage specificity for the individual proteases.

Finally, these identifications were cumulated to provide a list of nonredundant distance restraints (Lys-Lys contacts) for the whole data set (supplemental Tables S1 and S2). The complete data set provided a total of 240 restraints, with numbers for individual proteins ranging from 6 (catalase) to 57 (bovine transferrin). Trypsin-derived data alone accounted for a total of 137 restraints from these eight proteins. Although all other enzymes contributed less information, Asp-N provided the largest amount of complementary restraints, with 59 intramolecular connections out of a total of 78 not covered by trypsin (Table II). Again, Glu-C, Lys-C and Lys-N followed in the same order as for the total nonredundant identifications, contributing 32, 18, and 10 contacts not found using trypsin.

To illustrate the extensive cross-link coverage obtained for BSA, Fig. 5*A* visualizes the BSA restraints on a homology model obtained from ModBase (28). As shown in Fig. 5*B*, the majority of the observed distances conform to the expected span of the cross-linking reagent (C_α-C_α distance of 23 Å excluding any structural flexibility), and with the exception of two contacts, the bridged distances lie within 28 Å. The calculated span between residues 117 and 489 is 34.8 Å and could result from a deviation of the homology model to the actual structure, whereas the second outlier corresponds to a theoretical distance of 57.1 Å. Even if both cases are classified as false positives, the error rate would still be at an acceptable level of 3.6% (2 of 55).

As summarized in Table II, 34 of the 55 Lys-Lys contacts were obtained from the trypsin sample. However, not all regions of the protein are covered equally well by this enzyme. We highlight two exemplary regions where additional proteases provide substantial new structural information. First, few cross-links in the N-terminal region were identified from the tryptic digest. Cross-links containing Lys^{28} and Lys^{36} were identified in a total of six restraints, but the next position included in a cross-link is Lys^{140} (excluding the ambiguous cross-link 117 × 489 mentioned above). Within this span of ~100 residues, Asp-N and Glu-C derived contacts provide seven additional restraints (visualized in supplemental Fig. S3). A closer inspection of the amino acid composition reveals that the N-terminal region is relatively poor in arginine residues, but rich in lysines. Therefore, if exposed lysines are blocked following the reaction with the cross-linking reagent (therefore precluding cleavage by a protease) the resulting peptides would become excessively long. On the contrary, if lysines are not accessible in the native structure, these Lys-rich regions will present many cleavage sites upon denaturation, resulting in relatively short peptides that are challenging to identify and are underrepresented as a consequence of the

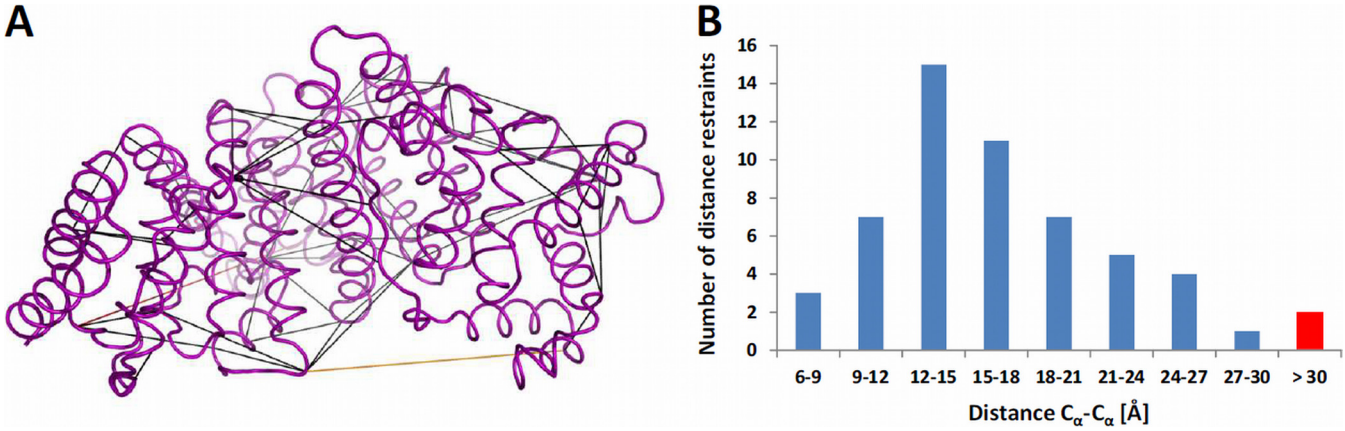

FIG. 5. ***A*, Lys-Lys contacts identified by the multiprotease approach mapped onto a bovine serum albumin homology structure obtained from ModBase.** Distances (C_α-C_α) of less than 30 Å, between 30 and 35 Å and above 35 Å are colored in black, orange and red, respectively. Visualization was performed using PyMOL 1.3 (Schrödinger LLC). *B*, Histogram showing the distribution of the BSA distance restraints shown in (*A*).

SEC fractionation. The more homogeneous distribution of acidic residues offers better coverage of this region.

As a second example, contacts only identified with Asp-N and Lys-C also covered a region near the C terminus more extensively. Lysines 561 and 568 were connected in peptides distant in the primary sequence, defining the orientation of this region toward the rest of the structure with the contacts 495 × 561 and 520 × 568 (supplemental Fig. S4).

Even with the expanded coverage achieved by the use of five proteases, the number of experimentally observed contacts was still roughly an order of magnitude below the theoretically possible. A simulation by the tool Xwalk (29) revealed that in excess of 500 contacts are possible within a reasonable distance restraint of up to 30 Å. Eventually, it is crucial for a cross-linking workflow to provide input for refining unknown structures of proteins and protein complexes. To achieve this, it has to be considered that part of the cross-links that are identified yield little relevant structural information because residues adjacent in the primary amino acid sequence are connected. For example, in our case about 20% of the nonredundant restraints connect residues less than 20 amino acids apart. In this context, the expanded coverage that is obtainable by multiple proteases becomes even more relevant.

Biological Application of the Optimized Workflow—To demonstrate the benefit of both SEC fractionation and multiprotease digestion, we applied the optimized workflow to a multisubunit protein complex of high biological interest, the proteasome. The proteasome is the end point of the ubiquitin-proteasome pathway for protein degradation (30, 31). It consists of two main compartments, the 19S regulatory particle (RP), responsible for the recognition of polyubiquitinated substrates, and a barrel-shaped 20S core particle (CP). Chemical cross-linking has recently contributed important information for deriving the structure of the CP and the AAA-ATPases that are part of the RP (25). Here, to demonstrate the value of the refined workflow, we focused on the CP that consists of 14 different subunits (α_1 - α_7 and β_1 - β_7), each present in two copies, which assemble to four stacked heteroheptameric rings ($\alpha\beta\beta\alpha$). High-resolution structures of CPs from several organisms are available (32, 33).

Samples From Two Species Were Evaluated. A rabbit 20S preparation was cross-linked with DSS at concentrations comparable to the standard proteins (using a starting amount of 50 μg at ~0.8 mg ml^{-1}). Additionally, *S. pombe* proteasome was reacted with DSS, although at much lower concentration, reflecting a typical sample-limited scenario. In this case, even after preconcentration, only around 10 μg of protein at ~0.2 mg ml^{-1} was recovered from the preparation. It is well known that cross-linking kinetics is not very favorable in this concentration range; we commonly observe that reaction yields drop substantially below 0.5 mg ml^{-1}. In addition, conditions for enzymatic digestion of such small sample amounts may also be suboptimal. In both cases, the cross-linked sample was split in half and digested with either trypsin or Asp-N. Asp-N was chosen because it provided the highest degree of complementary information to trypsin for the 8-protein mix. The digested samples were then fractionated by SEC and the two main fractions (0 and +1) were collected for LC-MS analysis.

For the rabbit sample, the trypsinized aliquot yielded 42 nonredundant cross-linked peptides, corresponding to 36 nonredundant contact sites. Among these, 18 restraints were within the same subunit, with one exception exclusively within α-subunits. 18 other restraints were located between distinct subunits. Also for this subset, a majority of the restraints was located within α-subunits, three were located between an α- and a β-subunit and one between two β-subunits. The aliquot digested with Asp-N yielded a much smaller set of identifications: Six intra-subunit cross-links and three inter-subunit cross-links, all within or between α-subunits. The overlap between the two data sets was however minimal, as only one

TABLE III

Identified cross-linking sites in the S. pombe 20S proteasome. Shown are the amino acid sequences and cross-linking positions within the peptide (a = α chain, b = ß chain); the corresponding proteins and the absolute position of the cross-linking sites; experimentally observed mass (M_r), mass-to-charge ratio(m/z), and charge state (z) of the highest scoring identification; the deviation of experimental to theoretical mass in ppm; fraction of total ion current (TIC) explained; xQuest score; and Euclidean C_α-C_α distance calculated from the homology model

Sequences	Protein 1	Pos. 1	Protein 2	Pos. 2	M_r (exp.)	m/z (exp.)	z	Error (ppm)	%TIC	Score	Distance (Å)
Trypsin data											
KIYNEYPPTK-KVAQTTYK-a1-b1	PSA2_SCHPO	99	PSA2_SCHPO	91	2327.237	582.817	4	−1.7	0.43	28.50	10.5
IITKEGVETR-RLLKLEEAMK-a4-b4	PSB1_SCHPO	212	PSB1_SCHPO	179	2512.421	503.492	5	−3.4	0.36	26.65	14.6
EYLEKNWKEGLSR-ASKAAR-a5-b3	PSA7_SCHPO	176	PSA7_SCHPO	168	2391.256	598.822	4	0.7	0.22	26.04	11.9
KPTSELAIGASLEK-ATAIGKSSTAAK-a1-b6	PSA2_SCHPO	50	PSA2_SCHPO	165	2685.48	672.378	4	−0.1	0.44	25.61	12.6
KVAQTTYK-VLVDKSR-a1-b5	PSA2_SCHPO	91	PSA2_SCHPO	88	1891.072	473.776	4	−2.9	0.15	25.51	5.1
IITKEGVETR-LLKLEEAMK-a4-b3[a]	PSB1_SCHPO	212	PSB1_SCHPO	179	2356.328	590.090	4	−0.3	0.24	21.48	14.6
ATSAGPKQTETINWLEK-KVPDKLIDASTVK-a7-b1	PSA6_SCHPO	169	PSA6_SCHPO	53	3423.852	856.971	4	0.7	0.28	19.88	14.5
KVPDKLIDASTVK-NELEKLNFSSLK-a5-b5	PSA6_SCHPO	57	PSA3_SCHPO	177	2971.649	743.920	4	0.4	0.22	18.67	7.1
Asp-N data											
DKCIKRLVKGRQD-DRGTTAVLKE-a9-b9	PSB3_SCHPO	200	PSB7_SCHPO	248	2841.552	474.600	6	1.1	0.29	20.38	4.9
DTTKNKMVCKIWKS-DIYKFVTVQ-a10-b4	PSA4_SCHPO	227	PSB7_SCHPO	253	2987.561	747.898	4	3.7	0.34	19.67	23.4
DKCIKRLVKGRQD-DRGTTAVLKE-a5-b9	PSB3_SCHPO	196	PSB7_SCHPO	248	2841.559	569.320	5	3.5	0.19	19.21	13.6
DEEKATPYRGYSKPN-ERATKQSKYTY-a13-b5	PSB7_SCHPO	226	PSB7_SCHPO	233	3265.594	654.127	5	1.5	0.13	18.34	19.1

[a] Redundant restraint.

Lys-Lys contact was shared by both enzymes. The preference for α-subunits can be readily explained by the fact that the β-subunits are located in the two central rings and have significantly less exposed surface than the α-rings and, consequently, less exposed cross-linkable sites. Some additional cross-links were possibly missed because the data was searched against a database containing the human proteasome subunits, which are likely not completely identical to the rabbit sequences. All the identifications are summarized in supplemental Table S3, and annotated spectra are provided in supplemental Fig. S5.

From the *S. pombe* sample, seven contacts from the trypsin sample and four from the Asp-N sample were identified, reflecting the very low sample amounts. The trypsin data set yielded five intra-subunit cross-links on α-subunits (three on α_2 plus additional ones on α_6 and α_7) plus one on the β_1-subunit. An intersubunit cross-link between subunits α_3 and α_6 was also observed. The Asp-N cross-links, interestingly, preferentially covered the β-subunits, including an intrasubunit link on β_7 and two inter-subunit links between β_3 and β_7. The remaining contact was observed between α_4 and β_7. In this case, no overlap between the trypsin and Asp-N restraints was found, and, importantly, all contacts were validated on a 20S homology model with C_α-C_α distances between 4.9 and 23.4 Å. Detailed information about the identifications is provided in Table III and supplemental Fig. S6.

Thus, although the increase in identifications from the use of a second enzyme was partially lower than for model proteins, it is apparent that additional contacts can be recovered using the same, well established cross-linking protocol. Practically, the starting amounts available for the *S. pombe* sample also seem to be the lower limit for providing any benefit by performing the fractionation step. However, the results from the rabbit proteasome compare favorably with a recent study by Kao *et al.* using the gas-phase cleavable cross-linking reagent, disuccinimidyl sulfoxide (21). In this work, similar starting amounts and concentrations (50 μl at a concentration of < 0.9 mg ml^{-1}) were used, and identical instrumentation was employed. A total of 13 nonredundant cross-linked peptides were identified, which should be at least partly attributable to the fact that no enrichment step was included in the protocol.

Concluding Remarks—Although cross-linking methodology has improved considerably in recent years, it still can be expected that only a small fraction of potential cross-linking sites are currently detected in typical assays. Despite the expectation that the introduction of more sensitive mass spectrometers will drive up the numbers in the future and improved software should increase the fraction of spectra that can be assigned to a particular arrangement of two connected peptides, the adoption of relatively straightforward experimental protocols immediately provides a convenient approach to increase the depth of cross-linking studies. Here, we demonstrated that the introduction of SEC fractionation and the use of multiple proteases led to a more comprehensive coverage of cross-links. On model proteins, the number of cross-links identified increased more than 3-fold upon adoption of SEC fractionation using only trypsin as the protease. Because two SEC fractions contain a large majority of the cross-link fractions, the increased demand for instrument time is reasonable. In contrast to SCX fractionation, the procedure is highly amenable to automation and directly compatible with downstream MS analysis. The use of several proteases resulted in a further increase of more than 70% on the level of nonredundant cross-linking sites by using four other proteases, and more than 45% using Asp-N alone, for model proteins. Similar

increases are achievable even for small sample amounts, as demonstrated by the application to the proteasome. Eventually, such improvements may depend on the particular properties of the protein(s) under study, mainly on the frequency and distribution of cross-linking and enzymatic cleavage sites.

The SEC fractionation described in this work has already been successfully applied in a previous study on the proteasome (25), and here we could show that the combined use of complementary proteases further increases the yield of cross-links. This is even the case for very low sample amounts, as could be demonstrated by the *S. pombe* sample, where the total number of Lys-Lys contacts increased from seven to eleven.

Acknowledgment—We thank Albert J. R. Heck (University of Utrecht) for providing a sample of Lys-N protease.

* This work was supported by the European Union 7th Framework project PROSPECTS (Proteomics Specification in Time and Space, grant HEALTH-F4-2008-201648). AL was partially supported by a Schrödinger fellowship of the Austrian Science Fund. The stay of RR was financially supported through a fellowship from the University of Vienna and the Österreichische Forschungsgemeinschaft (ÖFG). RA was supported by the ERC advanced grant "Proteomics v.3.0" (grant 233226).

S This article contains supplemental Figs. S1 to S6 and Tables S1 to S3.

‡‡ To whom correspondence should be addressed: Institute of Molecular Systems Biology, Eidgenössische Technische Hochschule (ETH) Zurich, Wolfgang-Pauli-Strasse 16, 8093 Zurich, Switzerland. Tel.: +41-44-633-2698; Fax: +41-44-633-1051; E-Mail: leitner@imsb.biol.ethz.ch; Ruedi Aebersold, Tel.: +41-44-633-3170; E-mail: aebersold@imsb.biol.ethz.ch.

REFERENCES

1. Robinson, C. V., Sali, A., and Baumeister, W. (2007) The molecular sociology of the cell. *Nature* **450,** 973–982
2. Konermann, L., Pan, J., and Liu, Y. H. (2011) Hydrogen exchange mass spectrometry for studying protein structure and dynamics. *Chem. Soc. Rev.* **40,** 1224–1234
3. Konermann, L., Stocks, B. B., Pan, Y., and Tong, X. (2010) Mass spectrometry combined with oxidative labeling for exploring protein structure and folding. *Mass Spectrom. Rev.* **29,** 651–667
4. Benesch, J. L., Ruotolo, B. T., Simmons, D. A., and Robinson, C. V. (2007) Protein complexes in the gas phase: Technology for structural genomics and proteomics. *Chem. Rev.* **107,** 3544–3567
5. Leitner, A., Walzthoeni, T., Kahraman, A., Herzog, F., Rinner, O., Beck, M., and Aebersold, R. (2010) Probing Native Protein Structures by Chemical Cross-linking, Mass Spectrometry, and Bioinformatics. *Mol. Cell. Proteomics* **9,** 1634–1649
6. Petrotchenko, E. V., and Borchers, C. H. (2010) Crosslinking combined with mass spectrometry for structural proteomics. *Mass Spectrom. Rev.* **29,** 862–876
7. Rappsilber, J. (2011) The beginning of a beautiful friendship: Cross-linking/mass spectrometry and modelling of proteins and multi-protein complexes. *J. Struct. Biol.* **173,** 530–540
8. Mayne, S. L., and Patteron, H. G. (2011) Bioinformatics tools for the structural elucidation of multi-subunit protein complexes by mass spectrometric analysis of protein–protein cross-links. *Brief. Bioinform.* **12,** 660–671
9. Trester-Zedlitz, M., Kamada, K., Burley, S. K., Fenyö, D., Chait, B. T., and Muir, T. W. (2003) A modular cross-linking approach for exploring protein interactions. *J. Am. Chem. Soc.* **125,** 2416–2425
10. Kang, S., Mou, L., Lanman, J., Velu, S., Brouillette, W. J., and Prevelige, P. E., Jr. (2009) Synthesis of biotin-tagged chemical cross-linkers and their applications for mass spectrometry. *Rapid Commun. Mass Spectrom.* **23,** 1719–1726
11. Nessen, M. A., Kramer, G., Back, J., Baskin, J. M., Smeenk, L. E., de Koning, L. J., van Maarseveen, J. H., de Jong, L., Bertozzi, C. R., Hiemstra, H., and de Koster, C. G. (2009) Selective enrichment of azide-containing peptides from complex mixtures. *J. Proteome Res.* **8,** 3702–3711
12. Rinner, O., Seebacher, J., Walzthoeni, T., Mueller, L. N., Beck, M., Schmidt, A., Mueller, M., and Aebersold, R., (2008) Identification of cross-linked peptides from large sequence databases. *Nat. Methods* **5,** 315–318
13. Chen, Z. A., Jawhari, A., Fischer, L., Buchen, C., Tahir, S., Kamenski, T., Rasmussen, M., Lariviere, L., Bukowski-Willis, J. C., Nilges, M., Cramer, P., and Rappsilber, J. (2010) Architecture of the RNA polymerase II–TFIIF complex revealed by cross-linking and mass spectrometry. *EMBO J.* **29,** 717–726
14. Lauber, M. A., and Reilly, J. P. (2010) Novel Amidinating Cross-Linker for Facilitating Analyses of Protein Structures and Interactions. *Anal. Chem.* **82,** 7736–7743
15. Zhang, H., Tang, X., Munske, G. R., Tolic, N., Anderson, G. A., and Bruce, J. E. (2009) Identification of Protein-Protein Interactions and Topologies in Living Cells with Chemical Cross-linking and Mass Spectrometry. *Mol. Cell. Proteomics* **8,** 409–420
16. Tang, X., and Bruce, J. E. (2010) A new cross-linking strategy: protein interaction reporter (PIR) technology for protein–protein interaction studies. *Mol. BioSyst.* **6,** 939–947
17. Zheng, C., Yang, L., Hoopmann, M. R., Eng, J. K., Tang, X., Weisbrod, C. R., and Bruce, J. E. (2011) Cross-linking measurements of in vivo protein complex topologies. *Mol. Cell. Proteomics* 10, M110.006841 (article number)
18. Lauber, M. A., and Reilly, J. P. (2011) Structural analysis of a prokaryotic ribosome using a novel amidinating cross-linker and mass spectrometry. *J. Proteome Res.* **10,** 3604–3616
19. Santos, L. F., Iglesias, A. H., and Gozzo, F. C. (2011) Fragmentation features of intermolecular cross-linked peptides using N-hydroxy- succinimide esters by MALDI- and ESI-MS/MS for use in structural proteomics. *J. Mass Spectrom.* **46,** 742–750
20. Trnka, M. J., and Burlingame, A. L. (2010) Topographic studies of the GroEL-GroES chaperonin complex by chemical cross-linking using diformyl ethynylbenzene. *Mol. Cell. Proteomics* **9,** 2306–2317
21. Kao, A., Chiu, C., Vellucci, D., Yang, Y., Patel, V. R., Guan, S., Randall, A., Baldi, P., Rychnovsky, S. D., and Huang, L. (2011) Development of a novel cross-linking strategy for fast and accurate identification of cross-linked peptides of protein complexes. *Mol. Cell. Proteomics* 10, M110.002212 (article number)
22. Swaney, D. L., Wenger, C. D., and Coon, J. J. (2010) Value of using multiple proteases for large-scale mass spectrometry-based proteomics. *J. Proteome Res.* **9,** 1323–1329
23. Tran, B. Q., Hernandez, C., Waridel, P., Potts, A., Barblan, J., Lisacek, F., and Quadroni, M. (2011) Addressing trypsin bias in large scale (phospho)proteome analysis by size exclusion chromatography and secondary digestion of large post-trypsin peptides. *J. Proteome Res.* **10,** 800–811
24. Saeki, Y., Isono, E., and Toh-E, A. (2005) Preparation of ubiquitinated substrates by the PY motif-insertion method for monitoring 26S proteasome activity. *Methods Enzymol.* **399,** 215–227
25. Bohn, S., Beck, F., Sakata, E., Walzthoeni, T., Beck, M., Aebersold, R., Förster, F., Baumeister, W., and Nickell, S. (2010) Structure of the 26S proteasome from *Schizosaccharomyces pombe* at subnanometer resolution. *Proc. Natl. Acad. Sci. U.S.A.* **107,** 20992–20997
26. Pedrioli, P. G. (2010) Trans-proteomic pipeline: a pipeline for proteomic analysis. *Methods Mol. Biol.* **604,** 213–238
27. Perkins, D. N., Pappin, D. J., Creasy, D. M., and Cottrell, J. S. (1999) Probability-based protein identification by searching sequence databases using mass spectrometry data. *Electrophoresis* **20,** 3551–3567
28. Pieper, U., Webb, B. M., Barkan, D. T., Schneidman-Duhovny, D., Schlessinger, A., Braberg, H., Yang, Z., Meng, E.C., Pettersen, E. F., Huang, C. C., Datta, R. S., Sampathkumar, P., Madhusudhan, M. S., Sjölander, K., Ferrin, T. E., Burley, S. K., and Sali, A. (2011) MODBASE, a database

of annotated comparative protein structure models and associated resources. *Nucleic Acids Res.* **39,** D465–D474
29. Kahraman, A., Malmström, L., and Aebersold, R. (2011) Xwalk: computing and visualizing distances in cross-linking experiments. *Bioinformatics* **27,** 2163–2164
30. Finley, D. (2009) Recognition and Processing of Ubiquitin-Protein Conjugates by the Proteasome. *Annu. Rev. Biochem.* **78,** 477–513
31. Weissman, A. M., Shabek, N., and Ciechanover, A. (2011) The predator becomes the prey: regulating the ubiquitin system by ubiquitylation and degradation. *Nat. Rev. Mol. Cell Biol.* **12,** 605–620
32. Lowe, J., Stock, D., Jap, B., Zwickl, P., Baumeister, W., and Huber, R. (1995) Crystal structure of the 20S proteasome from the archaeon *T. acidophilum* at 3.4 Å resolution. *Science* **268,** 533–539
33. Groll, M., Ditzel, L., Löwe, J., Stock, D., Bochtler, M., Bartunik, H. D., and Huber, R. (1997) Structure of 20S proteasome from yeast at 2.4Å resolution. *Nature* **386,** 463–471